

Spin Impurities, Wilson Lines and Semiclassics

Gabriel Cuomo,^{a,b} Zohar Komargodski,^{a,b} Márk Mezei^a and Avia Raviv-Moshe^a

^a*Simons Center for Geometry and Physics, SUNY, Stony Brook, NY 11794, USA*

^b*C. N. Yang Institute for Theoretical Physics, Stony Brook University, Stony Brook, NY 11794, USA*

E-mail: gcuomo@scgp.stonybrook.edu, zkomargodski@scgp.stonybrook.edu,
mmezei@scgp.stonybrook.edu, araviv-moshe@scgp.stonybrook.edu

ABSTRACT: We consider line defects with large quantum numbers in conformal field theories. First, we consider spin impurities, both for a free scalar triplet and in the Wilson-Fisher $O(3)$ model. For the free scalar triplet, we find a rich phase diagram that includes a perturbative fixed point, a new nonperturbative fixed point, and runaway regimes. To obtain these results, we develop a new semiclassical approach. For the Wilson-Fisher model, we propose an alternative description, which becomes weakly coupled in the large spin limit. This allows us to chart the phase diagram and obtain numerous rigorous predictions for large spin impurities in $2 + 1$ dimensional magnets. Using similar techniques, we also study $1/2$ -BPS Wilson lines in large representations of the gauge group in rank-1 $\mathcal{N} = 2$ superconformal field theories. We propose a universal effective field theory description that allows to compute several observables in a semiclassical expansion. We confirm some of our predictions using localization.

Contents

1	Introduction and summary	1
1.1	Spin Impurities	3
1.2	Wilson Lines in Large Representations	9
1.3	Structure of the paper	10
2	Spin defects at large s in free theory	10
2.1	Setup	10
2.2	Diagrammatic results	12
2.2.1	Perturbation theory and the beta function	12
2.2.2	The g -function and the breakdown of perturbation theory at large s	15
2.3	Semiclassics and the double-scaling limit	18
2.3.1	General considerations	18
2.3.2	The nonlocal theory on the line and the saddle-point	20
2.3.3	The one-point function of ϕ_a^2 and the phase diagram	22
2.3.4	The g -function	28
3	Spin defects at large s: the interacting theory	31
3.1	Setup	31
3.2	Diagrammatic results	32
3.3	The all-orders structure of perturbation theory	34
3.4	The phase diagram in $4 - \varepsilon$ dimensions	36
3.5	Large spin impurity as a pinning field	38
3.5.1	An interpretation of the small ε results for large s	38
3.5.2	Equivalence with the pinning field defect at large s	39
3.5.3	Subleading corrections	43
4	Wilson lines in large representations	46
4.1	Comments about non-supersymmetric Wilson lines in large representations	46
4.2	Supersymmetric Wilson loop in $\mathcal{N} = 2$ SCFTs	48
A	Details of the diagrammatic calculations in free theory	55
A.1	One-loop contribution to the one-point function	55
A.2	Two-loop contribution to g_γ for the bulk free theory	56
B	Details of the semiclassical calculations in free theory	57
B.1	The $1/s$ corrections to the one-point function of ϕ_a^2 close to four dimensions	57
B.2	Calculation of the \tilde{f}_0 function	59

C	Running from the classical profile for the defect coupling in the $O(3)$ model	62
C.1	Beta function in the physical renormalization scheme	62
C.2	Analytic results on the semiclassical beta function	64
C.3	Beta function in the interacting $O(3)$ model in dimensional regularization	67

1 Introduction and summary

The study of line defects (i.e. one-dimensional defects) in critical conformal bulk theories is of fundamental importance to the study of Quantum Field Theory (QFT). Line defects have a variety of applications ranging from condensed matter and statistical physics, such as models of magnetic impurities in metals and magnets [1, 2], to high energy physics, such as Wilson and 't Hooft lines in four-dimensional gauge theories [3, 4]. Studies of the Kondo problem, which emerged from models of impurities in two-dimensional systems, led to remarkable progress in the study of the renormalization group, as well as to developments in integrability; see [5] for a review.

Even if the bulk is tuned to a critical point, i.e. a conformal field theory (CFT), it is well known that line operators can undergo a nontrivial defect RG flow, which generically leads to a critical line at long distances. In two dimensions, Affleck and Ludwig conjectured that a renormalization group flow on a line defect leads to $g_{\text{UV}} \geq g_{\text{IR}}$, where g_{UV} (g_{IR}) refers to the universal part of the defect free energy in the UV (IR) [6]. This was subsequently proven in [7, 8]. A generalization of this statement to line defects in bulk CFTs of arbitrary number of spacetime dimensions d was recently obtained in [9]. This was done by identifying the following scheme-independent quantity

$$s_D = \left(1 - R \frac{\partial}{\partial R}\right) \log g(MR), \quad (1.1)$$

where R is the radius of the circular line defect, and M is a mass scale associated with the RG flow on the defect. The defect g -function $g(MR)$ is formally defined as the partition function of the full theory normalized by the partition function of the bulk theory without the defect. The above quantity s_D in eq. (1.1), which is referred to as the *defect entropy*, monotonically decreases under a defect RG flow and hence must obey the inequality $g_{\text{UV}} \geq g_{\text{IR}}$ for line defects in any number of spacetime dimensions d .

In quantum critical models, point-like impurities in space at zero temperature can be thought of as one-dimensional defects in spacetime. In this way the study of line defects in CFTs makes contact with the study of the phases of impurities in condensed matter.

The class of models of interest to us here are bulk models with global symmetry $SO(3)$ where an impurity in the spin s representation is present and interacts with the bulk in an $SO(3)$ invariant fashion, see figure 1. Models in this family are particularly interesting due to

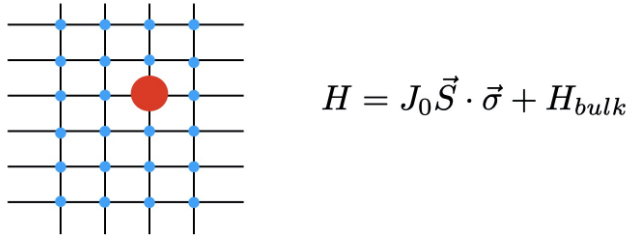


Figure 1: An impurity of spin s under $SO(3)$ interacts with the $SO(3)$ symmetric bulk. The operators \vec{S} are the spin s representation of $so(3)$ while the operators $\vec{\sigma}$ are the bulk spins (typically in the spin 1/2 representation) of the nearest neighbors and the bulk Hamiltonian H_{bulk} is tuned to a critical point.

their relation with magnets in three spacetime dimensions. Indeed, lattice realizations of $SO(3)$ bulk critical points are known and the insertion of a spin s impurity is rather straightforward to implement. Such spin s impurities are sometimes referred to as magnetic impurities but we will refer to them as spin impurities throughout this manuscript.

An interesting question concerning spin impurities is about their infrared behavior. Since the effective coupling on the impurity grows towards the infrared this is a very difficult problem in three spacetime dimensions. The main focus of this paper is to solve this problem in the large spin limit $s \gg 1$. This limit can be taken, of course, in any number of dimensions $3 \leq d \leq 4$, but it goes without saying that the most interesting case for the experimental setting is $d = 3$.

In a different context, several works focused on the study of conformal gauge theories in the presence of line operators, especially in supersymmetric theories (see e.g. [10–12] and references therein). Building on some remarkable similarities with the description of large spin impurities, in this work we will address the large representation limit of supersymmetric Wilson lines in $\mathcal{N} = 2$ superconformal gauge theories, that is 1/2-BPS Wilson loops in which the size s of the labeling representation becomes large.

It has been recently become clear that the bulk physics of CFTs simplifies when various quantum numbers are taken to be large.¹ A natural question which arises in this context is whether any simplification occurs for line defects with large quantum numbers and in particular for spin impurities in the large s limit.

We will show that indeed vast simplifications occur for impurities with large spin and, furthermore, we will see that similar simplifications occur in the context of supersymmetric Wilson lines in the large representation limit. The sections about Wilson loops and the spin impurities can be read independently of each other.

Let us now state briefly our main results before describing the setup in more detail.

¹Examples include CFTs in the regimes of large scaling dimensions [13–15], large spin [16–18] and large global charges [19–21].

- For the large s limit of spin impurities in the $O(3)$ Wilson Fisher model, we find a description which becomes increasingly more useful as $s \rightarrow \infty$. The description consists of two sectors, which are weakly interacting with each other: a quantum mechanical sector with S^2 target space and a first-order kinetic term, and another sector with no free parameters, which describes a previously studied conformal defect called the “pinning field defect” or “localized magnetic field defect” [22, 23]. While the pinning field defect is a strongly coupled conformal defect, some properties of it are known exactly and many others are known approximately. An example of an unexpected prediction that stems from this analysis is that there exists a primary defect operator in the vector representation of $SO(3)$ which is nearly marginal $\Delta_{\text{vector}} = 1 + O(\frac{1}{s})$. Another prediction is that the dimension of the lightest $SO(3)$ singlet should be approximately $\Delta_{\text{singlet}} \simeq 1.55$. Finally, we predict that the spin operator S on the defect, which acts on the defect Hilbert space, has dimension $\Delta_S \sim 1/s^2$.
- The second subject of this paper is 1/2-BPS Wilson lines in four-dimensional rank-1 $\mathcal{N} = 2$ SCFTs in a large representation of the gauge group. (This setup also makes sense for non-Lagrangian theories, as we later explain.) Here we argue that the large s limit leads to physics on the Coulomb branch. $1/s$ corrections are captured by higher derivative terms on the Coulomb branch. This allows us to make some universal predictions. For instance, for the g function of such line operators we find

$$\log g = \frac{g_{\text{CB}}^2 s^2}{4} + 4\Delta a \log s + O(s^0) . \quad (1.2)$$

where $\Delta a = a_{\text{UV}} - a_{\text{IR}}$ is the difference of the a -anomalies between the ultraviolet and the Coulomb branch² and g_{CB} is a parameter in the effective theory that is model-dependent. Interestingly, the g function of the 1/2-BPS Wilson loops grows exponentially fast as $s \rightarrow \infty$ (1.2) while for the spin impurities the g function grows only linearly as $s \rightarrow \infty$. We verify some of the predictions of the Coulomb branch effective theory, including (1.2), with localization (for Lagrangian theories).

We now delve into a more detailed summary of the content of the paper.

1.1 Spin Impurities

We will consider two different scenarios of bulk theories with $O(3)$ global symmetry: a free field theory with global $O(3)$ symmetry, and the interacting $O(3)$ Wilson-Fisher model [24–26].

In both cases, we will consider the theory in the presence of the following line defect operator:

$$D_s = \text{Tr}_{2s+1} \left[P \exp \left(\gamma_0 \int d\tau \phi \right) \right] , \quad (1.3)$$

²We work in units such that an Abelian free vector multiplet contributes with $a_{\text{VM}} = 5/24$ and a free Hypermultiplet with $a_{\text{HM}} = 1/24$.

where ϕ_a is the bulk scalar field ($a = \{1, 2, 3\}$), $\phi = \phi_a T^a$, and the matrices $\{T^a\}$ form a $2s + 1$ dimensional irreducible representation of the $su(2)$ algebra. Such a setting describes a spin s impurity inserted into a lattice site in the critical bulk and interacting with the bulk in an $SO(3)$ -invariant fashion, as in figure 1. The parameter γ_0 is a coupling constant and it is relevant for $d < 4$. We will see that for $d = 4$ it is marginally irrelevant for all s .

Even in the case of a free bulk theory, we cannot at present solve the model with the defect (1.3) for arbitrary number of dimensions and arbitrary s . The complication lies in the path-ordering in eq. (1.3) that makes the diagrammatic expansion rather intricate due to the appearance of an increasing number of commutators between $su(2)$ matrices at each order in perturbation theory.

The limit we will focus on in this paper is the $s \gg 1$ limit. Understanding the large s behavior of the defect QFT in both the free bulk case and the interacting $O(3)$ Wilson-Fisher bulk case will be our main goal throughout sections 2 and 3. Roughly speaking, the impurity backreacts on the bulk substantially and a new saddle-point emerges at large s . Then a new effective scale for quantum fluctuations emerges $s^{-1} \sim \hbar$. We will see that this intuition is partially true, indeed.

Several previous works already studied spin impurities in free theories and the $O(3)$ WF model [1, 2, 27–32].³ Of particular relevance for us are [1, 2, 27], that initiated the study of impurities from the field-theoretical viewpoint within the ε expansion. We also mention the Quantum Monte Carlo analysis of [30] for $s = 1/2$ impurities. No prior work addressed the large spin limit to our knowledge.

While this paper is focused on the spin impurities, there are various other interesting defects in the $O(N)$ model. For instance, the effect of a magnetic field localized in space, a setup which is particularly relevant for Monte Carlo simulations [38], was considered in [22, 23, 39, 40]. The line defect that describes a localized magnetic field will be referred to as the “pinning field defect QFT” (DQFT). The infrared conformal defect, when it exists, is referred to as the “pinning field DCFT.” Perhaps surprisingly, the results of these works, in particular of [23], will play an important role in our analysis later on. We will briefly review it in due course. Symmetry (twist) defects (which are not genuine line defects, since they are attached to a nontrivial topological surface) were considered in [41–45]. Finally, let us mention that the multi-channel Kondo problem has a rich set of various large N and large representation limits [5, 46–48].

³See also [33–37] and references therein for other field-theoretical studies of impurities in different models.

Free bulk In sec. 2 we discuss the defect (1.3) for a free scalar triplet. For any given fixed s , the model can be studied in $d = 4 - \varepsilon$ spacetime dimensions with $\varepsilon \ll 1$. In the limit where ε is the smallest parameter, the model admits an IR stable perturbative fixed point, that was studied in [2, 27].

As we will explain in detail in section 2.2, the perturbative expansion breaks down for sufficiently large spin, when $s \gtrsim 1/\varepsilon$. In section 2.3, we find that the model can be solved in a semiclassical expansion in powers of $1/s$ for arbitrary values of the spacetime dimensions d . Using this approach, we are able to chart the phases of the line defect (1.3). Let us now summarize our main findings:

- For $\varepsilon = 4 - d \ll 1$, the theory can be studied perturbatively in the double-scaling limit $s \gg 1$ with $\gamma_0^2 s = \text{fixed}$. This regime includes the perturbative fixed point mentioned above, which occurs at any fixed s for sufficiently small ε . However we find a richer phase diagram. For $\varepsilon s < 1/\pi$ we find two fixed points, one of which is novel and non-perturbative in the standard approach. For $\varepsilon s > 1/\pi$ we argue instead that no infrared fixed point exists and the defect g -function approaches zero in the IR, similarly to the free theory example discussed in [23]. The approach of g to zero means that the flow does not terminate in a healthy conformal defect in the infrared and instead one finds a certain runaway behavior. This is presumably only possible because the theory of a free triplet of scalars has a moduli space of vacua.
- For $\varepsilon = 4 - d$ fixed, the model can also be studied in a $1/s$ expansion, which is similar in spirit to the usual large N expansion for the $O(N)$ models [49] in the sense that s becomes effectively $1/\hbar$. We find that there is no fixed point in the IR in this limit for any finite $\varepsilon > 0$, and thus the flow never terminates in a DCFT. This result also applies to the large s limit of the theory in $d = 3$ spacetime dimensions.

The phase diagram of the theory is summarized in figure 2, where we colored blue the region of the (d, s) plane that we could analyze with our methods.

To further clarify the phase diagram we propose, let us give a “numerical” example: Consider for instance the case with spin $s = 10$ (corresponding to the purple dotted line in fig. 2). For $3 \leq d < d_c \simeq 3.97$ we expect no infrared DCFT to exist, and instead the flow from the trivial fixed point should never terminate and the defect entropy s_D would tend to $-\infty$ in the infrared. At some critical $d_c \simeq 3.97$ a nontrivial infrared fixed point would emerge.⁴ This infrared fixed point has a smaller defect entropy s_D than the trivial fixed point. It has an operator which is marginally relevant if added with one sign and marginally irrelevant if added with the other sign. For $d_c < d < 4$ there exist two fixed points, where one of them is continuously connected to the perturbative fixed point and is stable in the infrared for $SO(3)$ symmetric perturbations. The other fixed point has an $SO(3)$ invariant relevant operator, and has an increasingly large defect coupling as $d \rightarrow 4$, which is why it is non-perturbative. At

⁴Such a merger of a stable and unstable fixed points and disappearance to the complex plane is the standard situation, where Miransky scaling arises [50–52].

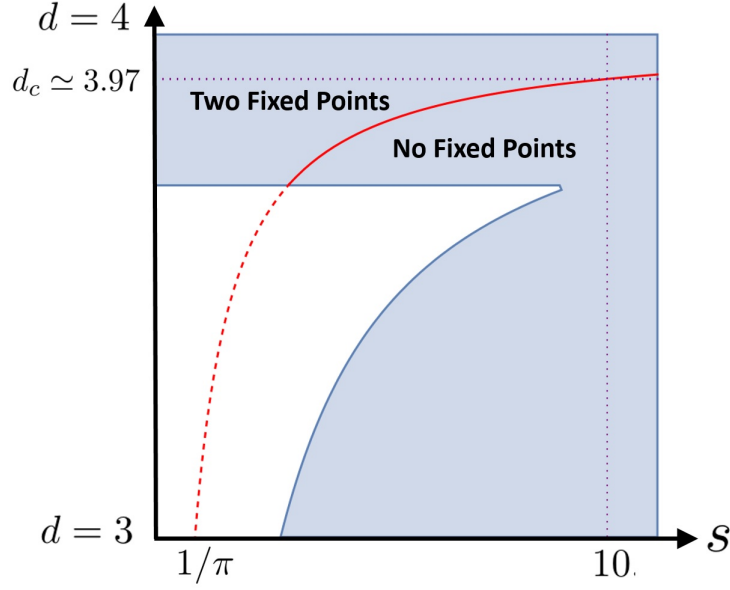


Figure 2: Phase diagram of the impurity (1.3) in a free bulk theory. The blue shaded region is the one that we could reliably study with our methods. The red solid line separates the region in which the theory admits two fixed points from the one in which the RG flow never terminates in a DCFT. The red dashed line is its *naive* extrapolation in the region that we do not control with present techniques. Notice that the extrapolation suggests that all physical impurities ($s \geq 1/2$) in $d = 3$ have no stable fixed points. Finally, the purple dotted lines refer to the numerical example for $s = 10$ in the main text.

$d = 4$ the latter fixed point drifts to infinite coupling while the former fixed point merges with the trivial fixed point.

As we said, for any fixed $3 \leq d < 4$, at large enough s , the flow never terminates in a healthy conformal infrared defect. We find that this runaway behavior is analogous to the one which is obtained considering the pinning field defect $\delta S \propto \int d\tau \phi_1$ in the free theory, see [23]. Also in that case, the defect renormalization group (DRG) flow never terminates, and the defect entropy s_D tends to $-\infty$ in the infrared. In fact, we will argue that to leading order in $1/s$, correlation functions of $SO(3)$ invariant operators in the presence of the defect (1.3) coincide with the ones in the presence of the pinning field defect. This relation between the large s limit of the spin impurity and the pinning field defect (which is a theory with no free parameters) will be especially useful in the interacting $O(3)$ model.

It is tempting to conjecture that in 3d the DRG flow never terminates in a healthy DCFT in the IR also for $s = O(1)$. At present, we can only prove this in a $1/s$ expansion.

The recent general results of [53, 54] guarantee that free scalar theories in $d = 3$ do not admit any nontrivial DCFT. This implies that the perturbative fixed points observed in the epsilon expansion cannot be extrapolated to $\varepsilon = 1$ also for small values of s . This is consistent

with the DRG runaway behavior we find at large s .⁵ Let us reiterate that we expect the runaway DRG behavior to be related to the existence of a moduli space of vacua in the bulk.

Interacting bulk In sec. 3 we consider the impurity (1.3) with an interacting $O(3)$ Wilson-Fisher bulk theory with potential $\lambda(\phi_a^2)^2$. For $d < 4$, both the bulk and the defect couplings are relevant, so that the physical three-dimensional model is strongly coupled in the IR.

The simplest approach is to perform a perturbative analysis for small $\varepsilon = 4 - d$ for finite values of $s = O(1)$ (see e.g. [1, 2, 28, 29]). In this limit it was found that, tuning the bulk to the critical point, the defect coupling admits a nontrivial IR stable fixed point for which $\gamma_*^2 \sim \lambda_* \sim \varepsilon$. This fixed point is analogous to the one mentioned at the beginning of sec. 1.1 for the free theory with $O(3)$ symmetry.

We are interested in the phases of this impurity for arbitrary s , including $s \gg 1$. As in the previous section, we should not trust the small ε expansion and some resummation is required in order to understand the phase diagram.

The central questions we would like to address are whether the theory admits new fixed points beyond the one seen in perturbation theory and whether the large s limit of the impurity in three spacetime dimensions can be understood. A particularly important point is that, unlike the free theory, the bulk interacting theory does not have a moduli space of vacua due to the potential $(\phi_a^2)^2$. Therefore, one should not expect an instability and consequently we do expect a healthy DCFT in any $3 \leq d < 4$ for any s .⁶

Our main results are the following:

- The model can be studied for all s as long as we have $d = 4 - \varepsilon$ with $\varepsilon \ll 1$. For fixed small s this can be accomplished using a standard perturbative analysis, while for $s \gtrsim \varepsilon^{-2}$ a resummation is required. We are able to achieve this resummation and obtain results that are trustworthy for all s using a new semiclassical limit, which allows to reorganize the perturbative series and to make non-perturbative statements at large s . (In particular, in this semiclassical limit, various terms in the beta function are obtained from the solution of a *classical* differential equation.)
- There is a unique nontrivial zero of the beta function for all values of s , describing an IR stable fixed point. A major simplification occurs for $s \rightarrow \infty$ for all d , including both $d \rightarrow 4$ and also for $d = 3$ which is the most interesting case experimentally. The prediction is that for $s \rightarrow \infty$ the theory breaks up into a weakly-decoupled sector of fluctuations with target space S^2 and a special DCFT that was studied before [22, 23, 39, 40] called hereafter the pinning field DCFT.

⁵In principle, it could be that the DRG for $s = O(1)$ in $d = 3$ terminates in a decoupled line defect, such as one with $s_{\text{IR}} < s$. This is why the case of $s = O(1)$ in $d = 3$ is not yet entirely settled, however, given the results about large s and fixed d and the results about the double scaling limit, it is reasonable to expect that the DRG flow for $s = O(1)$ in $d = 3$ indeed never terminates.

⁶One can hope that there exist rigorous lower bounds on s_D in $d > 2$ theories with no moduli space of vacua. See [55, 56] for results in $d = 2$.

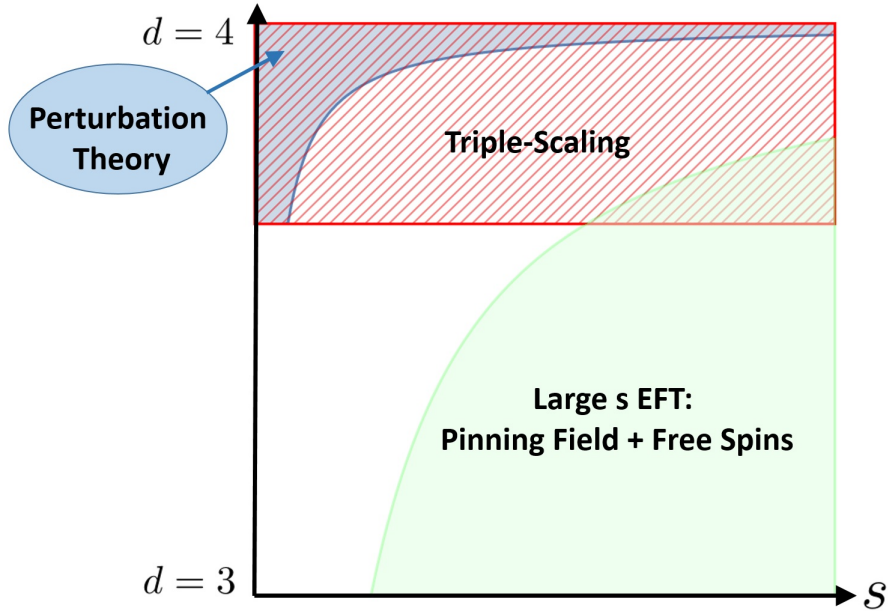


Figure 3: Regimes of applicability of different methods to capture the nontrivial DCFT fixed point of the spin impurity (1.3) in the $O(3)$ WF model. We expect that this DCFT exists for all d and s . The blue region corresponds to the standard ε expansion, the red hatched region to the new semiclassical resummation method, and the green region to an effective field theory (EFT) involving the pinning field DCFT weakly coupled to a first-order S^2 sigma model.

- We are able to verify this prediction for the large s limit of the spin impurity within the ε expansion. Additionally, we present the consequences of this prediction for the physically interesting case $d = 3$, including a determination of the scaling dimensions of certain operators, as well as some other observables. These predictions for $d = 3$ should be in principle testable.
- Finally, the nearly-decoupled sector of fluctuations with target space S^2 and the pinning field DCFT do couple to each other at finite large s , leading to some $1/s$ corrections to observables. We determine the leading coupling and use it to compute the anomalous dimension of the spin operator on the defect.

In fig. 3 we summarize the validity regimes of the various approaches, namely standard perturbation theory, the resummed ε expansion that we introduce, and the *effective* description that we propose in terms of the pinning field defect and a weakly coupled sector. As fig. 3 clearly shows, there are overlapping regimes between the different approaches. As a nontrivial benchmark of our ideas, we will verify explicitly the agreement between the different approaches in these regions.

1.2 Wilson Lines in Large Representations

The line defect (1.3) representing an impurity is remarkably similar to the familiar presentation of Wilson lines in gauge theories. It is therefore natural to wonder if ideas analogous to those discussed in the previous section can be applied to Wilson lines in large representations of the gauge group. In this paper we analyze in detail the case of 1/2-BPS Wilson lines in $\mathcal{N} = 2$ superconformal field theories (SCFTs) in four dimensions. For concreteness, we focus on rank-1 theories.⁷

1/2-BPS Wilson loops in $\mathcal{N} \geq 2$ superconformal field theories (SCFTs) are among the most studied examples of DCFTs in the literature [61–77] (for a general approach to supersymmetric line defects in diverse dimensions see [11, 12]). Notice that, in general, the large representation limit is of interest also for the study of non-Lagrangian theories, in which case superconformal defects are roughly labeled by the electric and magnetic charges of their IR representative in the Coulomb branch of the theory [68, 70, 74]. Importantly for us, localization techniques allow for exact predictions for certain supersymmetric observables [67, 78].

Analogously to the large s limit of the impurity in the free $O(3)$ model, the analysis of Wilson lines in large representations is carried out by identifying a new saddle-point. As a reminder, in Lagrangian theories, the 1/2-BPS loops includes both the gauge and scalar components of the vector multiplet:

$$D_s^{\text{BPS}} = \text{Tr}_{2s+1} \left[P \exp \left(\int_{\mathcal{C}} dt (i\dot{x}^\mu A_\mu + |\dot{x}| \Phi) \right) \right]. \quad (1.4)$$

Therefore, for $s \gg 1$, we expect that the classical trajectory dominating the path integral is characterized by a large scalar profile $\Phi \sim s$ and by a large Coulomb potential $A \sim s$. In particular the VEV of the scalar sets the largest gauge invariant scale. That the scalar field VEV is more important than the electric field is of crucial importance and this is what allows to reduce the problem to physics on the Coulomb branch. We therefore propose that the saddle-point and its fluctuations are *universally* described by the effective field theory (EFT) description for the theory on its Coulomb branch. In particular, we expect that the EFT description applies to all rank-1 SCFTs.

We use the EFT to compute several DCFT observables in a $1/s$ expansion. We consider in particular the g -function of the theory and the coefficient h_D of the one-point function of the stress-tensor. The result depends on a Wilson coefficient g_{CB} , identified with the IR gauge coupling, and on the difference in the “ a ”-conformal anomaly between the CFT and the Coulomb branch contribution as quoted in (1.2). We additionally find a general relation between h_D and $\log g$, that we conjecture to hold to all orders in the $1/s$ expansion. We also compare our findings with exact results from localization in Lagrangian theories, finding perfect agreement.

⁷For a complete classification of rank-1 $\mathcal{N} = 2$ SCFTs see [57–60].

1.3 Structure of the paper

The rest of this paper is organized as follows. In section 2 we study the spin impurity theory in the free bulk case in the large s regime. In section 3 we study the impurity theory in the interacting $O(3)$ Wilson-Fisher bulk case in the large s regime. In section 4 we study the large representation limit of 1/2-BPS Wilson lines in rank-1, $\mathcal{N} = 2$ superconformal field theories, and construct the EFT description explained above. Section 4 can be read without reading sections 2 and 3. In appendix A, technical details associated with the diagrammatic calculations of section 2 are given. Appendix B contains technical details related to the semiclassical calculations of section 2. In appendix C we obtain the four-dimensional beta function for the defect coupling in the interacting bulk theory studied in section 3 from the classical saddle-point equations.

Note added: while we were completing this work, we were informed of the upcoming paper [79], whose results overlap with part of our section 2. In particular, [79] also analyzes a model equivalent to the spin s impurity in free theory in the double-scaling limit $\gamma_0 \rightarrow 0$, $s \rightarrow \infty$ with $\gamma_0^2 s = \text{fixed}$. We are grateful to the authors for sharing with us a preliminary version of their draft.

2 Spin defects at large s in free theory

2.1 Setup

In this section we consider a free, massless $O(3)$ -symmetric scalar field theory in d spacetime dimensions. The bulk action is given by the free, massless action in flat space:

$$S_{\text{bulk}} = \frac{1}{2} \int d^d x (\partial \phi_a)^2, \quad (2.1)$$

where $a = \{1, 2, 3\}$, $(\partial \phi_a)^2 = \partial_\mu \phi_a \partial^\mu \phi_a$, and μ stands for spacetime indices, $\mu = 1, \dots, d$. As was explained in the introduction, we couple the free bulk theory to a line defect, physically representing an impurity in the spin s representation of the bulk global $SO(3)$ symmetry. This is achieved by adding the following line operator to the partition function:

$$D_s = \text{Tr}_{2s+1} \left[P \exp \left(\gamma_0 \int d\tau \phi \right) \right], \quad (2.2)$$

where γ_0 is the bare coupling, and, as was explained in sec. 1.1, $\phi = \phi_a T^a$ and $\{T^a\}$ are the $2s + 1$ dimensional representation of the $su(2)$ algebra. The defect worldline is parametrized by the embedding $x^\mu = x^\mu(\tau)$, where τ is a normalized affine parameter such that $|dx/d\tau| = 1$.

We will be interested both in circular and linear defects throughout this section. An equivalent representation of the defect in eq. (2.2) can be given in terms of a bosonic $su(2)$ spinor $z = \{z_1, z_2\}$ on the line, subject to the constraint $\bar{z}z = 2s$. In this formulation, the

total action (bulk and defect) of the defect quantum field theory (DQFT) reads (see e.g. [80])⁸

$$S = \frac{1}{2} \int d^d x (\partial \phi_a)^2 + \int_D d\tau \left[\bar{z} \dot{z} - \gamma_0 \bar{z} \frac{\sigma^a}{2} z \phi_a \right], \quad \bar{z} z = 2s. \quad (2.3)$$

The action (2.3) is invariant under $U(1)$ gauge transformations $z \rightarrow e^{i\alpha(\tau)} z$, which makes the target space into the two sphere. The canonical commutation relations imply that the operators $\{S^a = \bar{z} \frac{\sigma^a}{2} z\}$ satisfy the $su(2)$ algebra $[S^a, S^b] = i\epsilon^{abc} S^c$, while the constraint implies $S^a S^a = s(s+1)$, so that the worldline Hilbert space indeed corresponds to that of a spin s representation of $su(2)$. Since the kinetic term of z is first order in derivative, eq. (2.2) is just the evolution operator of the worldline variable. This proves the equivalence between the action (2.3) and the expectation value of the operator (2.2).

For future purposes, it is important to comment on the ordering in the definition of S^a . The variables \bar{z} and z form a canonical pair, and therefore do not commute. It turns out that the correct definition of the composite spin operator is obtained via the following point-splitting procedure (see e.g. [80, 83, 87] for similar discussions):

$$S^a(\tau) = \left(\bar{z} \frac{\sigma^a}{2} z \right) (\tau) \equiv \lim_{\eta \rightarrow 0^+} \bar{z}(\tau + \eta) \frac{\sigma^a}{2} z(\tau). \quad (2.4)$$

In terms of the path integral, such a definition prevents any issues with singularities at coincident points. The ordering in eq. (2.4) ensures that $\langle S^a(\tau) S^a(\tau') \rangle = s(s+1)$ for $\gamma_0 = 0$, as required.⁹

As was mentioned in the introduction, the coupling γ_0 is relevant for $d < 4$, and we will see that it is marginally irrelevant for $d = 4$. We are implicitly fine tuning to zero a defect cosmological constant term in the action (2.3). Note also that there are no wavefunctions renormalizations for the fields in the action (2.3). For ϕ this is obvious since it is a free field. For z this is because a nontrivial wavefunction renormalization factor would contradict the $U(1)$ gauge invariance. To see this it is convenient to promote the sliding scale to a spurionic function of the defect coordinate, $M = M(\tau)$, which transforms trivially under the action of the gauge group. Since the kinetic term for z is only invariant up to a total derivative under $U(1)$ gauge transformations, the coefficient of $\bar{z} \dot{z}$ cannot depend on the sliding scale $M(\tau)$, and it is therefore not renormalized at the quantum level.¹⁰

Our main findings which arise from the analysis presented in this section, including the phase diagram of the model, were already summarized in the introduction part of this paper (see sec. 1.1). In addition, we would like to comment that the results of this section will also prove useful at a technical level, as a warm-up for the analysis of a large spin impurity in the interacting $O(3)$ Wilson-Fisher fixed point.

⁸Similar actions to (2.3) have been studied in several different contexts, see e.g. [81–83]. In particular, the constrained spinor z is equivalent to a charged particle moving on a sphere with a charge s monopole at the center in the lowest Landau level [84–86].

⁹To verify this assertion, it is important to use the constraint in the form $(\bar{z} z)(\tau) = \lim_{\eta \rightarrow 0^+} \bar{z}(\tau + \eta) z(\tau) = 2s$.

¹⁰This result is similar to the nonrenormalization of the Chern-Simons term [88].

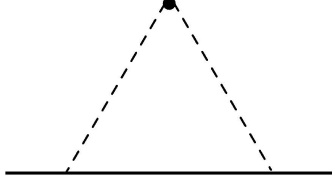


Figure 4: Diagram that contributes the leading order term in the one-point function $\langle \phi_a^2(x) \rangle$. Dashed lines represent bulk scalar field propagators. The solid line represents the defect.

This section is organized as follows. In section 2.2 we review the diagrammatic analysis of the theory in $d = 4 - \varepsilon$. The results will be useful later on when matching between results obtained by the semiclassical analysis with those obtained using standard perturbative techniques in their overlapping regime of validity at weak coupling. In section 2.3 we study the model in the large s limit. We will calculate various quantities, including the defect g -function and, for $\varepsilon \ll 1$, the β function associated with the defect coupling.

2.2 Diagrammatic results

2.2.1 Perturbation theory and the beta function

In this section we review the standard diagrammatic approach by considering the calculation of the one-point function of the operator ϕ_a^2 in the presence of a straight line defect. We focus on the regime of small $\varepsilon = 4 - d$ where the coupling is only weakly relevant and the full flow can be studied perturbatively. This will also allow us to extract the beta function of the renormalized coupling γ .¹¹

To calculate the one-point function of ϕ_a^2 , it is convenient to work in coordinates $x^\mu = (\mathbf{x}, \tau)$ with the defect located at $x^i = 0$, where $i = 1, \dots, d - 1$. The propagator of the free scalar is given by

$$\langle \phi_a(x) \phi_b(0) \rangle_{\gamma_0=0} = \delta_{ab} G(x), \quad G(x) \equiv \frac{1}{(d-2)\Omega_{d-1}} \frac{1}{(x^2)^{\frac{d-2}{2}}}, \quad (2.7)$$

where $\Omega_{d-1} = \frac{2\pi^{d/2}}{\Gamma(d/2)}$ is the volume of the $d - 1$ -dimensional sphere. Working with the representation (2.2) of the defect, the leading contribution to the one-point correlation function

¹¹As usual, the coupling is renormalized according to:

$$\gamma_0^2 = M^\varepsilon \left[\gamma^2 + \frac{\delta\gamma^2}{\varepsilon} + \frac{\delta_2\gamma^2}{\varepsilon^2} + \dots \right], \quad (2.5)$$

where M is the sliding scale and γ is the renormalized coupling constant. We work in the minimal subtraction scheme (MS) to one-loop order, for which only $\delta\gamma^2$ is non-vanishing, and the beta function can be extracted by requiring that γ_0^2 is independent of the sliding scale. This yields [89]:

$$\beta_{\gamma^2} = -\varepsilon\gamma^2 + \gamma^2 \frac{d\delta\gamma^2}{d\gamma^2} - \delta\gamma^2. \quad (2.6)$$

$\langle \phi_a^2(x) \rangle$ arises at order γ_0^2 from the diagram in fig. 4. It reads:¹²

$$\begin{aligned} \langle \phi_a^2(\mathbf{x}, 0) \rangle &\simeq \gamma_0^2 \frac{\text{Tr}[T^a T^a]}{2s+1} \left[\int d\tau G(x - x(\tau)) \right]^2 = \frac{\gamma_0^2 s(s+1)}{16\pi^{d-1} |\mathbf{x}|^{2d-6}} \Gamma\left(\frac{d-3}{2}\right)^2 \\ &\stackrel{d=4}{=} \frac{\gamma_0^2 s(s+1)}{16\pi^2 \mathbf{x}^2}, \end{aligned} \quad (2.8)$$

where we used $T^a T^a = s(s+1)$.

The first correction to the tree-level result (2.8) in four dimensions is given by the diagrams displayed in figure 5. After some matrix algebra only the diagrams in figs. 5d and 5e remain, giving:

$$\begin{aligned} (\text{1-loop}) &= -4\gamma_0^4 s(s+1) \int_{\tau_1 > \tau_2 > \tau_3 > \tau_4} d^4[\tau] G(x - x(\tau_1)) G(x(\tau_2) - x(\tau_3)) G(x - x(\tau_4)) \\ &= -\frac{1}{\varepsilon} \frac{\gamma_0^4 s(s+1)}{32\pi^4 \mathbf{x}^2} + O(\varepsilon^0). \end{aligned} \quad (2.9)$$

The evaluation of the integral in eq. (2.9) is detailed in appendix A.1.

Requiring that the one-point function $\langle \phi_a^2(\mathbf{x}, 0) \rangle$ is finite for $\varepsilon \rightarrow 0$ we obtain the counterterm $\delta\gamma^2 = \gamma^4/(2\pi^2)$ and the one-loop beta function for the physical coupling γ^2 (see footnote 11 for our conventions)

$$\beta_{\gamma^2} = -\varepsilon\gamma^2 + \frac{\gamma^4}{2\pi^2} + O(\gamma^6). \quad (2.10)$$

Eq. (2.10) is in agreement with previous studies in the literature [27, 28], and it implies the existence of a perturbative IR stable fixed point at

$$\gamma_*^2 = 2\pi^2\varepsilon + O(\varepsilon^2). \quad (2.11)$$

Note that the coupling γ is marginally irrelevant in four dimensions so the free DCFT with decoupled $2s+1$ states is attractive in $d=4$. For $0 < \varepsilon \ll 1$ sufficiently small, for any fixed s , we get a nontrivial infrared DCFT.

We also report the result for the one-point function to one-loop order:

$$\begin{aligned} \langle \phi_a^2(\mathbf{x}, 0) \rangle &= \frac{\mathcal{N}_d}{\mathbf{x}^{d-2}} \frac{\gamma^2 s(s+1)}{4\sqrt{6}} \left\{ 1 + \varepsilon \left[\log(4M|\mathbf{x}|) + \frac{1}{2}(\gamma_E + \log \pi) \right] \right. \\ &\quad \left. - \gamma^2 \frac{2\log(M|\mathbf{x}|) + \gamma_E + 2 + \log 4\pi}{4\pi^2} + O(\gamma^4, \gamma^2\varepsilon, \varepsilon^2) \right\}, \end{aligned} \quad (2.12)$$

where γ_E is the Euler constant and \mathcal{N}_d is the normalization of the bulk two point-function without the defect:

$$\langle \phi_a^2(x) \phi_a^2(0) \rangle = \frac{\mathcal{N}_d^2}{x^{2d-4}}, \quad \mathcal{N}_d = \frac{\sqrt{6}}{(d-2)\Omega_{d-1}}. \quad (2.13)$$

¹²Here and in the following all correlation functions are normalized by the expectation value of the unit operator in the presence of a straight line defect. The expectation value of the unit operator is $2s+1$ up to order γ_0^4 , which is all we shall use for the results in the main text.

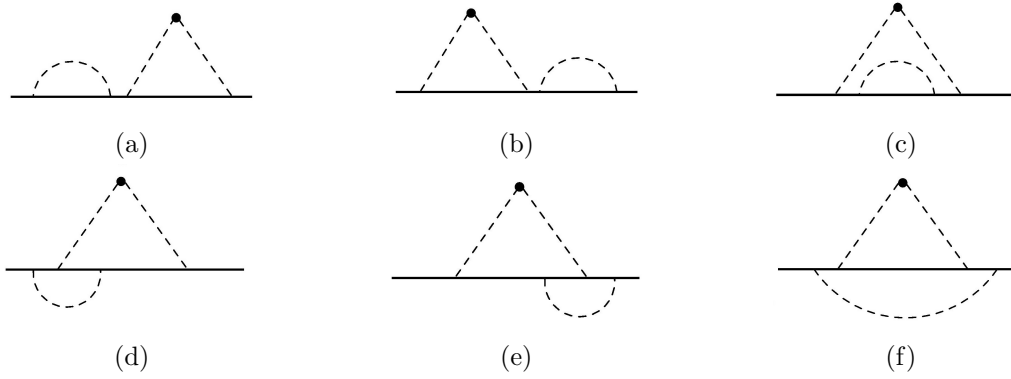


Figure 5: Diagrams contributing the next to leading order terms in the one-point function $\langle \phi_a^2(x) \rangle$.

At the infrared fixed point this implies the result:

$$\langle \phi_a^2(\mathbf{x}, 0) \rangle = \frac{\mathcal{N}_d}{\mathbf{x}^{d-2}} \frac{\pi^2 s(s+1)\varepsilon}{2\sqrt{6}} \left[1 - \varepsilon(1 - \log 2) + O(\varepsilon^2) \right]. \quad (2.14)$$

We will later see that the various higher order corrections that we have neglected in (2.12) and (2.14) are enhanced by powers of s for $s \gg 1$ and can become important if ε is not the smallest parameter in the problem.

Further perturbative results involving this defect, including the two-loop beta function and various thermal susceptibilities, can be found in [2, 27]. In particular in [2] it was argued diagrammatically that the defect spin operator S^a has exactly scaling dimension $\Delta_S = \varepsilon/2$, without further corrections. Let us briefly comment on an alternative proof of this fact which relies on the representation (2.3) of the defect. To this aim, notice that the bulk theory, besides the $su(2)$ currents, has three dimension $d/2$ conserved currents $J_{\text{shift}}^{\mu a} = -\partial^\mu \phi_a$ associated with the invariance under shifts of the scalars. This symmetry is explicitly broken at the defect. Indeed from eq. (2.3) we see that the bulk Ward identity is modified to

$$\partial_\mu J_{\text{shift}}^{\mu a} = \gamma_0 S^a \delta_D^{d-1}, \quad (2.15)$$

where δ_D^{d-1} is a delta function localized at the defect. Since the bulk current has protected dimension, the Ward identity (2.15) implies that at the fixed point the scaling dimension of S^a is $\Delta_S = \varepsilon/2$.¹³

¹³Defect operators which appear in Ward identities for internal symmetries broken by the defect are sometimes called *tilt* operators. The arguments about tilt operators having protected dimension date back to [90], a modern treatment is given in [91, 92] (see also [93]).

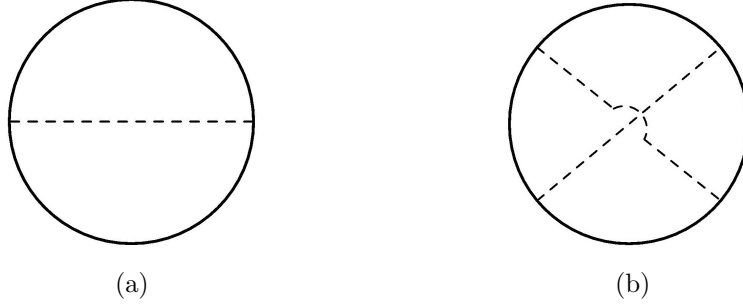


Figure 6: Sample diagrams contributing to the defect g -function.

2.2.2 The g -function and the breakdown of perturbation theory at large s

We denote by g_γ the defect g -function, defined according to the conventions in [9], as the partition function in the presence of the defect on a circle of radius R normalized by the partition function without it:

$$\log g_\gamma \equiv \log Z^{\text{bulk+defect}} - \log Z^{\text{bulk}}, \quad (2.16)$$

where $Z^{\text{bulk+defect}}$ refers to the partition function of the full theory including the defect (2.2), and Z^{bulk} refers to the partition function of the bulk theory alone. Note that for $\gamma = 0$ the defect is completely decoupled and $g_0 = 2s + 1$ regardless of the radius of the circle (in a scheme where a cosmological constant term is absent).

In this subsection we compute the defect g -function for a circular defect of radius R diagrammatically by expanding eq. (2.2) in terms of the bare coupling constant γ_0 . We will use this calculation to illustrate the structure of the diagrammatic expansion at large s . The discussion in this section will be largely analogous to the one in [94], where similar properties were observed in the study of the multi-legged amplitudes associated with large charge operators in the $O(2)$ Wilson Fisher point in $4 - \varepsilon$ dimensions.¹⁴ We will also use the result to provide an explicit check of the g -theorem recently proven in [9].

We can compute the defect partition function expanding the exponential in eq. (2.2):

$$\begin{aligned} g_\gamma/g_0 &= 1 + \frac{\gamma_0^2}{2} \frac{\text{Tr}[T^a T^b]}{2s+1} \int_{\mathcal{C}} d^2[\tau] d\tau_2 \langle P[\phi_a(x(\tau_1)) \phi_b(x(\tau_2))] \rangle_{\gamma_0=0} \\ &+ \frac{\gamma_0^4}{4!} \frac{\text{Tr}[T^a T^b T^c T^d]}{2s+1} \int_{\mathcal{C}} d^4[\tau] \langle P[\phi_a(x(\tau_1)) \phi_b(x(\tau_2)) \phi_c(x(\tau_3)) \phi_d(x(\tau_4))] \rangle_{\gamma_0=0} \\ &+ \dots, \end{aligned} \quad (2.17)$$

where P denotes the path-ordering and all the integrals are over the circle \mathcal{C} parametrized by $\tau \in [0, 2\pi R)$ via the embedding $x^\mu(\tau) = \{R \cos(\tau/R), R \sin(\tau/R), 0, \dots\}$.¹⁵ At order γ_0^2

¹⁴The breakdown of perturbation theory for multilegged amplitudes, and its relation to semiclassics, was first analyzed in the context of multi-particle production - see e.g. [95, 96].

¹⁵The bare coupling is related to the renormalized one as in eq. (2.5).

we have a unique contraction, represented in the diagram in fig. 6a, while at order γ_0^4 the path-ordering allows for several inequivalent contractions, see the diagram in fig. 6b for an example.

We focus now on the regime $s \gg 1$. We can evaluate the traces in the expansion (2.17) using $T^a T^a = s(s+1)$ and the commutator $[T^a, T^b] = i\varepsilon^{abc} T^c$. At each loop order ℓ we find contributions that range from $\gamma_0^{2\ell} s^{2\ell}$ down to $\gamma_0^{2\ell} s$. Every time we commute two matrices a suppression factor $1/s$ is brought about, as follows from the schematic scaling $T^a \sim s$. One might therefore conclude that perturbation theory breaks down when $s \gtrsim 1/\gamma_0$. This would be too quick however. A more careful analysis indeed shows that a remarkable exponentiation takes place.¹⁶ As a result, the logarithm of the g -function admits the following expansion in perturbation theory:

$$\log g_\gamma/g_0 = s \sum_{\ell=1} \gamma_0^{2\ell} P_\ell(s), \quad (2.18)$$

where the $P_\ell(s)$ are polynomials of order ℓ . We have checked eq. (2.18) diagrammatically only up to two-loops, but in the next section we shall give a simple general argument which bypasses the intricate diagrammatic analysis.

The structure of eq. (2.18) suggests the existence of a different expansion, directly in powers of $1/s$. Indeed by formally collecting all the leading order terms of the polynomials $P_\ell(s)$ in a new function $\tilde{f}_{-1}(\gamma_0^2 s)$, and similarly for the subleading powers, we recast the partition function in a double expansion as

$$\log g_\gamma/g_0 = \sum_{k=-1} s^{-k} \tilde{f}_k(\gamma_0^2 s) = s \tilde{f}_{-1}(\gamma_0^2 s) + \tilde{f}_0(\gamma_0^2 s) + \dots \quad (2.19)$$

As eq. (2.19) already suggests, we will show in the next section that the rewriting (2.19) is associated with a different loop expansion, valid for $s \rightarrow \infty$ with $\gamma_0^2 s = \text{fixed}$. This will be obtained by expanding the path integral around a new non-trivial classical trajectory.

We now present the explicit diagrammatic computation of the g -function to order $O(\gamma_0^4)$:

$$\log g_\gamma/g_0 = \frac{\pi \gamma_0^2 s(s+1)}{(d-2)\Omega_{d-1} R^{d-4}} I_1^{(d)} - \frac{\gamma_0^4 s(s+1)}{[(d-2)\Omega_{d-1} R^{d-4}]^2} I_2^{(d)} + O(\gamma_0^6), \quad (2.20)$$

where we defined the following integrals

$$I_1^{(d)} = \int_0^{2\pi} d\phi \frac{1}{\left[4 \sin^2 \frac{\phi}{2}\right]^{\frac{d-2}{2}}} = -\frac{\pi \sec\left(\frac{\pi d}{2}\right) \Gamma\left(\frac{d}{2}-1\right)}{\Gamma(d-2) \Gamma\left(-\frac{d}{2}+2\right)} = -\frac{\pi}{2} \varepsilon + O(\varepsilon^2), \quad (2.21)$$

$$I_2^{(d)} = \int_0^{2\pi} d\phi_1 \int_0^{\phi_1} d\phi_2 \int_0^{\phi_2} d\phi_3 \int_0^{\phi_3} d\phi_4 \frac{1}{\left(16 \sin^2 \frac{\phi_{13}}{2} \sin^2 \frac{\phi_{24}}{2}\right)^{\frac{d-2}{2}}} = -\frac{3\pi^2}{2} + O(\varepsilon). \quad (2.22)$$

¹⁶For instance, it is easy to verify that the sum over diagrams of order $\gamma_0^{2\ell} s^{2\ell}$, which are simply obtained by neglecting the path-ordering (i.e. dropping all the commutators) exponentiates the first $\gamma_0^2 s^2$ contribution in fig 6a. A similar exponentiation property of the one-loop contribution to the g -function was observed in the study of supersymmetric Wilson loops in $\mathcal{N} = 4$ SYM in [97, 98].

To obtain these expressions we used that the propagator of the scalar fields on the circle is given by:

$$\langle \phi_a(x(\tau)) \phi_b(x(0)) \rangle_{\gamma=0} = \frac{\delta_{ab}}{(d-2)\Omega_{d-1}} \frac{1}{[4R^2 \sin^2 \frac{\tau}{2R}]^{\frac{d-2}{2}}} . \quad (2.23)$$

The integral in eq. (2.22) is computed in appendix A.2. Notice that the $O(\gamma_0^2)$ contribution in eq. (2.20) vanishes for $\varepsilon = 0$ due to the vanishing of the integral (2.21) in four dimensions. This is because in four dimensions γ_0 is a marginal parameter at the classical level, and the g -function cannot depend on marginal defect couplings [9].

Rewriting the answer in terms of the physical coupling γ we obtain:

$$\log g_\gamma/g_0 = -\frac{\varepsilon s(s+1)}{8} \gamma^2 + \frac{\gamma^4 s(s+1)}{32\pi^2} + O(\gamma^6, \varepsilon \gamma^4, \varepsilon^2 \gamma^2) . \quad (2.24)$$

The result (2.24) depends on the radius R through the beta function (2.10) of the coupling $\gamma = \gamma(MR)$ (where M is the sliding scale); in particular, evaluating the coupling at the scale $M = 1/R$ resums the leading logarithmic corrections from higher orders in eq. (2.24). Specializing to the fixed point (2.11) we find the g -function of the DCFT:

$$\log(g_{\gamma^*}/g_0) = -\frac{\pi^2}{8} s(s+1) \varepsilon^2 + O(\varepsilon^3) . \quad (2.25)$$

We will use the results (2.24) and (2.25) to verify the validity of the semiclassical approach that we present in the next section.

We end this section by using our results to test the g -theorem recently proven in [9] (see also [6, 7, 99, 100]). To this aim, we consider the defect entropy s_D defined as:¹⁷

$$s_D = \left(1 - R \frac{\partial}{\partial R}\right) \log g_\gamma/g_0 . \quad (2.26)$$

The differential operator cancels the contribution from a possible cosmological constant counterterm on the defect (which we have ignored thus far) and ensures that s_D is a scheme-independent observable. The defect entropy is an important observable of the theory, since it decreases monotonically under the defect renormalization group flow. Using the Callan-Symanzik equation $(R\partial/\partial R + \beta_{\gamma^2}\partial/\partial\gamma^2) \log(g_\gamma/g_0) = 0$, we see that $\log(g_\gamma/g_0)$ and s_D in general coincide up to order $O(\gamma^6)$ corrections, and they are equal at the fixed points.¹⁸ This implies:

$$g_{\gamma^*} \leq g_0 , \quad (2.27)$$

in agreement with eq. (2.25). Additionally, the defect entropy obeys the following gradient equation [9]:

$$M \frac{\partial s_D}{\partial M} = - \int_0^{2\pi R} d\tau_1 \int_0^{2\pi R} d\tau_2 \langle T_D(\tau_1) T_D(\tau_2) \rangle \left[1 - \cos\left(\frac{\tau_1 - \tau_2}{R}\right) \right] , \quad (2.28)$$

¹⁷The definition of s_D in eq. (2.26) differs by a constant amount with respect to the definition (1.1) in the introduction due to the normalization factor g_0 .

¹⁸This is true only in mass independent schemes, such as the one we are using, where no cosmological constant counterterm is generated.

where T_D is the defect stress tensor. We may verify this equation in perturbation theory using that $T_D = \beta_\gamma T^a \phi_a$, where $2\gamma\beta_\gamma = \beta_{\gamma^2}$. Evaluating the derivative on the left hand side of eq. (2.28) using the Callan-Symanzik equation, the formula (2.28) to the leading non-vanishing order is equivalent to the following equality

$$\frac{\partial \log g_\gamma}{\partial \gamma^2} = \frac{\beta_{\gamma^2}}{4\gamma^2} \frac{\text{Tr}[T^a T^b]}{2s+1} \int_0^{2\pi R} d\tau_1 \int_0^{2\pi R} d\tau_2 \langle \phi_a(x(\tau_1)) \phi_b(x(\tau_2)) \rangle \left[1 - \cos\left(\frac{\tau_1 - \tau_2}{R}\right) \right]. \quad (2.29)$$

This is easily verified using eq. (2.23) and the beta function (2.10).

2.3 Semiclassics and the double-scaling limit

2.3.1 General considerations

In sec. 2.2.2 we showed that as the impurity spin s becomes large, standard diagrammatic perturbation theory breaks down. An alternative framework should be used in order to address the physics at large s . For instance, in (2.24) there could well be terms of order $\gamma^6 s^3$ which would render our analysis invalid for $\varepsilon s \sim O(1)$. Similarly, the analysis of the fixed point in (2.10) would have to be revisited for $\varepsilon s \sim O(1)$ due to terms such as $\gamma^6 s$ which we have not yet computed. Physically this is associated with the fact that a large spin has a strong backreaction on the bulk, and thus the expansion around the trivial bulk background becomes inadequate.

We now introduce a different *semiclassical* approach to study the theory in the large s regime. That a quasi-classical approach should exist is intuitively obvious, since an impurity with large spin *classically* sources a large response in the bulk order parameter $\phi_a \sim \gamma s$. The proper classical profile therefore resums all the s -enhanced contributions, allowing for a perturbative study of the theory.

Concretely, consider the one-point function of the operator ϕ_a^2 . Rescaling the bulk fields in eq. (2.3) as $\phi_a \rightarrow \sqrt{s}\phi_a$ and $z \rightarrow \sqrt{s}z$, one writes the corresponding path integral as^{19,20}

$$\langle \phi_a^2(\mathbf{x}, 0) \rangle = \frac{s \int \mathcal{D}\phi_a \mathcal{D}z \phi_a^2(\mathbf{x}, 0) \exp[-s S_{\text{rescaled}}]}{\int \mathcal{D}\phi_a \mathcal{D}z \exp[-s S_{\text{rescaled}}]}, \quad (2.30)$$

where we defined a rescaled action which depends only on $\gamma_0 \sqrt{s}$:

$$S = s \left[\frac{1}{2} \int d^d x (\partial \phi_a)^2 + \int_D d\tau \left(\bar{z} \dot{z} - \gamma_0 \sqrt{s} \bar{z} \frac{\sigma^a}{2} z \phi_a \right) \right] \equiv s S_{\text{rescaled}}, \quad \bar{z} z = 2. \quad (2.31)$$

It is clear from the above action that the model can be analyzed in a saddle-point expansion in the limit $s \rightarrow \infty$ by treating $\gamma_0 \sqrt{s}$ as a fixed parameter. Therefore the correlator admits

¹⁹ $\langle \phi_a^2(\mathbf{x}, 0) \rangle$ stands for the expectation value of the unscaled bulk field; we only do the field redefinition under the path integral.

²⁰In the following, to account for the trace in eq. (2.2), periodic boundary conditions on z are understood in the path integral: $z(\tau_i) = z(\tau_f)$.

the following double expansion

$$\langle \phi_a^2(\mathbf{x}, 0) \rangle = \frac{\mathcal{N}_d}{|\mathbf{x}|^{d-2}} \left[s \tilde{h}_{-1}(\gamma_0^2 s, |\mathbf{x}|, d) + \tilde{h}_0(\gamma_0^2 s, |\mathbf{x}|, d) + \dots \right], \quad (2.32)$$

where for convenience we isolated the factor \mathcal{N}_d , defined in eq. (2.13), in front of the right-hand-side. From eq. (2.32) it is clear that s^{-1} plays the role of the loop counting parameter similarly to \hbar . $\gamma_0^2 s$ instead is a fixed coupling, which near $4d$ is analogous to a 't Hooft coupling.

The interpretation of (2.32) is slightly different between the case of $\varepsilon = 4 - d \ll 1$ and the case of finite ε . For $\varepsilon = 4 - d \ll 1$ there are logarithmic corrections (e.g. terms such as $\gamma_0^2 s \log |\mathbf{x}|$) that can be nicely accounted for using the power of the renormalization group. Therefore we will switch to the physical coupling γ and consider the double-scaling limit²¹

$$\gamma \rightarrow 0, \quad s \rightarrow \infty, \quad \gamma^2 s = \text{fixed}. \quad (2.33)$$

For ε that is $O(1)$ (and in particular in $d = 3$) one might similarly worry that terms such as $\gamma_0^2 s |\mathbf{x}|^{4-d}$ become increasingly large in the infrared and would destroy the utility of the expansion (2.32). We will see that this does not happen and no large enhancement occurs in the infrared. The large s limit is fully analogous to the usual large N limit in the $O(N)$ model. All large IR effects are consistently resummed by the saddle-point, and the full renormalization group flow can be studied perturbatively in a $1/s$ expansion as in (2.32). Similar comments apply to other observables.

As promised, for $\varepsilon = 4 - d \ll 1$, we rewrite equation (2.32) using the physical coupling γ :

$$\langle \phi_a^2(\mathbf{x}, 0) \rangle = \frac{\mathcal{N}_d}{|\mathbf{x}|^{d-2}} \left[s h_{-1}(\gamma^2 s, |\mathbf{x}| M, \varepsilon) + h_0(\gamma^2 s, |\mathbf{x}| M, \varepsilon) + \dots \right], \quad (2.34)$$

where γ is defined so that h_{-1} and h_0 are finite for $\varepsilon \rightarrow 0$.

The beta function in the double-scaling limit takes the general form:

$$\beta_{\gamma^2} = \gamma^2 \left[-\varepsilon + \beta_0^{(4d)}(\gamma^2 s) + \frac{1}{s} \beta_1^{(4d)}(\gamma^2 s) + O\left(\frac{1}{s^2}\right) \right]. \quad (2.35)$$

In section 2.3.3 we will find that

$$\beta_0^{(4d)}(\gamma^2 s) = 0. \quad (2.36)$$

Furthermore, we will compute $\beta_1^{(4d)}(\gamma^2 s)$ (see eq. (2.59)). This will enable us to obtain the phase diagram of the theory summarized in sec. 1.1. At the fixed points the dependence on $|\mathbf{x}|$ in eq. (2.34) of course drops out.

Analogous considerations about the existence of a double scaling limit apply to other observables of the theory. We will consider in particular the g -function. Rescaling the fields as in (2.31), we see that the g -function admits the double scaling expansion

²¹This double-scaling limit is analogous to similar ones considered in the context of the large charge expansion [94, 101–104].

$$\log g_\gamma/g_0 = s\tilde{f}_{-1}(\gamma_0^2 s, R, d) + \tilde{f}_0(\gamma_0^2 s, R, d) + s^{-1}\tilde{f}_1(\gamma_0^2 s, R, d) + \dots \quad (2.37)$$

where R is the circle radius. For $\varepsilon \ll 1$ eq. (2.37) is conveniently rewritten in terms of the physical coupling as:

$$\log g_\gamma/g_0 = sf_{-1}(\gamma^2 s, RM, \varepsilon) + f_0(\gamma^2 s, RM, \varepsilon) + s^{-1}f_1(\gamma^2 s, RM, \varepsilon) + \dots \quad (2.38)$$

When specialized to a fixed point, there is no dependence on the size of the defect R and one finds the conformal defect entropy.

For $d < 4$ with fixed $\varepsilon = O(1)$, $s_D \rightarrow -\infty$ for $R \rightarrow \infty$ for large enough s . This indicates the lack of an infrared DCFT, as we anticipated in sec. 1.1. Instead, for $\varepsilon \ll 1$ there is a rich phase diagram.

As a final comment, we notice that the above expansions in the double-scaling limit (2.33) should match the result of the diagrammatic calculations discussed in sec. 2.2 for small $\gamma^2 s$. As previously noticed, this exponentiation is a very nontrivial fact from the diagrammatic viewpoint. We will therefore use the diagrammatic results as a benchmark of our semiclassical approach in the overlapping regime, thus providing a strong consistency check of our methodology.

The rest of this section is organized as follows. In subsec. 2.3.2 we consider a nonlocal one-dimensional theory on the defect that we obtain upon integrating out explicitly the bulk scalar field. This will set the stage for all the other calculations that we perform in this section. In subsec. 2.3.3 we study the one-point function of the operator ϕ_a^2 and derive the phase diagram of the theory in the large s limit as a function of d . Finally in subsec. 2.3.4 we compute the partition function of a circular defect and use our results to test the g -theorem.

2.3.2 The nonlocal theory on the line and the saddle-point

Let us consider the DQFT (2.3) for an arbitrary line geometry $x(\tau)$. Due to the simplicity of the bulk theory, we can integrate out explicitly ϕ_a on its equations of motion. Rescaling $z \rightarrow \sqrt{s}z$, this gives:

$$\phi_a(x) = -\frac{\gamma_0 s}{(d-2)\Omega_{d-1}} \int_D d\tau \frac{(\bar{z} \frac{\sigma_a}{2} z)(\tau)}{|x - x(\tau)|^{d-2}} + \delta\phi_a(x), \quad (2.39)$$

where $\delta\phi_a(x)$ is a free field fluctuation that completely decouples from the line. The defect action then reduces to the following nonlocal quantum mechanical model:

$$S = s \left[\int_D d\tau \bar{z} \dot{z} - \frac{\alpha_0}{2} \int_D d\tau \int_D d\tau' \frac{\bar{z} \frac{\sigma_a}{2} z \bar{z}' \frac{\sigma_a}{2} z'}{|x(\tau) - x(\tau')|^{d-2}} \right], \quad (2.40)$$

where $\bar{z}z = 2$, z' stands for $z(\tau')$ and we defined

$$\alpha_0 \equiv \frac{\gamma_0^2 s}{(d-2)\Omega_{d-1}}. \quad (2.41)$$

To proceed with the large s limit, we need to expand the action (2.40) around its saddle-point solution. By regulating the short distance divergence for $\tau \rightarrow \tau'$ in dimensional regularization, the saddle-point is simply given by:

$$z = z_0 = \text{const} . \quad (2.42)$$

There is a S^2 manifold of saddle-points: this is accounted for by the integration over the zero modes which rotate the solution as $z_0 \rightarrow U z_0$, where U is an arbitrary element of $U(2)$ modulo the $U(1)$ gauge transformations. The integration over the zero modes enforces the symmetry; for instance it implies that only $SO(3)$ singlet bulk operators can acquire a non-trivial one-point function.

It is useful to write z in terms of polar and azimuthal angles θ and ϕ , in the so called Bloch sphere parametrization:

$$z = \sqrt{2} \begin{pmatrix} \cos \frac{\theta}{2} \\ \sin \frac{\theta}{2} e^{i\phi} \end{pmatrix} . \quad (2.43)$$

We choose to expand around $\theta = \frac{\pi}{2}$ and $\phi = 0$.²² It is further convenient to recast the fluctuations $\delta\theta$ and $\delta\phi$ in terms of a complex variable χ as

$$\chi = \sqrt{\frac{s}{2}} (\delta\theta + i\delta\phi) . \quad (2.44)$$

The action then reads:

$$\begin{aligned} S = & -s \frac{\alpha_0}{2} \int_D d\tau \int_D d\tau' \frac{1}{|x(\tau) - x(\tau')|^{d-2}} \\ & + \int d\tau \bar{\chi} \dot{\chi} - \frac{\alpha_0}{2} \int d\tau \int d\tau' \frac{(\bar{\chi} \chi' + \bar{\chi}' \chi - \bar{\chi} \chi - \bar{\chi}' \chi')}{|x(\tau) - x(\tau')|^{d-2}} \\ & + O\left(\frac{1}{s}\right) \end{aligned} \quad (2.45)$$

The first line of eq. (2.45) will be important when we study the defect partition function, even though it does not depend on the fluctuation χ . The second line is the quadratic action for the fluctuations around the saddle-point, and it allows studying $1/s$ corrections to observables. The previous remark above eq. (2.4) implies that the equal time product $\bar{\chi} \chi$ is a formal notation for $\lim_{\eta \rightarrow 0^+} \bar{\chi}(\tau + \eta) \chi(\tau)$, and similarly for $\bar{\chi}' \chi'$. Finally $1/s$ suppressed quartic vertices arise both from the expansion of the kinetic term and the nonlocal interaction. The theory nonetheless remains under perturbative control at all scales for large s , since in the semiclassical approach the α_0 term behaves like a mass term for the fluctuations, so that the $1/s$ suppressed relevant couplings remain always parametrically small.²³ In this sense, the large s limit of the theory (2.40) resembles the large N limit of the three-dimensional $O(N)$ model, since in both cases the saddle-point allows resumming the leading effects of the relevant interaction term [49].

²²Notice that the parametrization (2.43) is singular at the south and north poles $\theta = 0$ and $\theta = \pi$.

²³This is analogous to the case of a three-dimensional theory with potential $V(\phi) = m^2 \phi^2 + \lambda \phi^4$, which is perturbative at all scales for $\lambda/m \ll 4\pi$.

2.3.3 The one-point function of ϕ_a^2 and the phase diagram

Here we illustrate our ideas by performing the semiclassical calculation of $\langle \phi_a^2(x) \rangle$, for a straight defect located at $x^i = 0$, to the first subleading order in the $1/s$ expansion. We will use this calculation to extract the beta function (2.35) in the double-scaling limit (2.33), and thus extract the phase diagram of the theory as a function of d in the large s limit. We will also comment on other observables.

To perform the calculation, we use (2.39) to express the one-point function of ϕ_a^2 as:

$$\langle \phi_a^2(\mathbf{x}, 0) \rangle = \frac{s\alpha_0}{(d-2)\Omega_{d-1}} \int d\tau \int d\tau' \frac{\langle \bar{z} \frac{\sigma_a}{2} z \bar{z}' \frac{\sigma_a}{2} z' \rangle}{(\mathbf{x}^2 + \tau^2)^{\frac{d-2}{2}} (\mathbf{x}^2 + \tau'^2)^{\frac{d-2}{2}}} . \quad (2.46)$$

To obtain the leading order result for the one-point correlation function, we simply plug the saddle-point solution (2.42) in eq. (2.46). This gives:

$$\begin{aligned} \langle \phi_a^2(\mathbf{x}, 0) \rangle &= \frac{s\alpha_0}{(d-2)\Omega_{d-1}} \left(\int d\tau \frac{1}{(\mathbf{x}^2 + \tau^2)^{\frac{d-2}{2}}} \right)^2 + O(s^0) \\ &= s \frac{\gamma_0^2 s}{16\pi^{d-1} |\mathbf{x}|^{2d-6}} \Gamma\left(\frac{d-3}{2}\right)^2 + O(s^0) . \end{aligned} \quad (2.47)$$

In terms of the expansion (2.32) this implies:

$$\tilde{h}_{-1}(\gamma_0^2 s, |\mathbf{x}|, \varepsilon) = \mathcal{N}_d^{-1} \frac{\gamma_0^2 s}{16\pi^{d-1} |\mathbf{x}|^{4-d}} \Gamma\left(\frac{d-3}{2}\right)^2 . \quad (2.48)$$

Eq. (2.48) exactly agrees with the leading order diagrammatic result (2.8), which is therefore *exact* in the double-scaling limit. We shall see in a moment that the first correction \tilde{h}_0 takes a more intricate (and interesting) form.

Before focusing on the next to leading order correction, a few comments are in order. The one-point function (2.47) in $d = 4$ reads:

$$\langle \phi_a^2(\mathbf{x}, 0) \rangle \stackrel{d=4}{=} \frac{\gamma_0^2 s^2}{16\pi^2 \mathbf{x}^2} + O(s^0) . \quad (2.49)$$

The one-point function is conformally invariant in $d = 4$, in agreement with the marginal nature of the coupling at tree level. We will soon show that quantum corrections provide logarithmic corrections in four dimensions, leading to a rich phase diagram for $\varepsilon = 4 - d \ll 1$. For $\varepsilon = O(1)$, the result instead deviates from the conformal scaling $\langle \phi_a^2(\mathbf{x}, 0) \rangle \propto 1/|\mathbf{x}|^{d-2}$, due to the relevant nature of the coupling. As anticipated in the discussion below eq. (2.45), we shall see that $1/s$ corrections do not change this qualitative behavior at long distances, and thus the theory never reaches an infrared fixed point. Finally we notice that the result (2.47) has a double pole in $d = 3$, associated with an infrared logarithmic divergence of the integral in three dimensions. To regulate the result, we introduce a cutoff length $L \gg |\mathbf{x}|$ on the extension of the line, so that to leading logarithmic accuracy the result reads:²⁴

$$\langle \phi_a^2(\mathbf{x}, 0) \rangle \stackrel{d=3}{\simeq} \frac{\gamma_0^2 s^2}{(4\pi)^2} \log^2(\mathbf{x}^2/L^2) + O(s^0) . \quad (2.50)$$

²⁴Alternatively, we could regulate the infrared divergence by considering a circular defect.

One conceptual point that will be crucial later is that the leading in s behavior is analogous to the one which is obtained by considering a symmetry breaking source localized on a line in the free theory, $\delta S \propto \int d\tau \phi_1$, i.e. the external field (or pinning field) defect, see [23]. In fact, as eq. (2.39) shows, the impurity behaves precisely as a localized source up to the zero-mode integration. This is also reflected in the result for the g -function, that we discuss in the next subsection. From this point of view, the lack of a fixed point for large s at any fixed $d < 4$ is therefore due to the same physics as the lack of a fixed point in the external field defect, which was explained in [23]. In other words, it is due to the moduli space of vacua in the bulk.

Let us now focus on the $O(s^0)$ correction to the result (2.47). To this aim, we write explicitly the quadratic action for the fluctuations in eq. (2.45) for a straight line:

$$\begin{aligned} S^{(2)} &\simeq \int d\tau \bar{\chi} \dot{\chi} - \frac{\alpha_0}{2} \int d\tau \int d\tau' \frac{(\bar{\chi}\chi' + \bar{\chi}'\chi - \bar{\chi}\chi - \bar{\chi}'\chi')}{|\tau - \tau'|^{d-2}} \\ &= \int \frac{d\omega}{2\pi} \bar{\chi}(\omega) G_\chi^{-1}(\omega) \chi(\omega), \end{aligned} \quad (2.51)$$

where $G_\chi(\omega)$ is the propagator associated with the fluctuations:

$$G_\chi(\omega) = \frac{1}{-i\omega - \alpha_0 \bar{c}^{(d)}(\omega)}. \quad (2.52)$$

The function $\bar{c}^{(d)}(\omega)$ is defined by

$$\bar{c}^{(d)}(\omega) = \int d\tau \frac{e^{-i\omega\tau} - 1}{|\tau|^{d-2}} = -2|\omega|^{d-3} \Gamma(3-d) \sin\left(\frac{d\pi}{2}\right) \quad \text{for } d > 3. \quad (2.53)$$

The case of $d = 3$ is special due to the infrared logarithmic divergence that we encountered before and we will discuss it separately at the end. Expanding eq. (2.46) in terms of the fluctuations around the saddle-point solution, we may now use the propagator (2.52) to write the next-to-leading order contribution to the one-point function as

$$\begin{aligned} \delta\langle\phi_a^2(\mathbf{x}, 0)\rangle &= \frac{\alpha_0}{(d-2)\Omega_{d-1}} \int d\tau \int d\tau' \frac{\langle\bar{\chi}'\chi + \bar{\chi}\chi' - \bar{\chi}\chi - \bar{\chi}'\chi'\rangle}{(\mathbf{x}^2 + \tau^2)^{\frac{d-2}{2}} (\mathbf{x}^2 + \tau'^2)^{\frac{d-2}{2}}} \\ &= \lim_{\eta \rightarrow 0^+} \frac{2\alpha_0}{(d-2)\Omega_{d-1}} \int \frac{d\omega}{2\pi} G_\chi(\omega) \left[|h_\mathbf{x}(\omega)|^2 - e^{i\omega\eta} |h_\mathbf{x}(0)|^2 \right], \end{aligned} \quad (2.54)$$

where the factor $e^{i\omega\eta}$ arise from the point-splitting regularization mentioned around eq. (2.4) and we have defined

$$h_\mathbf{x}(\omega) = \int d\tau \frac{e^{-i\omega\tau}}{(\mathbf{x}^2 + \tau^2)^{\frac{d-2}{2}}} = \frac{\sqrt{\pi} 2^{\frac{5-d}{2}} |\mathbf{x}|^{\frac{3-d}{2}} |\omega|^{\frac{d-3}{2}} K_{\frac{d-3}{2}}(|\mathbf{x}||\omega|)}{\Gamma\left(\frac{d}{2} - 1\right)}. \quad (2.55)$$

In the above $K_\nu(x)$ is the modified Bessel functions of the second kind. Eq. (2.55) simplifies in $d = 4$:

$$h_\mathbf{x}(\omega) \stackrel{d=4}{=} \frac{\pi}{|\mathbf{x}|} e^{-|\omega||\mathbf{x}|}. \quad (2.56)$$

The expression (2.54) holds for any value of $d > 3$. Nonetheless it is technically hard to obtain an explicit general result. Therefore, to proceed, it is technically convenient to discuss separately the case of small $\varepsilon = 4 - d$ and that of $4 - d = O(1)$.

We consider first the case of small ε . Noticing that $G_\chi(\omega) \sim 1/|\omega|$ for $\omega \rightarrow \infty$ in four dimensions, we see that the integral (2.54) would lead to a logarithmic divergence in the $\eta \rightarrow 0^+$ limit due to the integration over the $G_\chi(\omega) |h_{\mathbf{x}}(0)|^2$ term. The divergence needs to be renormalized by the coupling counterterm, and therefore leads to a nontrivial RG flow.

Explicitly, studying the integral in $4 - \varepsilon$ dimensions, we find that the next-to-leading order correction to the one-point function (2.47) is:

$$\begin{aligned} \delta \langle \phi_a^2(\mathbf{x}, 0) \rangle = & -\frac{1}{\varepsilon} \frac{\alpha_0 \arctan(\pi \alpha_0)}{2\pi \mathbf{x}^2} + \frac{\alpha_0}{4\pi \mathbf{x}^2} - \frac{2\alpha_0^2(\log |\mathbf{x}| + 1 + \log 2)}{4(1 + \pi^2 \alpha_0^2) \mathbf{x}^2} \\ & - \frac{\alpha_0 \arctan(\pi \alpha_0)(4 \log |\mathbf{x}| + \gamma_E + \log 16 + \log \pi)}{4\pi \mathbf{x}^2} + O(\varepsilon). \end{aligned} \quad (2.57)$$

We detail the computation in appendix B.1. Here we only remark that the second term on the right hand side of eq. (2.57), which is linear in α_0 , arises because of the point-splitting in eq. (2.4). When added to the leading order (2.49), it modifies the prefactor $\gamma_0^2 s^2$ to $\gamma_0^2 s(s+1)$, as expected.

Comparing eq. (2.57) with the leading order expression in four dimensions (2.49), we see that one obtains a finite result for the one-point correlation function of $\langle \phi_a^2(x) \rangle$ upon renormalizing the coupling α_0 according to:

$$\alpha_0 = \frac{4\pi^2 M^\varepsilon}{(2-\varepsilon)\Omega_{3-\varepsilon}} \left(\alpha + \frac{\delta\alpha}{\varepsilon} \right), \quad \delta\alpha = \frac{2\alpha \arctan(\pi\alpha)}{\pi s}, \quad (2.58)$$

where the prefactor $\frac{4\pi^2}{(2-\varepsilon)\Omega_{3-\varepsilon}} = 1 + O(\varepsilon)$ is there to compensate the ε -dependence in the definition (2.41). This ensures that eq. (2.58) corresponds to the same renormalization scheme used in sec. 2.2, allowing for a comparison with the results in that section also away from the fixed points. Using the above result, we find the following beta function:

$$\beta_\alpha = -\varepsilon\alpha + \frac{1}{s} \frac{2\alpha^2}{1 + \pi^2 \alpha^2}. \quad (2.59)$$

Notably, this result for the beta function agrees with the diagrammatic one (2.10) in the small α limit, as can be seen using $\alpha = \frac{\gamma^2 s}{4\pi^2}$. In eq. (2.35) it implies:

$$\beta_0^{(4d)} = 0, \quad \beta_1^{(4d)} = 2\alpha/(1 + \pi^2 \alpha^2). \quad (2.60)$$

Eq. (2.59) admits nontrivial zeros for:

$$\varepsilon s = \frac{2\alpha}{1 + \pi^2 \alpha^2}. \quad (2.61)$$

The solutions depend on the value of the double-scaling parameter εs and are summarized in figure 7. Strictly in $d = 4$, there is only one fixed point, which is stable and trivial (at $\alpha = 0$)

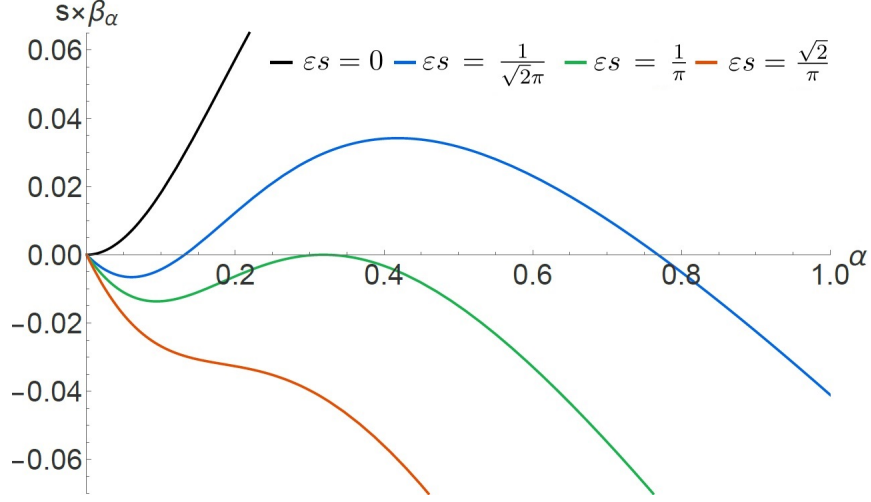


Figure 7: Plot of the beta function (multiplied by a factor of s) as a function of α for various values of fixed εs : strictly in four dimensions with $\varepsilon s = 0$ (black), in the range $0 < \varepsilon s < \frac{1}{\pi}$ with $\varepsilon s = \frac{1}{\sqrt{2}\pi}$ (blue), $\varepsilon s = \frac{1}{\pi}$ (green) and in the range $\varepsilon s > \frac{1}{\pi}$ with $\varepsilon s = \frac{\sqrt{2}}{\pi}$ (orange).

– see the black curve of figure 7. Interestingly, there are two solutions in the regime where $0 < \varepsilon s < 1/\pi$, as is demonstrated by the blue curve of figure 7. These are given by:

$$\alpha = \begin{cases} \frac{1 - \sqrt{1 - \pi^2(s\varepsilon)^2}}{\pi^2 s \varepsilon} \equiv \alpha_1 = \frac{\varepsilon s}{2} + O((\varepsilon s)^3), \\ \frac{1 + \sqrt{1 - \pi^2(s\varepsilon)^2}}{\pi^2(s\varepsilon)} \equiv \alpha_2 = \frac{2}{\pi^2 \varepsilon s} + O(\varepsilon s). \end{cases} \quad (2.62)$$

The fixed point with the smaller α , $\alpha = \alpha_1$, reduces to the weak-coupling perturbative fixed point studied in sec. 2.2 and it is the only stable fixed point. However, the semiclassical approach used in this subsection reveals the existence of a new fixed point, which appears for $\alpha = \alpha_2$; this is a nonperturbative fixed point in the standard perturbative approach valid only for $\varepsilon s \ll 1$. This new fixed point is unstable towards the first fixed point for $\alpha < \alpha_2$, and it flows to the strongly coupled regime for $\alpha > \alpha_2$; we expect that this latter flow never reaches an endpoint.

The two solutions coincide at $\varepsilon s = 1/\pi$ (as can be seen from the green curve of figure 7). No solutions exist for $\varepsilon s > 1/\pi$ (see the orange curve of figure 7). We will indeed see that for finite ε and large s the infrared limit of the defect is not described by a DCFT, rather, the flow never terminates and tends towards $s_D \rightarrow -\infty$.

We also comment on the defect operator spectrum at the fixed points. The comment below eq. (2.15) implies that the impurity spin operator S^a has dimension $\Delta_S = \varepsilon/2$ for both fixed points in eq. (2.61). The anomalous dimension of the operator $S^a \phi_a$ is extracted from

the beta function and to the first nontrivial order it reads

$$\gamma_{S\cdot\phi} = \Delta_{S\cdot\phi} - 1 = \left. \frac{\partial\beta_\alpha}{\partial\alpha} \right|_{\beta_\alpha=0} \simeq \begin{cases} +\varepsilon\sqrt{1-\pi^2s^2\varepsilon^2} & \text{for } \alpha = \alpha_1, \\ -\varepsilon\sqrt{1-\pi^2s^2\varepsilon^2} & \text{for } \alpha = \alpha_2. \end{cases} \quad (2.63)$$

As expected, the anomalous dimension is positive at the stable fixed point and negative at the unstable one. The operator is marginal when the two fixed points collide.

Finally, we provide the result for the one-point correlation function to the next-to-leading order. In terms of the expansion (2.34), we find:

$$\begin{aligned} h_{-1}(\gamma^2s, |\mathbf{x}|M, \varepsilon) &= \frac{\gamma^2s}{4\sqrt{6}} \left\{ 1 + \varepsilon \left[\log(4M|\mathbf{x}|) + \frac{1}{2}(\gamma_E + \log \pi) \right] + O(\varepsilon^2) \right\}, \\ h_0(\gamma^2s, |\mathbf{x}|M, \varepsilon) &= \frac{\gamma^2s}{4\sqrt{6}} - \frac{\gamma^4s^2}{\sqrt{6}(16\pi^2 + \gamma^4s^2)} [2\log(M|\mathbf{x}|) + \gamma_E + 2 + \log 4\pi] + O(\varepsilon). \end{aligned} \quad (2.64)$$

The expansion of eqs. (2.64) for $\gamma^2s \ll (4\pi)^2$ is in perfect agreement with the diagrammatic results (2.12). From eq. (2.64) we also obtain the correlator at the fixed points α_1 and α_2 in eq. (2.62):

$$\langle \phi_a^2(\mathbf{x}, 0) \rangle = \frac{\mathcal{N}_d}{|\mathbf{x}|^{2-\varepsilon}} \frac{s \left(1 \mp \sqrt{1 - \pi^2\varepsilon^2s^2} \right)}{\sqrt{6}\varepsilon s} \left\{ 1 + \frac{1}{s} [1 + \varepsilon s (\log 2 - 1)] + O\left(\frac{1}{s^2}\right) \right\}, \quad (2.65)$$

where the $-$ and $+$ sign refer, respectively, to the fixed points α_1 and α_2 . This concludes the discussion for $\varepsilon \ll 1$.

We now wish to evaluate the $1/s$ correction in eq. (2.54) for generic d with $\varepsilon = O(1)$. In this case no renormalization is required since there are no divergences in (2.54). Thus, we will work directly in terms of the bare coupling α_0 .

To obtain an analytic expression, we focus on the long distance limit of $\langle \phi_a^2(\mathbf{x}, 0) \rangle$, specified by $\alpha_0|\mathbf{x}|^{4-d} \gg 1$. In this limit, the leading result arises from the second term in square parenthesis in eq. (2.54), which is proportional to a tadpole integral of the propagator. This term indeed behaves as $|h_{\mathbf{x}}(0)|^2 \propto 1/|\mathbf{x}|^{2d-6}$ like the leading order (2.47), while we shall soon see that the first contribution in the square parenthesis in eq. (2.54) decays faster at large distances. We find:

$$\lim_{\eta \rightarrow 0^+} \int \frac{d\omega}{2\pi} e^{i\omega\eta} G_\chi(\omega) = \frac{1}{2(4-d)} - \frac{1}{2}. \quad (2.66)$$

While the propagator (2.52) depends on α_0 the result is independent of it, as expected from dimensional analysis.²⁵ The $-1/2$ arises from the point-splitting prescription (2.4). We

²⁵Technically, this can be seen rescaling $\omega \rightarrow \omega\alpha_0^{\frac{1}{4-d}}$ in the integral (2.66).

may also evaluate the leading long distance contribution from the first term in the square parenthesis of eq. (2.54) by expanding the propagator (2.52) for small ω :²⁶

$$\begin{aligned} \int \frac{d\omega}{2\pi} G_\chi(\omega) |h_{\mathbf{x}}(\omega)|^2 &= \frac{-1}{\alpha_0 \bar{c}^{(d)}(1)} \int \frac{d\omega}{2\pi} \frac{|h_{\mathbf{x}}(\omega)|^2}{|\omega|^{d-3}} \left[1 + O\left(\frac{1}{\alpha_0^2 |\mathbf{x}|^{2(4-d)}}\right) \right] \\ &= \frac{\pi \Gamma\left(\frac{d-3}{2}\right)^2}{\Gamma\left(\frac{d-2}{2}\right)^2} \frac{\sigma(d)}{\alpha_0 |\mathbf{x}|^{d-2}} \left[1 + O\left(\frac{1}{\alpha_0^2 |\mathbf{x}|^{2(4-d)}}\right) \right], \end{aligned} \quad (2.67)$$

where for convenience we defined a positive coefficient $\sigma(d)$ as:

$$\sigma(d) = \frac{(3-d) \cot\left(\frac{\pi d}{2}\right) \Gamma\left(\frac{d}{2}-1\right)^2}{2^{5-d} \pi \Gamma(d-3)} > 0 \quad \text{for } 3 < d < 4. \quad (2.68)$$

The coefficient $\sigma(d)$ has a pole for $d \rightarrow 4$ and vanishes in $d = 3$.

Using eqs. (2.47), (2.66) and (2.67) in the expression (2.54), we write the final result for the one-point function (2.47) in $3 < d < 4$ as

$$\begin{aligned} \langle \phi_a^2(\mathbf{x}, 0) \rangle &= \frac{s \alpha_0 \pi \Gamma\left(\frac{d-3}{2}\right)^2}{(d-2) \Gamma\left(\frac{d-2}{2}\right)^2 \Omega_{d-1} |\mathbf{x}|^{2d-6}} \\ &\times \left\{ 1 + \frac{1}{s} \left[\frac{3-d}{4-d} + \frac{\sigma(d)}{\alpha_0 |\mathbf{x}|^{4-d}} + O\left(\frac{1}{\alpha_0^3 |\mathbf{x}|^{3(4-d)}}\right) \right] + O\left(\frac{1}{s^2}\right) \right\}. \end{aligned} \quad (2.69)$$

Notice that the expansion breaks down for $d \rightarrow 4$, which is why we had to perform renormalization in that case. Otherwise, we see that $1/s$ corrections only change the prefactor of the leading $1/|\mathbf{x}|^{2d-6}$ term at large distances. From eq. (2.69) we also see that the first subleading correction at long distances is independent of α_0 (but depends on s) and obeys a conformal scaling law $1/|\mathbf{x}|^{d-2}$.

A qualitatively similar behavior describes other correlation functions. For instance, an analogous calculation shows that the two-point function of the spin operator on the line takes the following form:

$$\langle S^a(\tau) S^b(0) \rangle = \frac{\delta^{ab}}{3} s^2 \left\{ 1 + \frac{1}{s} \left[\frac{3-d}{4-d} + \frac{(3-d) \cot\left(\frac{\pi d}{2}\right)}{\pi \alpha_0 |\tau|^{4-d}} + O\left(\frac{1}{\alpha_0^3 |\tau|^{3(4-d)}}\right) \right] + O\left(\frac{1}{s^2}\right) \right\}. \quad (2.70)$$

We see from these examples that $1/s$ corrections for $d < 4$ are indeed small and do not alter the long distance behavior. In addition, as promised, we see that the long distance behavior is not compatible with a DCFT (which would require a leading $1/|\tau|^{4-d}$ dependence because of eq. (2.15)), rather, the RG flow at large s and fixed $d < 4$ never terminates.

While our treatment so far focused on $3 < d < 4$, a similar discussion applies in $d = 3$, provided one carefully regulates the infrared logarithmic divergences associated with the infinite extent of the line. In particular, $1/s$ corrections again do not lead to a well defined

²⁶This can be seen explicitly rescaling $\omega \rightarrow \omega/|\mathbf{x}|$ in the integral (2.67).

DCFT at long distances. Technically, these infrared singularities arise because $\bar{c}^{(3)}(\omega)$ in (2.52) reads:

$$\bar{c}^{(3)}(\omega) = \int d\tau \frac{e^{-i\omega\tau} - 1}{|\tau|} = -2 \log(|\omega|L) + \text{const}, \quad (2.71)$$

where L is the IR cutoff length of the defect. Because of the ambiguities related to how precisely we perform the IR regularization, we postpone the discussion of $d = 3$ to circular defects, for which no ambiguities of this sort arise.

We summarize: at fixed $3 \leq d < 4$, for large s , there is no infrared DCFT. Our large s -result leads to a never-ending flow with correlation functions scaling as in the presence of a localized external source (up to the zero-mode integration). We expect (but cannot prove) that the DQFT behaves analogously also for $s = O(1)$ in $3 \leq d < 4$.

2.3.4 The g -function

In this subsection we compute the defect g -function for a circular defect of radius R in the large s limit. We will also use our results to check the g -theorem for the fixed points we have found at $\varepsilon \ll 1$.

To perform the calculation, we consider the defect on a circle of radius R , $x^\mu(\tau) = R(\cos \tau/R, \sin \tau/R, 0 \dots)$. The leading order result arises from the classical value of the action (2.45) on the saddle-point $z = \text{const}$. In terms of the expansion (2.37), we find

$$\tilde{f}_{-1}(\gamma_0^2 s, R, d) = \frac{\alpha_0 R^{4-d}}{2} \int d\phi \int d\phi' \frac{1}{\left(4 \sin^2 \frac{\phi - \phi'}{2}\right)^{\frac{d-2}{2}}} = \pi \alpha_0 R^{4-d} I_1^{(d)}, \quad (2.72)$$

where we set $\tau = R\phi$ and $I_1^{(d)}$ is defined in eq. (2.21). As for the leading \tilde{h}_{-1} contribution to $\langle \phi_a^2(\mathbf{x}, 0) \rangle$ before, eq. (2.72) exactly agrees with the leading order diagrammatic result in eq. (2.20). As expected, the result (2.72) also exactly coincides with that of a localized source $\int d\tau \phi_1$ on the defect discussed in [23], where the result was also shown to satisfy the gradient formula (2.28).

The function $I_1^{(d)}$ in eq. (2.21) vanishes for $d = 4$, in agreement with the classical marginality of the coupling. Notice that, since $I_1^{(d)} = -\pi\varepsilon/2 + O(\varepsilon^2)$, to obtain the value of $\log g$ for small $\varepsilon \sim 1/s$ we also need to compute the one-loop correction \tilde{f}_0 in eq. (2.37). We will soon do that.

Before discussing subleading corrections, let us comment on the result for $d < 4$ with $\varepsilon = O(1)$. We find that $I_1^{(d)}$ has a pole for $d = 3$. The divergence can be renormalized by adding a cosmological constant counterterm on the line, since it is linear in R , and results in a $R \log R$ contribution²⁷ to $\log g$ in $d = 3$:

$$\tilde{f}_{-1}(\gamma_0^2 s, R, 3) = 2\pi\alpha_0 R \log(RM) + \text{const} \times MR, \quad (2.73)$$

²⁷As commented in footnote 9 of [23] for the case of localized symmetry breaking source, this term is associated to an anomaly in coupling space [105–107].

where M is an arbitrary cutoff scale. To obtain a scheme-independent quantity for arbitrary d we compute the defect entropy as in eq. (2.26),

$$s_D = -s\pi\alpha_0 R^{4-d}\rho(d) \left[1 + O\left(\frac{1}{s}\right) \right], \quad (2.74)$$

where we defined a function $\rho(d)$ which is positive and regular for $2 < d < 4$ and vanishes in $d = 4$:

$$\rho(d) \equiv \frac{\sqrt{\pi}2^{4-d}\Gamma\left(\frac{5}{2} - \frac{d}{2}\right)}{\Gamma\left(2 - \frac{d}{2}\right)} = \begin{cases} 0 & \text{for } d = 4, \\ 2 & \text{for } d = 3. \end{cases} \quad (2.75)$$

The result (2.74) therefore implies that $s_D \rightarrow -\infty$ in the infrared ($R \rightarrow \infty$) for fixed $d < 4$ and large s . This is compatible with the previously discussed scenario of a defect renormalization group flow that does not terminate in a healthy DCFT (that would have $g > 0$). At the end of this section we will see that $1/s$ corrections do not change the IR behaviour of s_D .

Let us now discuss the first $1/s$ correction to the result for small $\varepsilon \sim 1/s$. In particular, to obtain the g -function at the previously discussed fixed points we need to compute the next to leading order correction \tilde{h}_0 strictly in $d = 4$. This follows from the one-loop determinant of the fluctuations χ defined in eq. (2.44). The details of the calculation can be found in appendix B.2, while here we report the main result:

$$\tilde{f}_0(\gamma_0^2 s, R, 4 - \varepsilon) = \frac{1}{2} \log(1 + \pi^2 \alpha_0^2) + \pi \alpha_0 \arctan(\pi \alpha_0) + O(\varepsilon). \quad (2.76)$$

We now have all the information we need in order to compute the physical g -function to the leading nonvanishing order in the double-scaling limit (2.33). In terms of the physical, renormalized, coupling, we find the following results for the coefficient f_{-1} and f_0 (2.38):

$$\begin{aligned} f_{-1}(\gamma^2 s, RM, \varepsilon) &= -\frac{\varepsilon}{2} \pi^2 \alpha + O(\varepsilon^2), \\ f_0(\gamma^2 s, RM, \varepsilon) &= \frac{1}{2} \log(1 + \pi^2 \alpha^2) + O(\varepsilon). \end{aligned} \quad (2.77)$$

Using $\alpha = \frac{\gamma^2 s}{4\pi^2}$ and expanding for small $\gamma^2 s$, eqs. (2.77) can be seen to agree with the previous diagrammatic result in eq. (2.24). As already commented below eq. (2.24), the result depends on RM through the running of the coupling constant $\alpha = \alpha(RM)$. This implies in particular that $\log g$ and s_D coincide to the first nontrivial order.

At the fixed points that satisfy (2.61), the g -function is conveniently expressed in terms of α as

$$\log g_\gamma / g_0 = \frac{1}{1 + \pi^2 \alpha^2} + \frac{1}{2} \log(\pi^2 \alpha^2 + 1) - 1 + O\left(\frac{1}{s}\right). \quad (2.78)$$

Eq. (2.78) is plotted in figure 8. It has a minimum at $\alpha = 1/\pi$, where the two fixed points (2.62) coincide.

We may use eq. (2.78) to further test the g -theorem as in sec. 2.2.2. To this aim, we denote by $g^{(i)}$ the values of the defect g -function at the fixed points (2.62), i.e. $g^{(i)} = g_\gamma / g_0|_{\alpha=\alpha_i}$.

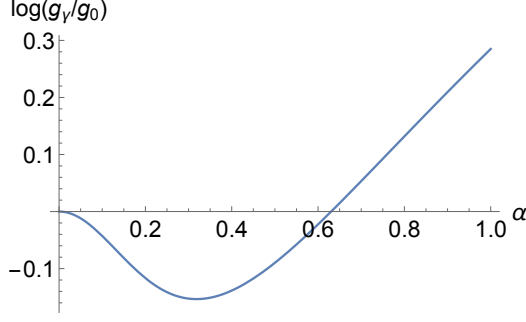


Figure 8: Plot of $\log(g_\gamma/g_0)$ at the fixed points as a function of α .

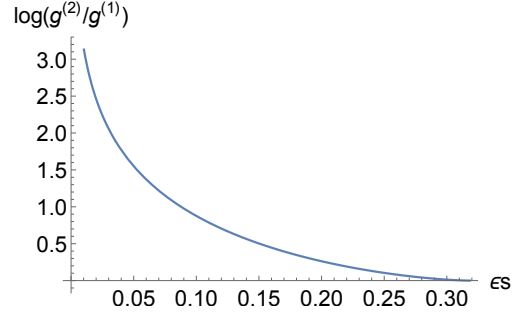


Figure 9: The difference $\log g^{(2)} - \log g^{(1)}$ as a function of εs .

One can verify that the (normalized) g -function at the fixed points satisfies:

$$\log g^{(1)} \leq 0, \quad \log g^{(1)} \leq \log g^{(2)}, \quad (2.79)$$

for $\varepsilon s \in [0, \pi^{-1}]$. This is in agreement with the g -theorem [9], which predicts that the most stable fixed point corresponds to the lowest value of g . The difference $\log g^{(2)} - \log g^{(1)}$ is plotted in fig. 9.

We may also use eq. (2.77) to verify explicitly the gradient formula (2.28). On the right hand side of the above, the defect stress tensor reads $T_D = \beta_\gamma \mathcal{O}$, where \mathcal{O} is the following defect operator:

$$\mathcal{O} = s \bar{z} \frac{\sigma^a}{2} z \phi_a = -\frac{s \alpha_0}{\gamma_0} \int d\tau' \frac{\bar{z} \frac{\sigma^a}{2} z \bar{z}' \frac{\sigma^a}{2} z'}{|x(\tau) - x(\tau')|^{d-2}} + s \bar{z} \frac{\sigma^a}{2} z \delta \phi_a. \quad (2.80)$$

To obtain the connected two-point function of the defect stress tensor we also have to expand the z field around the saddle $z = z_0$. All field fluctuations are of order $1/\sqrt{s}$, hence to leading order we can make the replacement $\mathcal{O} = s \bar{z}_0 \frac{\sigma^a}{2} z_0 \delta \phi_a$, and the condition (2.28) then reads:

$$-\beta_\alpha \frac{\partial}{\partial \alpha} \log g_\gamma/g_0 = -s^2 \beta_\gamma^2 2\pi \int d\phi \langle \delta \phi_a(x(\phi)) \delta \phi_b(x(0)) \rangle \bar{z}_0 \frac{\sigma^a}{2} z_0 \bar{z}_0 \frac{\sigma^b}{2} z_0 [1 - \cos(\phi)]. \quad (2.81)$$

Proceeding similarly to the discussion around eq. (2.29), the above condition (2.81) reduces to:

$$\frac{\partial}{\partial \alpha} \log g_\gamma/g_0 = \frac{\pi^2 s \beta_\alpha}{2\alpha}, \quad (2.82)$$

which is easily verified using eq. (2.59) and plugging in eq. (2.77).

We now discuss the $1/s$ correction \tilde{f}_0 for fixed $d < 4$. As for the correlation function discussed in the previous section, we focus on the IR limit $\alpha_0 R^{4-d} \gg 1$. The calculation is detailed in appendix B.2. For $d > 3$ the result reads:

$$\tilde{f}_0(\gamma_0^2 s, R, d) = \pi R^{4-d} \alpha_0 I_1^{(d)} \frac{5-d}{4-d} + \text{c.c.} + O\left(\left(R^{4-d} \alpha_0\right)^0, \left(R^{4-d} \alpha_0\right)^{1-\frac{d-3}{4-d}}\right), \quad (2.83)$$

where we neglected a scheme-dependent cosmological constant term, denoted by c.c.. Eq. (2.83) scales as $R^{4-d}\alpha_0$ in the IR, like the leading order (2.72). From eq. (2.83) we compute the $1/s$ corrections to the defect entropy (2.74) in the $R \rightarrow \infty$ limit:

$$s_D \stackrel{R \rightarrow \infty}{=} -s\pi\alpha_0 R^{4-d}\rho(d) \left[1 + \frac{1}{s} \frac{5-d}{4-d} + O\left(\frac{1}{s^2}\right) \right]. \quad (2.84)$$

The case of $d = 3$ needs to be discussed separately, as the expansion in eq. (2.83) takes a more intricate form due to the logarithmic behavior of the propagator mentioned above eq. (2.71). Neglecting again a cosmological constant contribution, the final result reads:

$$\tilde{f}_0(\gamma_0^2 s, R, 3) = -2\pi\alpha_0 R \log(\log(\alpha_0 R)) + \text{c.c.} + O\left(\alpha_0 R \frac{\log^2(\log(\alpha_0 R))}{\log(\alpha_0 R)}\right). \quad (2.85)$$

Eq. (2.85) scales as $R \log(\log R)$ in the IR, differently than the leading order (2.72) which is proportional to $R \log R$. Subleading terms in the expansion are suppressed by powers of $\frac{\log(\log(\alpha_0 R))}{\log(\alpha_0 R)}$. From eq. (2.85), we find that the defect entropy reads:

$$s_D \stackrel{d=3}{=} -s2\pi R\alpha_0 \left\{ 1 - \frac{1}{s} \left[\frac{1}{\log(\alpha_0 R)} + O\left(\frac{\log^2(\log(\alpha_0 R))}{\log^2(\alpha_0 R)}\right) \right] + O\left(\frac{1}{s^2}\right) \right\}, \quad (2.86)$$

and indeed in the infrared $s_D \rightarrow -\infty$, consistently with the absence of an infrared DCFT.

3 Spin defects at large s : the interacting theory

3.1 Setup

In this section we consider the $O(3)$ Wilson-Fisher model:

$$S_{\text{bulk}} = \int d^d x \left[\frac{1}{2}(\partial\phi_a)^2 + \frac{\lambda_0}{4!}(\phi_a)^4 \right], \quad (3.1)$$

where a mass term has been tuned to zero. We will be interested in the model (3.1) in the presence of a spin s impurity. As in the free theory, this is modeled by inserting in the path integral the line operator (2.2). We can write the corresponding DQFT action with our constrained bosonic spinor satisfying $\bar{z}z = 2s$ similarly to eq. (2.3):

$$S = \int d^d x \left[\frac{1}{2}(\partial\phi_a)^2 + \frac{\lambda_0}{4!}(\phi_a)^4 \right] + \int_D d\tau \left[\bar{z}\dot{z} - \gamma_0 \bar{z} \frac{\sigma^a}{2} z \phi_a \right], \quad \bar{z}z = 2s. \quad (3.2)$$

The same comments below eq. (2.3) apply to the action (3.2). In this section we will analyze the theory (3.2) for $s \gg 1$. Our main findings were already summarized in the introduction in sec. 1.1.

The rest of this section is organized as follows. In subsec. 3.2 we review the diagrammatic perturbative approach to the impurity. In subsec. 3.3 we study a certain triple scaling limit, and obtain the *classical* beta-function in four dimensions. In sec. 3.4 we study the large spin fixed point within the ε expansion. Finally in sec. 3.5 we analyze the large spin limit in an arbitrary number of spacetime dimensions $d < 4$ and make some concrete predictions for the physical case of the $O(3)$ model in three spacetime dimensions.

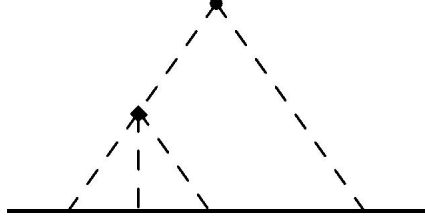


Figure 10: Diagram for the $O(\lambda\gamma^4 s^4)$ two-loop contribution to $\langle\phi_a^2(\mathbf{x}, 0)\rangle$.

3.2 Diagrammatic results

As well known, the theory (3.1) flows to a weakly coupled fixed points in $d = 4 - \varepsilon$ dimensions with $\varepsilon \ll 1$.²⁸ The theory admits the following beta function:

$$\beta_\lambda = -\varepsilon\lambda + \frac{11}{48\pi^2}\lambda^2 + O\left(\frac{\lambda^3}{(4\pi)^4}\right), \quad (3.4)$$

which leads to an IR stable perturbative fixed point at:

$$\frac{\lambda_*}{(4\pi)^2} = \frac{3}{11}\varepsilon + O(\varepsilon^2). \quad (3.5)$$

The fixed point (3.5) describes the critical $O(3)$ Wilson-Fisher model.

We now consider the theory in the presence of the defect (3.2). The diagrammatic analysis in the limit where ε is the smallest parameter proceeds similarly to that in sec. 2.2 and was performed first in [1, 2]. Here we reproduce a few results that will be necessary for what follows.

By considering corrections to the one-point function $\langle\phi_a^2(\mathbf{x}, 0)\rangle$, one easily finds that to one-loop order the beta function of the defect coupling coincides with the free theory result (2.10).²⁹ At two loops order there are several new contributions. The most important one for our purposes scales as $\lambda\gamma^4 s^4$ and arises from the two-loop diagram correction described in fig. 10. From this diagram we extract a contribution to the counterterm, which we add to the counterterm for the free bulk to obtain $\delta\gamma^2 = \frac{\gamma^4}{2\pi^2} + \frac{\lambda\gamma^4}{96\pi^2}s(s+1) + O(\lambda^3 s^0)$, from which one obtains the following beta function:

$$\beta_{\gamma^2} = -\varepsilon\gamma^2 + \frac{\gamma^4}{2\pi^2} + \frac{\lambda\gamma^4}{48\pi^2}s(s+1) + O(\varepsilon^3 s^0). \quad (3.6)$$

²⁸We remind that the bare coupling λ_0 in the minimal subtraction scheme is renormalized according to [108]:

$$\lambda_0 = M^\varepsilon \left[\lambda + \frac{\delta\lambda}{\varepsilon} + \frac{\delta_2\lambda}{\varepsilon^2} + \dots \right], \quad \delta\lambda = \frac{11}{3} \frac{\lambda^2}{(4\pi)^2} + O\left(\frac{\lambda^3}{(4\pi)^4}\right), \quad (3.3)$$

where λ is the renormalized coupling associated with the quartic interaction of the bulk theory, M is the sliding scale and, as in the previous section, we work in the $\overline{\text{MS}}$ scheme. We will not need higher orders or the value of $\delta_2\lambda$ for what follows. Also note that the wavefunction renormalization of the fundamental field starts at two-loop order and it will not be needed in what follows.

²⁹There is a divergent $O(\lambda\gamma^2 s^2)$ contribution to the correlation function, but this is renormalized by the ϕ_a^2 wavefunction.

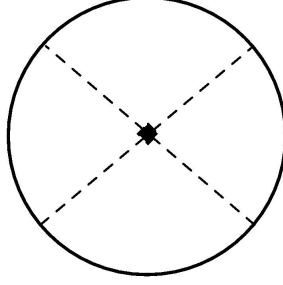


Figure 11: Diagram that contributes the leading order new contribution to the defect g -function defined in (2.16) due to the bulk self-interaction.

In deriving the above result we have used the counting $\lambda \sim \gamma^2 \sim \varepsilon$ and neglected $O(\varepsilon^4)$ (three-loop) contributions. Furthermore, we neglected $O(\varepsilon^3 s^0)$ contributions (of order $\gamma^6 s^0$, $\lambda \gamma^4 s^0$ and $\lambda^2 \gamma^2 s^0$), since we would like to think about s which is $s \gg 1$ (but not as large as to require a resummation, yet). Later on we will reproduce the $\lambda \gamma^4 s^2$ term from a classical calculation. Eq. (3.6) implies that the coupling in the IR flows to a perturbative fixed point at:

$$\gamma_*^2 = 2\pi^2 \varepsilon \left[1 - \frac{2\pi^2}{11} \varepsilon s(s+1) + O(\varepsilon s^0) \right]. \quad (3.7)$$

Various quantities of interest were computed to two-loop order in the ε expansion in [1, 2, 28, 29]. For instance, differently from the free theory case discussed in the previous section, the scaling dimension of the defect spin operator is not protected by the Ward identity (2.15) anymore, and receives a correction at order ε^2 [2]:

$$\Delta_S = \frac{\varepsilon}{2} \left[1 - \frac{2\pi^2}{11} \varepsilon s(s+1) + O(\varepsilon s^0) \right], \quad (3.8)$$

where again we retained only the largest two-loop contribution for $s \gg 1$ and neglected three-loop corrections. Clearly, the above expressions should only be trusted for $\varepsilon \rightarrow 0$ with fixed s , since otherwise one may get a negative γ_*^2 and Δ_S , which is of course disallowed.

Finally, we consider the g -function of the theory. The leading order result for the defect partition function coincides with the free theory one (2.24). At the next order we find a $\gamma^6 s^2$ correction, while the coupling λ contributes at order $\lambda^2 \gamma^2 s^2$ and $\lambda \gamma^4 s^4$.³⁰ We compute this last contribution, which is dominant for $s \gg 1$. It comes from a diagram in which four defect insertions are connected through a bulk quartic vertex (see figure 11). The leading s^4 term is obtained by neglecting all commutators and it reads:

$$\begin{aligned} \delta g_\gamma / g_0 &= - \lim_{\varepsilon \rightarrow 0} \frac{\gamma_0^4 \lambda_0}{4!} [s(s+1)]^2 \int d^4[\tau] \int d^{2-\varepsilon} x_\perp d^2 x_\parallel \prod_{i=1}^4 \frac{1}{4\pi^2 [x_\perp + x_\parallel - x_\parallel(\tau_i)]^{2-\varepsilon}} \\ &= [s(s+1)]^2 \frac{\gamma_0^4 \lambda_0}{384\pi^2}, \end{aligned} \quad (3.9)$$

³⁰One might naively expect a contribution $\lambda \gamma^2 s^2$, but this is proportional to a bulk tadpole and vanishes in dimensional regularization.

where x_{\parallel} and x_{\perp} are in the plane of the defect and perpendicular to it respectively and in the last line we used the result obtained in appendix B of [23] for the value of the integral. Adding (3.9) to the leading order (2.24) and writing the result in terms of the physical couplings γ and λ (see footnotes 11 and 28 for our conventions) we obtain:

$$\begin{aligned} \log g_{\gamma}/g_0 = & -\frac{\varepsilon}{8}s(s+1)\gamma^2 + \frac{\gamma^4 s(s+1)}{32\pi^2} + \frac{\gamma^4 \lambda [s(s+1)]^2}{768\pi^2} + O(\varepsilon^3 s^2) \\ \stackrel{\text{fix.pt.}}{=} & -\frac{\pi^2}{8}s(s+1)\varepsilon^2 + \frac{\pi^4}{44}[s(s+1)]^2\varepsilon^3 + O(\varepsilon^3 s^2) . \end{aligned} \quad (3.10)$$

3.3 The all-orders structure of perturbation theory

To begin our exploration into the physics of large s it is very useful to understand systematically the structure of the beta function and other physical quantities as a function of γ, λ, s . Our analysis in the previous subsection only allows to understand the regime of small γ, λ and fixed s , and we clearly need to go beyond that to understand the true large s limit.

By the same arguments as in the free bulk theory in section 2, as the spin s of the impurity increases the standard perturbative approach becomes less and less accurate, and eventually breaks down. It turns out that perturbation theory nicely reorganizes as an expansion in γ^2 with arbitrary functions of $\gamma^2 s, \lambda s$. This reorganization would be very useful to us, so let us prove it: We implement the rescalings $\phi_a \rightarrow \phi_a/\sqrt{\lambda}$ and $z \rightarrow \sqrt{s}z$ in eq. (3.2):

$$S = \frac{1}{\lambda} \int d^d x \left[\frac{1}{2}(\partial\phi_a)^2 + \frac{1}{4!}(\phi_a)^4 \right] + s \int d\tau \left[\bar{z}\dot{z} - \frac{\gamma}{\sqrt{\lambda}} \bar{z} \frac{\sigma^a}{2} z \phi_a \right] , \quad \bar{z}z = 2 . \quad (3.11)$$

From requiring that all terms in the action scale the same way, we obtain a new semiclassical limit:

$$\begin{aligned} s \rightarrow \infty , \quad \gamma \rightarrow 0 , \quad \lambda \rightarrow 0 , \\ \alpha = \frac{\gamma^2 s}{4\pi^2} = \text{fixed} , \quad y \equiv \frac{\sqrt{\lambda} \gamma s}{4\pi} = \text{fixed} . \end{aligned} \quad (3.12)$$

This of course reduces to the semiclassical limit (2.33) for $y = 0$, i.e. a free bulk.

From this it follows that the beta function and Δ_S admit the following expansions:

$$\beta_{\gamma^2} = \gamma^2 \left[-\varepsilon + \beta_0^{(4d)}(\alpha, y) + \gamma^2 \beta_1^{(4d)}(\alpha, y) + \dots \right] , \quad (3.13)$$

$$\Delta_S = \gamma^2 \left[\Delta_0(\alpha, y) + \gamma^2 \Delta_1(\alpha, y) + \dots \right] . \quad (3.14)$$

In (3.14) we have extended the notion of Δ_S away from the fixed point – to obtain the physical scaling dimension of the spin operator at the fixed point we must evaluate Δ_S for solutions of $\beta_{\gamma^2} = 0$.

The perturbative result (3.6) corresponds to $\beta_0 = \frac{1}{3}y^2 + \dots$ and $\beta_1 = \frac{1}{2\pi^2} + \dots$. Unlike in the free theory case, for the bulk interacting theory the leading term $\beta_0^{(4d)}(\alpha, y)$ in eq. (3.13) is nonzero.

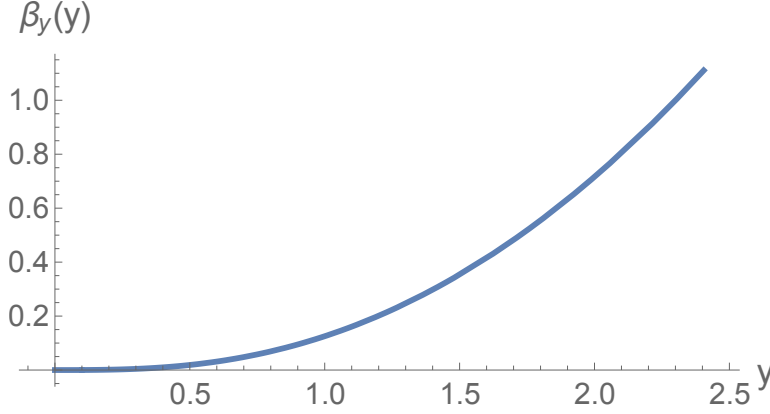


Figure 12: Plot of the 4-dimensional beta function $\beta_y(y)$ as a function of y , extracted from the solution of the saddle-point equation (given by the ODE (C.5)).

Due the semiclassical nature of the expansion (3.13), $\beta_0^{(4d)}$ can be completely understood from the properties of a new classical solution. Since developing this direction is somewhat tangential to our main thrust, we detail this conceptually and technically interesting analysis in appendix C.

For us, the most important conclusion is that $\beta_0^{(4d)}$ is only a function of y , $\beta_0^{(4d)} = \beta_0^{(4d)}(y)$ and that $\beta_0^{(4d)}(y)$ is a monotonically increasing function, implying that $\beta_0^{(4d)}(y)$ has no zeroes other than at $y = 0$. From this and fig. 12 we conclude that there is no interacting DCFT fixed point in 4 dimensions, which is not surprising. The only fixed point is the decoupled one with $y = 0$. However, the major difference from the previous section, in that we have a nonzero $\beta_0^{(4d)}$, leads to rather different conclusions also in $4 - \varepsilon$ dimensions. Since now $\beta_0^{(4d)} \neq 0$ we must solve $\varepsilon = \beta_0^{(4d)}(y)$ in order to find fixed points in $4 - \varepsilon$ dimensions. Since $\beta_0^{(4d)}(y)$ has no zeroes other than at $y = 0$ and does not tend to zero at infinity, the only solution is at infinitesimal y ,

$$y_* = \sqrt{3\varepsilon} . \quad (3.15)$$

The semiclassical approach (3.12) is very useful to understand the form of the beta function, scaling dimensions etc. We will use it further below. But there are no new fixed

points in this semiclassical limit.³¹

3.4 The phase diagram in $4 - \varepsilon$ dimensions

With the large amount of results that we have amassed both in the standard ε expansion and the semiclassical regime (3.12) we can now systematically understand the phases of the defect for small ε but arbitrary s . We will see that a major simplification occurs in the large s limit and we will argue that the same simplification happens in any number of dimensions, which would lead us, finally, to a solution of the model in $d = 3$ for large s as well.

In our exploration of the phase diagram we will fix a finite small ε and let s vary. The bulk coupling is going to be fixed to its fixed point (3.5). For small s the standard perturbative analysis holds. We find a healthy infrared DCFT. The defect coupling scales as

$$s \sim O(1), \quad d \rightarrow 4, \quad \gamma_* \sim \sqrt{\varepsilon}. \quad (3.17)$$

As we keep increasing s the corrections of order εs^2 in (3.7), (3.8) begin to increase in importance and eventually, for $\varepsilon s^2 \sim 1$ we must switch to a different description, which is accurately provided by our analysis around (3.15). Therefore for large s we find

$$s \rightarrow \infty, \quad d \rightarrow 4, \quad \gamma_* = \frac{\sqrt{11}}{s}. \quad (3.18)$$

Throughout this whole regime, and for arbitrary s , the terms beyond the three terms quoted in (3.6) always remain parametrically small, provided only that ε is sufficiently small and regardless of s .³² Therefore we can in fact find results that cover the whole range of s near four dimensions:

$$\gamma_*^2 = \frac{2\pi^2\varepsilon}{1 + 2\pi^2\varepsilon s^2/11} \left[1 - \varepsilon^{1/2} \frac{2\pi^2\sqrt{\varepsilon s^2}}{11 + 2\pi^2\varepsilon s^2} + O(\varepsilon) \right]. \quad (3.19)$$

This formula clearly interpolates between the regimes (3.17) and (3.18). For $\varepsilon s^2 \ll 1$ the fixed point (3.19) reduces to the one in eq. (3.7) that was analyzed in [1, 2, 28, 29]. In the opposite regime, $\varepsilon s^2 \gg 1$, we get the scaling (3.18) and in this regime our results are new to the best of our knowledge.

³¹Yet the results from the classical analysis, which allow to fix $\beta_0^{(4d)}(y)$, lead to a wealth of information about various perturbative corrections to the β function which correspond to high-order effects in the usual diagrammatic methods. For instance, from the next to leading order in the expansion of $\beta_0^{(4d)}(y)$ around $y = 0$ given in (C.19) (and remembering that the running of λ is subleading in four dimensions), we infer that in four dimensions

$$\beta_{\gamma^2}^{(4d)} = \frac{\lambda\gamma^4 s^2}{48\pi^2} - \frac{\lambda^2\gamma^6 s^4}{1536\pi^4} + \dots, \quad (3.16)$$

We have thus reproduced the s^2 piece of the third term from (3.6) and essentially computed a new (scheme-independent) 4-loop term which should be possible, in principle, to verify also from the standard diagrammatic approach.

³²This can be justified by a careful analysis of the implications of the structure (3.13) in the perturbative regime, together with the observation that powers of s are always multiplied by a greater than equal power of γ .

We can compute many other observables in this framework. Let us quote a few. All of them apply for arbitrary s and small ε .

Let us consider first the correlation function $\langle \phi_a^2(\mathbf{x}, 0) \rangle$. Up to order $O(\varepsilon)$ corrections, the one-point function $\langle \phi_a^2(\mathbf{x}, 0) \rangle$ coincides with the tree-level free theory result (2.8). Using eq. (3.19), at the fixed point we obtain

$$\langle \phi_a^2(\mathbf{x}, 0) \rangle \stackrel{\text{fix.pt.}}{\equiv} \frac{\mathcal{N}_d}{\mathbf{x}^{d-2}} a_{\phi^2}, \quad (3.20)$$

$$a_{\phi^2} = \frac{\pi^2 \varepsilon s^2}{2\sqrt{6}(1 + 2\pi^2 \varepsilon s^2/11)} \left[1 + \varepsilon^{1/2} \frac{1}{\sqrt{\varepsilon s^2}(1 + 2\pi^2 \varepsilon s^2/11)} + O(\varepsilon) \right]. \quad (3.21)$$

Next we consider the spectrum of defect operators, and in particular the spin operator S . Using the two-loop result in [2] and combining with (3.19) we can read the dimension of the spin operator S^a :³³

$$\Delta_S = \frac{\gamma_*^2}{4\pi^2} [1 + O(\varepsilon)] = \frac{\varepsilon/2}{1 + 2\pi^2 \varepsilon s^2/11} \left[1 - \varepsilon^{1/2} \frac{2\pi^2 \sqrt{\varepsilon s^2}}{11 + 2\pi^2 \varepsilon s^2} + O(\varepsilon) \right]. \quad (3.22)$$

From the beta-function we obtain the scaling dimension $\Delta_{S \cdot \phi}$ of the perturbation $S^a \phi_a$:

$$\gamma_{S \cdot \phi} = \Delta_{S \cdot \phi} - 1 = \left. \frac{\partial \beta_{\gamma^2}}{\partial \gamma^2} \right|_{\beta_{\gamma^2}=0} = \varepsilon + O(\varepsilon^2). \quad (3.23)$$

Finally we consider the g -function of the theory at the fixed point. We find that this is given by the diagrammatic result (3.10) up to relative $O(\varepsilon)$ corrections. At the fixed point the result reads:

$$\log g_\gamma/g_0 \stackrel{\text{fix.pt.}}{\equiv} -\frac{\pi^2 s^2 \varepsilon^2}{8(1 + 2\pi^2 s^2 \varepsilon/11)} \left[1 + \varepsilon^{1/2} \frac{1}{\sqrt{\varepsilon s^2}(1 + 2\pi^2 s^2 \varepsilon/11)} + O(\varepsilon) \right]. \quad (3.24)$$

The result is negative for arbitrary values of εs^2 in agreement with the attractive nature of the fixed point. Away from the fixed points, the result (3.10) satisfies:

$$\gamma^2 \frac{\partial \log g_\gamma/g_0}{\partial \gamma^2} = \frac{s(s+1)}{8} \beta_{\gamma^2}, \quad (3.25)$$

from which it is possible to check that the defect entropy obtained from eq. (3.10) obeys the gradient formula (2.28).

³³Incidentally, we notice that the extrapolation of eq. (3.22) to $\varepsilon \rightarrow 1$ and $s = 1/2$ gives $\Delta_S \approx 0.1 \div 0.3$, which is not too different from the result $\Delta_S = 0.20(1)$ of Quantum Monte Carlo simulations [30].

3.5 Large spin impurity as a pinning field

3.5.1 An interpretation of the small ε results for large s

Above we have quoted several predictions, valid for small ε and large s . Here we would like to give an alternative description of the large s limit. To motivate it consider (3.22) in the large s limit: $\Delta_S \sim 1/s^2$. Therefore the spin operator on the defect becomes decoupled at large s . This suggests that the large s theory might have a free sector.

We claim that at large s the defect (2.3) flows to the pinning field DCFT in which the symmetry $O(3)$ is explicitly broken to $O(2)$ but in addition there is a decoupled QM with $2s+1$ degrees of freedom which induces, at large s , an integral over the direction of the magnetic field inside $SO(3)$ so that the full system at large s is still manifestly $SO(3)$ invariant.

Therefore, the large s limit is identified with the DCFT that describes a localized (pinning) magnetic field, averaged over the two sphere. The z variables do not fluctuate at large s , which is why the dimension Δ_S tends to zero in that limit. This picture receives $1/s$ corrections that we will later compute.

The advantage of this new description at very large s is that a lot is known about the $O(N)$ theories with a localized magnetic field [23]. (We will also briefly review it in the next section.) In particular a lot is also known about the pinning field also away from the ε expansion, allowing us to make rigorous predictions also in $d=3$. For now, however, we focus on matching some of the explicit calculations above at large s with the previously-known results about the pinning field DCFT, finding remarkable agreement.

The mysterious $\sqrt{11}$ factor in (3.18) can now be simply understood. Since the z degrees of freedom do not fluctuate at large s , $\gamma_* s$ is simply the magnitude of the effective localized magnetic field in the fixed point. The magnitude of the effective localized field was found to leading order in [23] to be $\sqrt{N+8}$ in the $O(N)$ theory. Plugging $N=3$ we see that this nicely matches the $\sqrt{11}$ factor. As another example, the large s limit of (3.24) gives $\log g_\gamma/g_0 \rightarrow \frac{-11\varepsilon}{16}$, while for the localized magnetic field defect it was found in [23] that the leading order result for $\log g$ is $-\frac{8+N}{16}\varepsilon$, which again nicely matches our present result upon plugging $N=3$. Finally, for the one-point function (3.21) we obtain in the large s limit $a_{\phi^2} = \frac{11}{4\sqrt{6}}$. The corresponding one-point function in the pinning field DCFT was computed in [23] for small ε and exactly the same result was found.

The fact that the large s limit of the spin impurity is described by the pinning field with an integration over the direction of the external magnetic field is correct not only at the infrared DCFT – it extends to the RG flow, as the reader can verify.

3.5.2 Equivalence with the pinning field defect at large s

On the one hand, we have the large s limit of the spin impurity which, in the lattice system, would describe an external atom with large spin interacting with the bulk in an $SO(3)$ invariant fashion. On the other hand, we have the $SO(3)$ system with an external, localized in space, magnetic field, explicitly breaking $SO(3)$ to $SO(2)$.

These two systems are essentially claimed to be equivalent at $s \rightarrow \infty$, after properly averaging over the direction of the external localized magnetic field inside $SO(3)$. We have demonstrated this equivalence close to four dimensions above.

In fact this equivalence extends to any d . Furthermore, at large finite s one can set up a systematic perturbation theory around the pinning field DCFT and hence we have a systematic $1/s$ expansion at hand in any d . The leading coupling between the two sectors is through the tilt operator of the pinning DCFT which allows us to control the $1/s$ expansion.

The purpose of this section is to formalize the above statements and show some examples of how the $1/s$ expansion around the pinning field DCFT can be performed. We will use this correspondence to write down some explicit predictions about the large s limit of the spin impurity in $d = 3$ as well as to discuss $1/s$ corrections in $d = 3$.³⁴

Let us formally consider the path integral for an arbitrary observable \mathcal{O} in the DQFT that we obtain by coupling the $O(3)$ critical model in arbitrary $d \leq 4$ to the spin s impurity:

$$\langle \mathcal{O} \rangle = \mathcal{Z}^{-1} \int_{\bar{z}z=2} \mathcal{D}\phi \mathcal{D}z \mathcal{O} \exp \left(-S_{O(3)} - s \int_D d\tau \bar{z}\dot{z} - \gamma_0 s \int_D d\tau \bar{z} \frac{\sigma^a}{2} z \phi_a \right), \quad (3.26)$$

where as usual we work in the normalization $\bar{z}z = 2$, $\mathcal{D}\phi e^{-S_{O(3)}}$ is a formal notation for the measure of the (generically strongly coupled) path integral describing the $O(3)$ critical point and \mathcal{Z} is the vacuum partition function.

We have argued that in the large s limit the fluctuations of the z variables are suppressed and hence in the $s \gg 1$ limit we should expand around a constant profile for the quantum-mechanical spinor:

$$\bar{z} \frac{\sigma^a}{2} z = \hat{n}^a = \text{const}. \quad (3.27)$$

We therefore recast the path integral (3.26) as:

$$\langle \mathcal{O} \rangle = \mathcal{Z}^{-1} \int_{S^2} d^2 \hat{n} \int \mathcal{D}\phi \mathcal{D}\chi \mathcal{O} \exp \left[-S_{O(3)} - \int_D d\tau \bar{\chi} \dot{\chi} - \gamma_0 s \int_D d\tau \hat{n}^a \phi_a + O \left(\frac{1}{\sqrt{s}} \right) \right], \quad (3.28)$$

where we separated the two-dimensional integral over the zero-mode rotating \hat{n} from the path integral over the τ -dependent fluctuations defined similarly to eq. (2.44). In eq. (3.28) we neglected a $\sim \gamma_0 \sqrt{s}$ coupling between ϕ_a and the fluctuation χ , as this is $1/\sqrt{s}$ suppressed compared to the $\gamma_0 s \hat{n}^a \phi_a$ term. Therefore (3.28) is a useful description at very large s .

³⁴As in the rest of this paper, our analysis will concern only with the DCFT at zero temperature; in the future it would be interesting to study with this method also thermal susceptibilities, for which results from Quantum Monte Carlo simulations are available [30, 31].

Let us now imagine performing the path integral over ϕ and the fluctuations χ for a fixed direction \hat{n} . The variable χ is decoupled from the bulk field up to $1/\sqrt{s}$ corrections. The path integral over ϕ coincides with the one obtained by perturbing the critical $O(3)$ model with a *pinning* magnetic field $h = \gamma_0 s$ localized on a line. This is precisely the setup which defines the pinning field DCFT studied in [23]. Let us briefly review this construction.

Consider for a moment a general Wilson-Fisher $O(N)$ fixed point. We can consider perturbing it with a magnetic field h localized on a line as:

$$\delta S = h \int_D d\tau \hat{n}^a \phi_a. \quad (3.29)$$

The coupling h breaks $O(N) \rightarrow O(N-1)$ explicitly and constitutes a relevant perturbation of the trivial line defect. The g -theorem implies that the RG flow results in a stable nontrivial DCFT in the IR; we will call such a DCFT the *pinning* field DCFT in the following. The pinning field DCFT is obviously strongly coupled in $d = 3$, but it admits a perturbative description in the ε expansion or in the large N -limit, for which several results were obtained in [23] (see also [40]). Additionally, a few Monte Carlo results for $N = 1$ and $N = 3$ were obtained in [22] (see also [39]).

We conclude that, neglecting $1/s$ corrections, the ϕ path integral in the IR coincides with that of the $O(3)$ pinning field DCFT. We therefore obtain

$$\langle \mathcal{O} \rangle_{\text{IR}} = \mathcal{Z}_{\text{IR}}^{-1} \int_{S^2} d^2 \hat{n} \int \mathcal{D}\phi \mathcal{D}\chi \mathcal{O} \exp \left[-S_{\text{pinning}}(\hat{n}) - \int_D d\tau \bar{\chi} \dot{\chi} + O\left(\frac{1}{\sqrt{s}}\right) \right], \quad (3.30)$$

where $\mathcal{D}\phi e^{-S_{\text{pinning}}(\hat{n})}$ is a formal notation for the path integral measure associated with the pinning field DCFT, which is obtained perturbing the $O(3)$ Wilson-Fisher critical point with a localized magnetic field in the direction \hat{n} . The observable $\langle \mathcal{O} \rangle_{\text{IR}}$ is therefore computed in a product of the free theory of the fluctuations χ and the pinning field DCFT.

We will discuss the $1/\sqrt{s}$ corrections in the next subsection. Finally, the zero-mode integral in eq. (3.30) restores the $SO(3)$ symmetry by averaging over the direction of the symmetry breaking field $h\hat{n}$. Notice that the partition function \mathcal{Z}_{IR} has a similar expression, and thus for $s \gg 1$ it factorizes as follows:

$$\mathcal{Z}_{\text{IR}} = 4\pi \times \mathcal{Z}_{\text{pinning}} \times \mathcal{Z}_{\chi} \times \left[1 + O\left(\frac{1}{s}\right) \right], \quad (3.31)$$

where the factor $4\pi = \int d^2 \hat{n}$ arises from the zero-mode integral, and the remaining terms are associated with the two decoupled path integrals.

The relation (3.30) between the pinning field DCFT and the $s \rightarrow \infty$ limit of the impurity is one of our main results, as it provides access to the large s limit of the spin impurity and also, as we will see, allows to consider $1/s$ corrections systematically.³⁵ In the following we will illustrate some implications by discussing specific observables.

³⁵In fact, as eq. (3.28) shows, the relation holds also for the DQFTs away from the fixed points.

The simplest observables to be discussed are bulk one-point functions. In the pinning field DCFT, one finds the following results for the normalized one-point functions of ϕ_a and ϕ_a^2 :

$$\begin{aligned}\frac{\langle \phi_a(\mathbf{x}, 0) \rangle_{\text{pin}}}{\sqrt{\langle \phi_1(\infty) \phi_1(0) \rangle_{O(3)}}} &= \hat{n}_a \frac{a_{\phi}^{(\text{pin})}}{|\mathbf{x}|^{\Delta_{\phi}}}, \\ \frac{\langle \phi_a^2(\mathbf{x}, 0) \rangle_{\text{pin}}}{\sqrt{\langle \phi_a^2(\infty) \phi_b^2(0) \rangle_{O(3)}}} &= \frac{a_{\phi^2}^{(\text{pin})}}{|\mathbf{x}|^{\Delta_{\phi^2}}},\end{aligned}\tag{3.32}$$

where Δ_{ϕ} and Δ_{ϕ^2} are the corresponding bulk scaling dimensions (see e.g. [24–26]), the subscript $\langle \dots \rangle_{\text{pin}}$ denotes pinning field correlators and we normalized by the two-point functions in the absence of a defect, distinguished by the subscript $\langle \dots \rangle_{O(3)}$. The coefficients $a_{\phi}^{(\text{pin})}$ and $a_{\phi^2}^{(\text{pin})}$ were computed in [23] in the ε expansion (to one-loop order) and in the large N limit.

To relate (3.32) with one-point functions in the presence of a spin $s \gg 1$ impurity all we have to do is to integrate over the zero-mode. Clearly this simply projects one-point functions onto the singlet sector and thus we find:

$$\begin{aligned}\frac{\langle \phi_a(\mathbf{x}, 0) \rangle}{\sqrt{\langle \phi_1(\infty) \phi_1(0) \rangle_{O(3)}}} &= 0, \\ \frac{\langle \phi_a^2(\mathbf{x}, 0) \rangle}{\sqrt{\langle \phi_a^2(\infty) \phi_b^2(0) \rangle_{O(3)}}} &= \frac{a_{\phi^2}^{(\text{pin})}}{|\mathbf{x}|^{\Delta_{\phi^2}}} \left[1 + O\left(\frac{1}{s}\right) \right].\end{aligned}\tag{3.33}$$

We have already checked in the previous section that this method agrees with explicit computations in the large s limit of the spin impurity near four dimensions, as both approaches give $a_{\phi^2} = \frac{11}{4\sqrt{6}}$. For $d = 3$ there is not yet a prediction for $a_{\phi^2}^{(\text{pin})}$ of the pinning field DCFT that is entirely reliable, however, even in the absence of such a prediction, our methods show that the two quantities should agree between an impurity at large spin and an localized magnetic field in the infrared.

The lowest dimensional operator (other than the unit operator) of the pinning field DCFT is the *tilt* operator $\hat{t}_{\hat{a}}$, where the index \hat{a} runs over the components orthogonal to \hat{n} . The tilt is thus an $O(2)$ vector and its dimension is protected to be 1 nonperturbatively in the pinning field DCFT. This predicts that at large s the spin impurity DCFT must have an $SO(3)$ vector defect operator that we denote $\hat{\phi}_a$, whose scaling dimension is therefore marginal to leading order in s :

$$\Delta_{\hat{\phi}_a} = 1 + O\left(\frac{1}{s}\right).\tag{3.34}$$

The existence of a marginal operator is a highly non-generic fact for the spin impurity DCFT and therefore constitutes a very nontrivial prediction of our approach!

In fact, one can construct several marginal composites made out of $\hat{\phi}_a$ and S , since they are decoupled at leading order in the $1/s$ expansion and S has scaling dimension 0 at leading order.

We will now analyze these composites and their quantum numbers. First let us construct the $SO(3)$ vector $\hat{\phi}_a$ from the tilt operator $\hat{t}_{\hat{a}}$ of the pinning field DCFT. The procedure is completely analogous to the one used in the pion Lagrangian to construct operators transforming in a $SU_L(N_f) \times SU_R(N_f)$ representation out of operators linearly transforming in a representation of the diagonal subgroup [89]. We discuss it below for completeness.

It is convenient to define a $SO(3)$ matrix $\tilde{\Omega}_n^{-1}$ which aligns the saddle-point in the direction “1”:

$$(\tilde{\Omega}_n^{-1})_b^a \hat{n}^b = \delta_1^a. \quad (3.35)$$

Using this matrix we can now parametrize the space dependent fluctuations χ and $\bar{\chi}$ precisely as in eqs. (2.43) and (2.44) of sec. 2.3.2. For our purposes, it is convenient to do this as follows

$$\bar{z} \frac{\sigma^a}{2} z = (\tilde{\Omega}_n)_b^a (\Omega_{\chi, \bar{\chi}})_c^b \delta_1^c = (\Omega_{\text{full}})_b^a \hat{n}^b, \quad (3.36)$$

where we defined two other matrices as

$$\Omega_{\chi, \bar{\chi}} = e^{-i\delta\phi Q_3} e^{-i\delta\theta Q_2}, \quad \Omega_{\text{full}} = \tilde{\Omega}_n \Omega_{\chi, \bar{\chi}} \tilde{\Omega}_n^{-1}; \quad (3.37)$$

the relation between $\delta\theta$, $\delta\phi$ and χ , $\bar{\chi}$ is as in eq. (2.44), and $(Q_a)_c^b = -i\varepsilon_{abc}$ are the $SO(3)$ matrices in the fundamental representation.

It is now straightforward to use the $SO(3)/SO(2)$ coset in eq. (3.37) to construct a vector out of the pinning field tilt operator $\hat{t}_{\hat{a}}$. This is simply done as:

$$\hat{\phi} = \Omega_{\text{full}} \cdot \hat{t} = \tilde{\Omega}_n \cdot \Omega_{\chi, \bar{\chi}} \cdot \begin{pmatrix} 0 \\ \hat{t}_2 \\ \hat{t}_3 \end{pmatrix} = \tilde{\Omega}_n \cdot \begin{pmatrix} \hat{t}_3 \frac{\chi + \bar{\chi}}{\sqrt{2s}} + i\hat{t}_2 \frac{\chi - \bar{\chi}}{\sqrt{2s}} + O\left(\frac{1}{s^{3/2}}\right) \\ \hat{t}_2 + O\left(\frac{1}{s}\right) \\ \hat{t}_3 + O\left(\frac{1}{s}\right) \end{pmatrix}, \quad (3.38)$$

where we defined in obvious notation

$$\begin{pmatrix} 0 \\ \hat{t}_2 \\ \hat{t}_3 \end{pmatrix} \equiv \tilde{\Omega}_n^{-1} \cdot \hat{t}. \quad (3.39)$$

A similar analysis allows to reconstruct operators in the $2n' + 1$ dimensional $SO(3)$ representation out of pinning field operators with charge n under $O(2)$ as long as $n' \geq |n|$. Notice also that the operator (3.38) so defined is orthogonal to the impurity spin, $S \cdot \hat{\phi} = 0$, and therefore we cannot build $O(3)$ singlets by considering composites of S and $\hat{\phi}$. In the large s limit there is therefore no marginal singlet of $SO(3)$ but there is a marginal vector of $SO(3)$ (and in fact there is a marginal operator of any positive integer spin), as we said.

It was argued in [23] that the lowest dimensional neutral defect operator (besides the identity) in the pinning field DCFT is irrelevant and it is identified with the infrared version of the perturbation $\hat{\phi}_n \equiv \hat{n}^a \phi_a|_{\mathbf{x}=0}$ on the defect. On the impurity side of our correspondence, this operator is naturally identified with the infrared version of the operator coupling the

impurity spin with the bulk order parameter, $(S \cdot \phi) \equiv S^a \phi_a \simeq s \hat{n}^a \phi_a + O(\sqrt{s})$. From the results of [23] we conclude that its scaling dimension reads:³⁶

$$\Delta_{S \cdot \hat{\phi}} = \Delta_{\phi_n}|_{\text{pin}} + O\left(\frac{1}{s}\right), \quad \Delta_{\hat{\phi}_n}|_{\text{pin}} = \begin{cases} 1 + \varepsilon + O(\varepsilon^2) & \varepsilon = 4 - d \ll 1, \\ \sim 1.55 & d = 3. \end{cases} \quad (3.40)$$

Again, we happily find that the epsilon expansion result from the pinning field DCFT in eq. (3.40) matches the independent calculation of the previous section, whose result in eq. (3.23) does not depend on s to one-loop order. In $d = 3$, eq. (3.40) makes a concrete prediction for the scaling dimension of the leading irrelevant (symmetry preserving) perturbation of the spin impurity DCFT for $s \gg 1$. This concludes our discussion of the defect operator spectrum to leading order.

Finally, we comment that the equivalence (3.30) implies that the g -function of the defect is given by the product of the pinning field g -function and that of a decoupled spin s impurity:

$$g = g_{\text{pin}} g_0 \left[1 + O\left(\frac{1}{s}\right) \right], \quad (3.41)$$

where $g_0 = 2s + 1$. Since the pinning field g function satisfies $g_{\text{pin}} < 1$, we see that $g < 2s + 1$ and is hence consistent with the g theorem. Further, in the previous subsection we checked (3.41) near four dimensions.³⁷

3.5.3 Subleading corrections

The $1/s$ corrections to the factorized ansatz (3.30) are quite interesting. As we show below, their form is fixed by the requirement that the path integral is $SO(3)$ invariant. The interesting problem is to write down the couplings that restore the $SO(3)$ invariance of the fixed point using the pinning field infrared DCFT operators. Our analysis will be analogous to and inspired by that in [109]. In what follows, we assume for simplicity that all bulk and defect operators of the pinning field DCFT have canonically normalized two-point functions.

Working at leading order in the fields, the most general form of the interaction term involves a linear coupling between the angular fluctuations $\delta\theta$, $\delta\phi \sim O(1/\sqrt{s})$ and the pinning

³⁶The result for $d = 3$ was obtained in [23] interpolating between a two-loop epsilon expansion calculation and the two-dimensional exact value; it is in agreement with the large N prediction and the Monte Carlo estimate of [22].

³⁷One can similarly extend the discussion to correlation functions, matching large s correlators of the spin impurity and the pinning field correlation functions. Consider for concreteness the two-point function of the bulk order parameter ϕ_a . In the pinning field DCFT it is convenient to decompose it in parallel and orthogonal components to the magnetic field $h\hat{n}$:

$$\phi_a \stackrel{\text{pinning}}{=} \hat{n}_a \phi_n + \phi_a^\perp. \quad (3.42)$$

We then obtain for the two-point function of ϕ_a in the $SO(3)$ invariant impurity case:

$$\langle \phi_a(x) \phi_b(0) \rangle = \frac{\delta_{ab}}{3} \left[\langle \phi_n(x) \phi_n(0) \rangle_{\text{pin}} + \langle \phi_c^\perp(x) \phi_c^\perp(0) \rangle_{\text{pin}} \right] + O\left(\frac{1}{s}\right). \quad (3.43)$$

field tilt operator. In the notation (3.39) this reads:

$$S_{\text{int}} = -\kappa \int_D d\tau (\hat{t}_2 \delta\phi - \hat{t}_3 \delta\theta) + \delta S + \dots, \quad (3.44)$$

where the structure of the coupling is fixed by $SO(2)$ invariance, δS consist of counterterms that are adjusted to ensure $SO(3)$ invariance order by order in $1/s$ and we neglected additional interactions that will not play a role in what follows, including those arising from the expansion of the kinetic term $\bar{z}\dot{z}$ and nonlinear couplings between the tilt operator and the angular fluctuations. Because the tilt operator has dimension 1, the coupling (3.44) is dimensionless.

We now want to argue that the coupling κ is fixed by $SO(3)$ invariance. To this aim, we momentarily consider the pinning field theory that we obtain by freezing $\hat{n}^a = \delta_1^a$. In this theory we have:

$$\langle \phi_1(\mathbf{x}, 0) \rangle = \frac{a_\phi^{(\text{pin})}}{|\mathbf{x}|^{\Delta_\phi}}, \quad \langle \phi_2(\mathbf{x}, 0) \rangle = \langle \phi_3(\mathbf{x}, 0) \rangle = 0. \quad (3.45)$$

If we rotate \hat{n} by an infinitesimal angle α in the direction “2”, we should find:

$$\langle \phi_2(\mathbf{x}, 0) \rangle \simeq \alpha \frac{a_\phi^{(\text{pin})}}{|\mathbf{x}|^{\Delta_\phi}}. \quad (3.46)$$

At the same time, an infinitesimal rotation of the unit vector \hat{n} can be understood as originating from an infinitesimal perturbation proportional to the tilt operator. Locality implies that the coefficient of this perturbation exactly coincides with the coupling in eq. (3.44). Therefore, setting $\delta\theta = 0$ and $\delta\phi = \alpha$ in eq. (3.44) we conclude that we can express the one-point function of ϕ_2 as:

$$\begin{aligned} \langle \phi_2(\mathbf{x}, 0) \rangle &\simeq \alpha \kappa \int_D d\tau \langle \phi_2(\mathbf{x}, 0) \hat{t}_2(\tau) \rangle = \alpha \kappa \int_D d\tau \frac{b_{\phi\hat{t}} |\mathbf{x}|^{1-\Delta_\phi}}{(\mathbf{x}^2 + \tau^2)} \\ &= \alpha \frac{\pi \kappa b_{\phi\hat{t}}}{|\mathbf{x}|^{\Delta_\phi}}. \end{aligned} \quad (3.47)$$

In eq. (3.47) we used that the scaling dimension of the tilt operator is 1 and that the bulk-to-defect two-point function of ϕ and the tilt is completely fixed in terms of a single OPE coefficients $b_{\phi\hat{t}}^{(\text{pin})}$ [110, 111], defined as:

$$\phi_{\hat{a}}(\mathbf{x}, 0) \sim \frac{b_{\phi\hat{t}}^{(\text{pin})}}{|\mathbf{x}|^{\Delta_\phi-1}} \hat{t}_{\hat{a}}(0) + \dots \quad (3.48)$$

By comparing eqs. (3.46) and (3.47) we conclude:

$$\kappa = \frac{a_\phi^{(\text{pin})}}{\pi b_{\phi\hat{t}}^{(\text{pin})}}. \quad (3.49)$$

We have therefore expressed κ in terms the pinning field DCFT data, $a_\phi^{(\text{pin})}$ and $b_{\phi\hat{t}}^{(\text{pin})}$.

We can now use the result (3.49) to compute the leading nontrivial correction to the scaling dimension of the impurity spin operator in terms of the DCFT coefficients $a_{\phi}^{(\text{pin})}$ and $b_{\phi\hat{t}}^{(\text{pin})}$. To this aim, we notice that the free propagator for the fluctuations χ reads:

$$G_{\chi}(\tau) = \langle \chi(\tau) \bar{\chi}(0) \rangle_{s \rightarrow \infty} = \frac{1}{2} \text{sgn}(\tau) + \text{const} , \quad (3.50)$$

where the constant term drops from all physical observables (its value depends on the boundary conditions, which are not important for what follows). Using eq. (3.50), we immediately find that:

$$\begin{aligned} \langle S^a(\tau) S^a(0) \rangle &= s^2 + s \langle \bar{\chi}(\tau) \chi(0) + \bar{\chi}(0) \chi(\tau) - \bar{\chi}(\tau) \chi(\tau) - \bar{\chi}(0) \chi(0) \rangle_{s \rightarrow \infty} + O(s^0) \\ &= s(s+1) + O(s^0) , \end{aligned} \quad (3.51)$$

where we remind that, as explained below eq. (2.4), the equal time product is regulated by a point-splitting procedure $\bar{\chi}(\tau) \chi(\tau) = \lim_{\eta \rightarrow 0^+} \bar{\chi}(\tau + \eta) \chi(\tau)$. To obtain the anomalous dimension of the operator S^a we need to compute the logarithmic $O(s^0 \log |\tau|)$ corrections to eq. (3.51). These arise upon lowering twice the interaction term between the tilt and the angular fluctuations (3.44), which in terms of χ reads:³⁸

$$S_{int} \supset -\frac{\kappa}{\sqrt{2s}} \int_D d\tau [\chi(\hat{t}_3 + i\hat{t}_2) + \bar{\chi}(\hat{t}_3 - i\hat{t}_2)] . \quad (3.52)$$

Using that $\langle \hat{t}_a(\tau) \hat{t}_b(0) \rangle = \delta_{ab}/\tau^2$, the logarithmic correction arises from³⁹

$$\begin{aligned} \delta \langle S^a(\tau) S^a(0) \rangle &= \kappa^2 \int_D d\tau_1 \int_D d\tau_2 \frac{G_{\chi}(\tau - \tau_1) G_{\chi}(\tau_2) + G_{\chi}(-\tau_1) G_{\chi}(\tau_2 - \tau)}{(\tau_1 - \tau_2)^2} + \dots \\ &\sim -2\kappa^2 \log(|\tau|\Lambda) , \end{aligned} \quad (3.53)$$

where Λ is a cutoff scale and we neglected all τ -independent contributions. Using eq. (3.53) we can write:

$$\langle S^a(\tau) S^a(0) \rangle = s(s+1) - 2\kappa^2 \log(|\tau|\Lambda) + O(s^0 |\tau|^0) \approx \frac{s(s+1)}{|\tau|^{2\kappa^2/s^2}} . \quad (3.54)$$

Therefore, using (3.49), we finally obtain the result:

$$\Delta_S \simeq \frac{\kappa^2}{s^2} = \frac{1}{s^2} \left(\frac{a_{\phi}^{(\text{pin})}}{\pi b_{\phi\hat{t}}^{(\text{pin})}} \right)^2 . \quad (3.55)$$

³⁸The $1/s$ interaction terms arising from the expansion of the kinetic term exist also for a free decoupled impurity and thus cannot change the result (3.51); the counterterms in δS are needed instead only to compute the τ -independent term.

³⁹A simple way to isolate the logarithmic contribution that we are interested in is to compute $\frac{\partial^2}{\partial \tau \partial \tau'} \langle S^a(\tau) S^a(\tau') \rangle$ for $\tau \neq \tau'$ and then integrate the result twice. To order $O(s^0)$, only the terms explicitly shown in the first line of eq. (3.53) yield a nontrivial contribution to the derivative (where for arbitrary $\tau' \neq 0$ we should change $G_{\chi}(\tau_2) \rightarrow G_{\chi}(\tau_2 - \tau')$ and $G_{\chi}(-\tau_1) \rightarrow G_{\chi}(\tau' - \tau_1)$). The result then follows immediately using eq. (3.50).

This prediction for the dimension of the spin field can be explicitly tested in the epsilon expansion. To this aim, we use that at leading order in the epsilon expansion the tilt and the fundamental field coincide in the pinning field DCFT, and thus $b_{\phi\hat{t}} = 1$. Using $a_{\phi}^{(\text{pin})} = \sqrt{\frac{11}{4}} + O(\varepsilon)$ which was derived in [23], we find:

$$\Delta_S \approx \frac{11}{4\pi^2 s^2}. \quad (3.56)$$

Eq. (3.56) exactly agrees with the large εs^2 limit of the anomalous dimension explicitly computed in eq. (3.22). This provides a very nontrivial check of our methodology.

By using eq. (3.49) in eq. (3.44) we can in principle compute (or parameterize) $1/s$ corrections to other observables as well. In practice, this is generically hard to do without more data about the pinning field DCFT, since, for instance, corrections to bulk one- and two-point functions are proportional to integrals of three- and four-point bulk to defect correlation functions, whose form is not fully constrained by symmetry and about which we generically know little at the moment.

4 Wilson lines in large representations

In the previous section we demonstrated that impurities in the large spin limit can be studied in a semiclassical expansion in inverse powers of s . It is therefore natural to wonder if similar results hold for other line defects. A natural setup is provided by Wilson and 't Hooft lines in four-dimensional conformal gauge theories, in the limit in which the size s of the labelling representation becomes large. In this section we will make comments about an effective field theory which captures the large s limit and corrections thereof for 1/2-BPS Wilson lines in SCFTs. We begin, however, from some comments about the more general case.

4.1 Comments about non-supersymmetric Wilson lines in large representations

Consider for concreteness a generic $SU(2)$ conformal gauge theory; for instance, this could be the infrared phase of a $SU(2)$ gauge field coupled to five Weyl fermions in the adjoint [112], or one of the several familiar supersymmetric conformal gauge theories we will discuss later. We are interested in the DCFT that we obtain by considering the theory in the presence of a Wilson line in the $2s + 1$ -dimensional representation:

$$D_s = \text{Tr}_{2s+1} \left[P \exp \left(i \int_C dx^\mu A_\mu \right) \right]. \quad (4.1)$$

By the defect version of the state-operator correspondence [113], the DCFT spectrum is obtained quantizing the theory on the conformally flat manifold $AdS_2 \times S^2$:

$$ds^2 = R^2 \left(\frac{d\tau^2 + dr^2}{r^2} + d\Omega_2^2 \right) = \frac{ds_{\text{flat}}^2}{r^2} \quad (4.2)$$

where $d\Omega_2^2$ is the S^2 metric and R is the radius of both AdS_2 and S^2 . The defect sits at the boundary of AdS_2 , $r = 0$, and we work in Euclidean signature.

Arguments essentially identical to those we have seen in the previous section concerning impurities in the Wilson-Fisher magnets, lead to the following picture for the large s limit of Wilson lines: The world-line degrees of freedom are expected to be frozen which means that the color of the probe quark is approximately fixed at large s . This creates a large Coulomb potential $A_\tau \sim sg_{\text{YM}}^2/r$ in the direction of the color of the quark (g_{YM} schematically represents the gauge coupling of the conformal gauge theory; it could be order $O(1)$).

Such a Coulomb potential leads to an electric field. In $AdS_2 \times S^2$ this defines a constant scale

$$m_{\text{el}}^2 \equiv |F_{\tau r}^2 g^{\tau\tau} g^{rr}|^{1/2} \sim \frac{sg_{\text{YM}}^2}{R^2} . \quad (4.3)$$

For $sg_{\text{YM}}^2 \gg 1$, which is certainly achievable at large s , this defines a scale much larger than the radius of $AdS_2 \times S^2$

$$1/R \ll m_{\text{el}} . \quad (4.4)$$

To understand an effective theory description below the scale m_{el} we can consider the infinite volume limit $R \rightarrow \infty$ with fixed m_{el} .⁴⁰ The infinite volume limit would constrain the EFT allowing to use the full power of the symmetries in flat space. We should be therefore considering conformal gauge theories in the background of a constant electric field at the scale (4.3) in flat space. One generically expects an instability related to the Schwinger effect [123].⁴¹ At present, the implications of such an instability are not clear to us. For this reason we will not pursue an EFT description of the Wilson lines (4.1). We plan to come back to this issue in the future.

We will instead analyze in detail the case of a 1/2-BPS loop in $\mathcal{N} = 2$ rank-1 superconformal gauge theories. The fundamental difference in this case, as we will soon explain, is that in addition to the scale set by the electric field there is another, larger, gauge invariant scale which clearly gaps out all degrees of freedom other than an Abelian $\mathcal{N} = 2$ vector supermultiplet. This will allow us to set up an EFT and we will show that the EFT predictions remarkably agree with exact results obtained via localization. This provides a highly nontrivial check of our approach.

⁴⁰This is what one calls the macroscopic limit, which plays an important role in the study of heavy operators in CFTs [13, 114, 115]. Particularly relevant for us is the case of large charge operators in conformal field theories invariant under internal symmetries [19–21]. In that case, the state-operator correspondence and EFT techniques enables the study of correlation functions of operators charged under the internal group in an expansion in inverse powers of their charge. It is perhaps related to the present setup that in that context it was argued that such a universal EFT description also applies to monopole operators in $3d$ gauge theories [116, 117], which are roughly analogous to 't Hooft lines in $4d$ gauge theories (see [118–121]). It was also found that large charge defect operators in boundary and defect CFTs admit a semiclassical description [91, 122].

⁴¹We thank O. Aharony, S. Bolognesi and E. Rabinovici for discussions on this. Such an instability was studied in holographic CFTs too [124, 125].

4.2 Supersymmetric Wilson loop in $\mathcal{N} = 2$ SCFTs

In this subsection we will provide an analysis of 1/2-BPS Wilson loops in large representations for the case of rank-1 $\mathcal{N} \geq 2$ SCFTs. As already mentioned in the introduction, our analysis will also be of interest for non-Lagrangian theories, in which case superconformal defects are roughly labeled by the electric and magnetic charges of their IR representation in the Coulomb branch of the theory [68, 70, 74]. For these theories our description is expected to apply to defects with large electric or magnetic charge. For Lagrangian models we will be able to explicitly verify our predictions against exact localization results [67, 78].

In Lagrangian theories, the 1/2-BPS loops take a form similar to (4.1) except that we must also include the real part of the vector multiplet scalar:

$$D_s^{\text{BPS}} = \text{Tr}_{2s+1} \left[P \exp \left(\int_C dt (i\dot{x}^\mu A_\mu + |\dot{x}| \Phi) \right) \right]. \quad (4.5)$$

There is a SUSY-breaking generalization of these line operators where the coefficient of the vector multiplet scalar is arbitrary but we will not discuss it here.⁴²

The crucial new element in (4.5) is that the 1/2-BPS Wilson loop sources both the scalar (ϕ) and the gauge (A_μ) components of the $\mathcal{N} = 2$ vector multiplet [65] in the direction of the color of the probe quark. After performing the mapping to $AdS_2 \times S^2$ again, we therefore have $A_\tau \sim sg_{\text{YM}}^2/r$ and $\phi \sim sg_{\text{YM}}^2/R$. The novelty here is that in addition to the electric field scale (4.3) we have a new gauge-invariant scale

$$m_{\text{gap}}^2 \sim |\phi|^2 \sim \frac{s^2 g_{\text{YM}}^4}{R^2}. \quad (4.6)$$

Comparing this scale to that of the electric field we see $m_{\text{gap}}^2/m_{\text{el}}^2 \sim sg_{\text{YM}}^2$ and hence at any fixed g_{YM} for large enough s the effect of the scalar field ϕ is more important than the electric field.

The macroscopic limit of the EFT is achieved by taking the large radius limit of $AdS_2 \times S^2$ such that ϕ remains fixed, hence, we need to scale $sg_{\text{YM}}^2 \sim R$. Therefore, in this macroscopic limit, the electric field is zero in the infinite volume limit and we should not worry about it to leading order. Therefore, in the macroscopic flat space limit we simply have a rank-1 $\mathcal{N} \geq 2$ SCFT theory on the Coulomb branch! This leads to major simplifications in the large s limit, since much is known about $\mathcal{N} \geq 2$ SCFT theory on the Coulomb branch. We emphasize again that an important ingredient in the logic above is that at large s the color fluctuations on the probe are highly suppressed which allows one to pick the direction in color space of ϕ .

Therefore, the description of the DCFT defined by a 1/2-BPS Wilson loop in a large representation in a $\mathcal{N} = 2$ SCFT is given by the EFT on the Coulomb branch of the theory. To leading order in derivatives, the EFT consists of the free action for a single $\mathcal{N} = 2$ vector

⁴²We note that we do not obtain a conformal line for arbitrary values of this coefficients. An interesting defect RG flow related to this coefficient in $\mathcal{N} = 4$ SYM was the subject of some previous studies [126] (see also [99, 127, 128]).

multiplet plus, in some cases (as in $\mathcal{N} = 4$ SYM), some free decoupled Hypermultiplets:

$$\mathcal{L}/\sqrt{g} = \frac{1}{g_{\text{CB}}^2} \left(\partial_\mu \phi^\dagger \partial^\mu \phi + \frac{1}{6} \mathcal{R} \phi^\dagger \phi + \frac{1}{4} F^2 \right) + \text{fermions} + \text{Hypers}, \quad (4.7)$$

where \mathcal{R} is the Ricci scalar. The free action of the vector multiplet in particular depends on a unique Wilson coefficient g_{CB} . Due to the VEV of the scalar and the gauge field, the action scales as $\sim s^2$ on the saddle-point. An important point is that the EFT (4.7) captures all analytic $1/s$ corrections upon adding higher derivative terms to this Abelian effective theory. This is different from sections 2 and 3 where in the large s limit we needed to also integrate over zero modes and compute their $1/s$ effects in order to connect the pinning field DCFT to the large s physics of the spin impurity.

Higher derivative corrections are suppressed by inverse powers of $\phi^\dagger \phi \sim s^2$ and naively start at order $O(s^0)$ (see e.g. [129] for examples). However, there is an exception to this expectation: the (supersymmetric) Wess-Zumino term. This is required to match the UV conformal anomaly in the EFT [130, 131] and scales as $O(\log s)$. Its supersymmetric form on the Coulomb branch of $\mathcal{N} = 2$ theories can be found in [132–134] (see also [135] for the explicit integration over superspace). Here we will only need the leading term, whose form is:

$$\mathcal{L}_{\text{WZ}} \supset -\Delta a E_4 \log(\phi^\dagger \phi), \quad (4.8)$$

where E_4 is the Euler invariant, normalized so that $\int_{S^4} E_4 = 2$. The contribution from the c -anomaly is proportional to W^2 , the square of the Weyl tensor, but we will work only on conformally flat manifolds, for which $W^2 = 0$, so we do not discuss it further. The coefficient $\Delta a = a_{\text{UV}} - a_{\text{IR}}$ represents the difference in the conformal a -anomalies between the SCFT and the Coulomb branch contribution, in units such that an Abelian free vector multiplet contributes with $a_{\text{VM}} = \frac{5}{24}$ and a free Hypermultiplet with $a_{\text{HM}} = \frac{1}{24}$. We will not need additional subleading EFT terms for what follows.

The 1/2-BPS Wilson loop in the EFT is represented as follows [65]:⁴³

$$D_s^{\text{BPS}} \longrightarrow \exp \left[i s \int_{\mathcal{C}} d\tau \left(\dot{x}^\mu A_\mu - i \frac{\phi + \phi^*}{\sqrt{2}} \right) \right] + \exp \left[-i s \int_{\mathcal{C}} d\tau \left(\dot{x}^\mu A_\mu - i \frac{\phi + \phi^*}{\sqrt{2}} \right) \right], \quad (4.9)$$

where we omit for simplicity the possibility that there are nontrivial integer multiplicities for some of the lines (adding multiplicities is straightforward, of course). The relative sign in front of the scalar terms in (4.9) is fixed by supersymmetry.

⁴³More formally, the loop is represented through the sum of its components on the Coulomb branch [68]. Those with maximal electric charge (in the duality frame in which the magnetic one is zero) provide the leading contribution, with the other simple line contributions being exponentially suppressed in s ; these are negligible in the EFT. Therefore in the appropriate duality frame the loop generically reduces to a sum of two electric lines as in eq. (4.9).

Results from EFT Here we consider the EFT predictions for the expectation values of the circular loop and the one-point function of the stress-tensor.

From equations (4.7) and (4.9) one can compute the saddle-point profile. In flat space, before the transformation to $AdS_2 \times S^2$, the scalar profile reads

$$\phi = \pm \frac{1}{\sqrt{2}} \frac{g_{\text{CB}}^2 s}{4\pi^2} \int_{\mathcal{C}} d\sigma \frac{1}{[x - x(\sigma)]^2}, \quad (4.10)$$

where the two signs refer to the two different simple components in eq. (4.9) and we left the line contour unspecified. As before, a Weyl rescaling allows to obtain the profile on other manifolds of interest. In particular, for a straight contour, after the transformation to $AdS_2 \times S^2$, the profile becomes a constant.

We can use the classical solution as we did before to evaluate the expectation value of the circular loop (i.e. the g function). It turns out that the scalar contributes only to a perimeter divergence without affecting the defect entropy. The leading order contribution to the defect entropy arises from the gauge field and is given by⁴⁴

$$\log g = \frac{s^2 g_{\text{CB}}^2}{4} + O(\log s). \quad (4.12)$$

The leading correction arises from the Wess-Zumino term (4.8) and it is of order $O(\log s)$. To evaluate it, it is convenient to consider the theory on the sphere. The results is obtained by integrating eq. (4.8) with ϕ evaluated on the saddle-point profile (4.10); in practice we only need that ϕ scales as $g_{\text{CB}}^2 s$ since we neglect $O(s^0)$ contributions and the field appears as the argument of a logarithm. In conclusion, we find the following result for the g -function⁴⁵

$$\log g = \frac{g_{\text{CB}}^2 s^2}{4} + 4\Delta a \log(g_{\text{CB}}^2 s) + O(s^0). \quad (4.13)$$

A table with the values of Δa for all rank-1 $\mathcal{N} = 2$ theories can be found in [135].

We can also compute the coefficient h_D of the one-point function of the stress-tensor within the EFT. We define it according to the conventions of [71]:

$$\langle T_{00}(x) \rangle_{\mathbb{R}^4} = \frac{h_D}{r^4}. \quad (4.14)$$

⁴⁴Let us review the g function in Abelian gauge theory. The saddle-point solution in Feynman gauge reads:

$$A_{\pm}^{\nu} = \pm i \frac{g_{\text{CB}}^2 s}{4\pi^2} \int_{\mathcal{C}} d\sigma \frac{\dot{x}^{\nu}(\sigma)}{[x - x(\sigma)]^2}, \quad (4.11)$$

where the $+$ ($-$) refers to the solution sourced by the first (second) simple line in eq. (4.9). The profile (4.11) can be translated to S^4 and $AdS_2 \times S^2$ by a Weyl rescaling. In particular, the solution (4.11) can be used to compute the defect partition function by evaluating the DCFT action, e.g. in flat space or on S^4 , with the defect placed on a great circle. Subtracting a perimeter divergent term, the result for the universal part is quoted in the text, see for instance [100]; our construction shows that to leading order in $s \gg 1$ the same result holds also for a generic non-Abelian supersymmetric conformal gauge theory.

⁴⁵The one-loop contribution to the partition function of the theory coincides with the partition function of a relativistic free theory; its UV divergent part is associated with the Weyl anomaly a_{IR} [136] and its finite part contributes to (4.13) at order $O(s^0)$.

In supersymmetric theories h_D is related to the Bremsstrahlung function parametrizing the energy radiated by the line and it has been computed in various examples [69, 72, 73, 76, 77]. In the EFT, at leading order in s , this is just given by the sum of the results for a free gauge field and a free real scalar. To the leading order in s we find

$$h_D = h_D^{\text{gauge}} + h_D^{\text{scalar}} = \frac{s^2 g_{\text{CB}}^2}{32\pi^2} + \frac{s^2 g_{\text{CB}}^2}{96\pi^2} = \frac{s^2 g_{\text{CB}}^2}{24\pi^2}. \quad (4.15)$$

Notice that we can rewrite this formula in terms of a derivative of the partition function (4.13)

$$h_D \simeq \frac{s}{12\pi^2} \frac{\partial \log g}{\partial s}. \quad (4.16)$$

At this stage eq. (4.16) may seem like a coincidence associated with working to leading order, but in fact we will argue in the remaining of this subsection that in theories for which the localization formulas apply, eq. (4.16) is exact up to exponentially small corrections in the large s limit. It is therefore natural to conjecture that eq. (4.16) holds for all rank-1 $\mathcal{N} = 2$ SCFTs up to exponentially small corrections in s . Indeed both h_D and $\log g$ are protected observables and therefore receive contribution only from F -terms in the EFT [137]. The only F -terms are the kinetic term of the vector multiplet and the Wess-Zumino term [138], and they take the same universal structure on the Coulomb branch for all rank-1 $\mathcal{N} = 2$ SCFTs. Similar arguments were used in [135, 138] to extract the correlation function of two charge n chiral primaries to all order in the $1/n$ expansion, up to exponentially small corrections. We therefore expect that to all orders in the $1/s$ expansion in eq. (4.13) (and hence in (4.16)) is likewise uniquely fixed in terms of g_{CB} and Δa .

Finally we also provide a few comments on non-protected observables. In $\mathcal{N} = 2$ superspace notation a generic scalar long multiplet of dimension Δ would map in the EFT to

$$\mathcal{O}_\Delta(x, \theta, \bar{\theta}) = C_\mathcal{O}(\bar{\Phi}\Phi)^{\Delta/2} + \dots \quad (4.17)$$

Here Φ is a $\mathcal{N} = 2$ chiral superfield whose bottom component coincides with ϕ . Evaluating the scalar field on the solution (4.10), it follows that one-point functions obey a simple scaling law of the form:

$$\langle \mathcal{O}_\Delta |_{\theta=\bar{\theta}=0} \rangle \propto (g_{\text{CB}}^2 s)^\Delta. \quad (4.18)$$

Localization results We now focus on two specific Lagrangian examples of $SU(2)$ superconformal gauge theories: $\mathcal{N} = 4$ SYM and $\mathcal{N} = 2$ SQCD with $N_f = 4$ Hypermultiplets in the fundamental representation. In these theories localization provides exact expressions for the g -function and the h_D coefficient in terms of a one-dimensional integral. We will evaluate these integrals in the double-scaling limit for weak coupling g_{YM}^2 and large representation s with fixed $g_{\text{YM}}^2 s$. We will also briefly discuss the large representation limit $s \rightarrow \infty$ with fixed arbitrary values of the coupling g_{YM}^2 .

Let us study first the defect partition function on the equator of the four-sphere. This can be written in terms of a one-dimensional integral as [67, 139]:

$$g = \frac{\int_{\mathbb{R}} da (2a^2) e^{-\frac{16\pi^2}{g_{\text{YM}}^2} R^2 a^2} Z(aR) \sum_{q=-s}^s e^{4\pi R q a}}{\int_{\mathbb{R}} da (2a^2) e^{-\frac{16\pi^2}{g_{\text{YM}}^2} R^2 a^2} Z(aR)}, \quad (4.19)$$

where R is the sphere radius and $Z(aR)$ represents the contribution from the fluctuations determinant. The denominator is the sphere partition function with no Wilson loop insertion. In the first line, the Wilson loop is represented as a sum over all eigenvalues q of the Cartan generator in the $2s + 1$ -dimensional representation. In $\mathcal{N} = 4$ we have $Z = 1$, while in $\mathcal{N} = 2$ with $N_f = 4$ we can write Z as the product of the one-loop contribution and the instanton partition function: $Z = Z_{1\text{-loop}} Z_{\text{inst}}$. In the following we will need the explicit expression for the one-loop part:

$$Z_{1\text{-loop}}^{(\mathcal{N}=2)}(aR) = \frac{H(2iaR)H(-2iaR)}{|H(iaR)H(-iaR)|^4}, \quad H(x) = e^{(1+\gamma_E)x^2} G(1+x)G(1-x), \quad (4.20)$$

where γ_E is the Euler constant and G is the Barnes G-function. For details about the instanton contribution see [140–142]; instantons are exponentially suppressed in the limit of $s \rightarrow \infty$ with fixed $g_{\text{YM}}^2 s$ and therefore we will neglect them in what follows. It is further convenient to rescale $a \rightarrow a/R$, so that the dependence on R drops explicitly, and perform the sum in eq. (4.19) in order to write the localization integral as:

$$g = \frac{\int_{\mathbb{R}} da (2a^2) \exp \left[-\frac{16\pi^2}{g_{\text{YM}}^2} a^2 + (2s+1)2a\pi \right] Z(a)/\sinh(2a\pi)}{\int_{\mathbb{R}} da (2a^2) e^{-\frac{16\pi^2}{g_{\text{YM}}^2} a^2} Z(a)}. \quad (4.21)$$

In the double-scaling limit $s \rightarrow \infty$ with fixed $g_{\text{YM}}^2 s$ we can compute the first integral in eq. (4.21) by expanding around the saddle-point obtained via extremizing the exponent:

$$a_{\text{saddle}} = \frac{g_{\text{YM}}^2 (2s+1)}{16\pi}. \quad (4.22)$$

The partition function in the denominator is obtained by expanding $Z(a)$ around $a = 0$. Accounting for the measure, the general structure of the result is:

$$\log g = \frac{1}{g_{\text{YM}}^2} f_{-1}(g_{\text{YM}}^2 s) - \log g_{\text{YM}}^2 + f_0(g_{\text{YM}}^2 s) + O(g_{\text{YM}}^2 s), \quad (4.23)$$

where the $-\log g_{\text{YM}}^2$ term arises since the numerator and the denominator in eq. (4.21) are expanded around different saddle-points. We are interested in the EFT regime $g_{\text{YM}}^2 s \gg (4\pi)^2$.

For $\mathcal{N} = 4$ SYM we find the following result:

$$f_{-1}(g_{\text{YM}}^2 s)|_{\mathcal{N}=4} = \frac{(g_{\text{YM}}^2 s)^2}{4}, \quad (4.24)$$

$$f_0(g_{\text{YM}}^2 s)|_{\mathcal{N}=4} = 2 \log(g_{\text{YM}}^2 s) + e^{-g_{\text{YM}}^2 s/2} + O(e^{-g_{\text{YM}}^2 s}). \quad (4.25)$$

Comparing with the EFT prediction (4.13) and, using the known value $\Delta a = 1/2$ [135], we find perfect agreement for both the leading and the subleading terms with the identification $g_{\text{YM}} = g_{\text{CB}}$ (as expected since the gauge coupling does not receive corrections in this case). The exponentially small correction in eq. (4.25) cannot be reproduced in the EFT and are interpreted as the worldline action associated with the propagation of a massive BPS particle - see e.g. [138, 143–145] for discussions of similar contributions in a related context.

Similarly, in $\mathcal{N} = 2$ SQCD with $N_f = 4$ we find:

$$f_{-1}(g_{\text{YM}}^2 s) |_{\mathcal{N}=2} = \frac{(g_{\text{YM}}^2 s)^2}{4}, \quad (4.26)$$

$$f_0(g_{\text{YM}}^2 s) |_{\mathcal{N}=2} = -\frac{g_{\text{YM}}^4 s^2 \log 2}{8\pi^2} + 3 \log(g_{\text{YM}}^2 s) + O((g_{\text{YM}}^2 s)^0). \quad (4.27)$$

Using that $\Delta a = 3/4$ in this case [135], we see that eqs. (4.26) and (4.27) are consistent with the EFT predictions, and allow to identify the EFT coupling in terms of the UV one as $g_{\text{CB}}^2 = g_{\text{YM}}^2 - \frac{g_{\text{YM}}^4}{2\pi^2} \log 2 + O(g_{\text{YM}}^6)$. Also in this case the expansion in eq. (4.27) contains exponentially suppressed terms, whose interpretation is similar to $\mathcal{N} = 4$, but we did not display them explicitly. Notice that the leading order results (4.24) and (4.26) in the double-scaling limit are the same in both cases, as anticipated.

We also briefly comment on the results in the large s limit with fixed coupling g_{YM}^2 . In this limit it is useful to use the representation (4.19) of the integral. To perform the calculation we retain only the weights $q = -s$ and $q = s$ in the sum, since all the other give an exponentially small contribution in this limit. In $\mathcal{N} = 4$ SYM the integrals can be performed exactly and one finds:

$$\log g |_{\mathcal{N}=4} \stackrel{s \rightarrow \infty}{=} \frac{g_{\text{YM}}^2 s^2}{4} + \log \left(\frac{g_{\text{YM}}^2 s^2}{2} + 1 \right) + \log 2 + O\left(e^{-\frac{1}{2} g_{\text{YM}}^2 s}\right), \quad (4.28)$$

again in agreement with eq. (4.13).

To perform the same calculation in this limit in the $\mathcal{N} = 2$ with $N_f = 4$ theory in principle we should retain the full instanton contribution in $Z(a)$. However, most of this can be avoided by the following observation: We can organize the full integrand besides the Wilson loop term in (4.19) according to the genus expansion as

$$e^{F_{-1} a^2 R^2 + F_0 \log(aR) + F_1 \frac{1}{a^2 R^2} + \dots}. \quad (4.29)$$

The large Ra expansion is tantamount to the standard expansion at small $\epsilon_1 = \epsilon_2$, which is analogous to the genus expansion of topological string theory, see for instance [146]. If we now insert the highest weight contribution from the Wilson line, $e^{4\pi s Ra}$, then the saddle-point occurs for $aR \sim s$ and hence the genus expansion becomes the $1/s$ expansion. This is obvious also from the EFT of the Abelian vector multiplet (4.7) because the genus expansion is nothing but the derivative expansion in the bulk.

The instantons are needed to determine the F_i . But for large s we only need F_{-1} and F_0 , and the latter does not receive instanton corrections due its relation with the conformal

anomalies. Hence all the instantons would do in the large s limit is to dictate the exact relation between g_{YM} and g_{CB} . We therefore find in the large s limit with fixed g_{YM} :

$$\log g = \frac{g_{\text{CB}}^2 s^2}{4} + 3 \log s + O(s^0) , \quad (4.30)$$

which as expected agrees with the EFT prediction (4.13). $g_{\text{CB}}^2 = g_{\text{CB}}^2(g_{\text{YM}}^2)$ is in general a complicated function that receives contributions from instantons, but it is easy to determine it to all orders in perturbation theory: $g_{\text{CB}}^2 = \frac{g_{\text{YM}}^2}{1 + \frac{g_{\text{YM}}^2}{2\pi^2} \log 2}$. Therefore, the expansion of (4.30) for small g_{YM} agrees with the double-scaling limit results (4.26) and (4.27).

Let us now focus on the stress-tensor one-point function. In localization this is given by the derivative with respect to the squashing parameter b of the ellipsoid partition function g_b [71, 73, 76, 77]:

$$h_D = \frac{1}{12\pi^2} \frac{\partial \log g_b}{\partial b} \Big|_{b=1} , \quad (4.31)$$

for b close to one g_b is obtained from eq. (4.19) by replacing $q \rightarrow qb$:

$$g_b = \frac{\int_{\mathbb{R}} da (2a^2) e^{-\frac{16\pi^2}{g_{\text{YM}}^2} R^2 a^2} Z(aR) \sum_{q=-s}^s e^{4\pi R q b a}}{\int_{\mathbb{R}} da (2a^2) e^{-\frac{16\pi^2}{g_{\text{YM}}^2} R^2 a^2} Z(aR)} + O((1-b)^2) . \quad (4.32)$$

We may evaluate this integral in the $s \rightarrow \infty$ limit with fixed $g_{\text{YM}}^2 s$. Dropping exponentially small corrections, we retain only the terms with $q = -s$ and $q = s$ in eq. (4.32). One can therefore trade derivatives with respect to b for derivatives with respect to s in eq. (4.31) in this limit. We thus obtain the relation:

$$h_D \simeq \frac{s}{12\pi^2} \frac{\partial \log g}{\partial s} . \quad (4.33)$$

Exactly the same argument allows to conclude that eq. (4.33) holds up to exponentially small corrections in the limit $s \rightarrow \infty$ with $g_{\text{YM}}^2 = \text{fixed}$. The relation (4.16) thus holds for the Lagrangian $\mathcal{N} = 2$ rank-1 SCFTs up to theory-dependent exponentially small corrections in the large s limit.

Remarks Our intuition was largely guided by analogous results for large R -charge operators in SCFTs [21, 135, 138, 144, 145, 147]. In particular, refs. [135, 138] argued that the two-point function of two chiral primary operators of charge n in rank-1 $\mathcal{N} = 2$ SCFTs can be determined to all order in $1/n$ via the effective description of the theory on the Coulomb branch, up to exponentially small corrections. A similar analysis might allow for the determination of the g -function to all orders in $1/s$ in our setup; we leave this as an interesting open question for the future.

We also mention that a double-scaling limit analogous to $s \rightarrow \infty$ with fixed $g_{\text{YM}}^2 s$ was explored for large R -charge correlators within localization in [143, 148, 149], where it was also shown to be associated with a dual matrix model description.

Finally, the EFT for supersymmetric Wilson lines in large representations can be generalized to SCFTs with rank $N \geq 2$. It would be interesting to address the large N limit, and compare our EFT findings with holography, where Wilson lines in large representations are described by a “bubbling” geometry [150, 151].

Acknowledgements

We thank O. Aharony, S. Bolognesi, S. Komatsu, G. Korchemsky, P. Kravchuk, E. Lauria, E. Rabinovici, L. Rastelli, S. Sachdev, A. Sever, S. Shao, B. Van Rees, and S. Yankielowicz for useful discussions. GC is supported by the Simons Foundation (Simons Collaboration on the Non-perturbative Bootstrap) grants 488647 and 397411. ZK, MM and ARM are supported in part by the Simons Foundation grant 488657 (Simons Collaboration on the Non-Perturbative Bootstrap) and the BSF grant no. 2018204. The work of ARM was also supported in part by the Zuckerman-CHE STEM Leadership Program.

A Details of the diagrammatic calculations in free theory

A.1 One-loop contribution to the one-point function

The one-loop contribution (2.9) to the one-point function $\langle \phi_a^2(\mathbf{x}, 0) \rangle$ in the presence of the defect is proportional to the following integral:

$$\begin{aligned} \mathcal{I}_1 &= \int_{\tau_1 > \tau_2 > \tau_3 > \tau_4} d[\tau] G(x - x(\tau_1)) G(x(\tau_2) - x(\tau_4)) G(x - x(\tau_3)) \\ &= \frac{1}{[(2 - \varepsilon)\Omega_{3-\varepsilon}]^3} \int_{\tau_1 > \tau_2 > \tau_3 > \tau_4} d[\tau] \frac{1}{(\mathbf{x}^2 + \tau_1^2)^{\frac{2-\varepsilon}{2}} (\mathbf{x}^2 + \tau_3^2)^{\frac{2-\varepsilon}{2}} |\tau_2 - \tau_4|^{2-\varepsilon}}. \end{aligned} \quad (\text{A.1})$$

It is convenient to evaluate first the integrals over τ_2 and τ_4 . This leads to

$$\mathcal{I}_1 = \frac{1/2}{\varepsilon(1 - \varepsilon) [(2 - \varepsilon)\Omega_{3-\varepsilon}]^3} \iint d\tau_1 d\tau_3 \frac{|\tau_1 - \tau_3|^\varepsilon}{(\mathbf{x}^2 + \tau_1^2)^{\frac{2-\varepsilon}{2}} (\mathbf{x}^2 + \tau_3^2)^{\frac{2-\varepsilon}{2}}}, \quad (\text{A.2})$$

where we used the symmetry of the integrand under exchanges of τ_1 and τ_3 to extend the integration over the full real axis for both variables. Notice that, while the prefactor of eq. (A.2) diverges for $\varepsilon \rightarrow 0$, the remaining integral is convergent. We may therefore evaluate \mathcal{I}_1 expanding the integrand to first order in ε . To this aim we rescale $(\tau_1, \tau_2) \rightarrow |\mathbf{x}|(\tau_1, \tau_2)$ and use the following results:

$$\int d\tau \frac{1}{1 + \tau^2} = \pi, \quad \int d\tau \frac{\log(1 + \tau^2)}{1 + \tau^2} = 2\pi \log 2, \quad (\text{A.3})$$

$$\iint d\tau_1 d\tau_2 \frac{\log |\tau_1 - \tau_2|}{(1 + \tau_1^2)(1 + \tau_2^2)} = \pi^2 \log 2. \quad (\text{A.4})$$

Eventually, we arrive at

$$\mathcal{I}_1 = -\frac{1}{128(\pi^4 \mathbf{x}^2)^\varepsilon} - \frac{\log(64\pi^3 \mathbf{x}^6) + 3\gamma_E + 2}{256\pi^4 \mathbf{x}^2} + O(\varepsilon), \quad (\text{A.5})$$

where γ_E is the Euler constant.

A.2 Two-loop contribution to g_γ for the bulk free theory

The two-loop contribution to the g -function studied in sec. 2.2.2 is proportional to the following integral, see eq. (2.22) :

$$I_2^{(4-\varepsilon)} = \int_0^{2\pi} d\phi_1 \int_0^{\phi_1} d\phi_2 \int_0^{\phi_2} d\phi_3 \int_0^{\phi_3} d\phi_4 \frac{1}{\left(16 \sin^2 \frac{\phi_{13}}{2} \sin^2 \frac{\phi_{24}}{2}\right)^{\frac{2-\varepsilon}{2}}}. \quad (\text{A.6})$$

We can evaluate it following the strategy outlined in the appendix B.2 of [99]. This consists in expanding the denominator using the following Fourier representation

$$\frac{1}{\left[4 \sin^2 \left(\frac{\phi}{2}\right)\right]^{\frac{2-\varepsilon}{2}}} = \frac{1}{2\pi} c_0(\varepsilon) + \frac{1}{\pi} \sum_{n=1}^{\infty} c_n(\varepsilon) \cos(n\phi), \quad (\text{A.7})$$

where we defined for $n \in \mathbb{N}$:

$$c_n(\varepsilon) = \int_0^{2\pi} d\phi \frac{\cos(n\phi)}{\left[4 \sin^2 \frac{\phi}{2}\right]^{\frac{2-\varepsilon}{2}}} = \frac{2 \cos(\pi n) \Gamma(\varepsilon - 1)}{\Gamma\left(\frac{\varepsilon}{2} - n\right) \Gamma\left(n + \frac{\varepsilon}{2}\right)} = -|n|\pi + O(\varepsilon). \quad (\text{A.8})$$

One then evaluates the integrals over the Fourier components using the following identity:

$$\int_0^{2\pi} d\phi_1 \int_0^{\phi_1} d\phi_2 \int_0^{\phi_2} d\phi_3 \int_0^{\phi_3} d\phi_4 \cos(n\phi_{13}) \cos(m\phi_{24}) = \begin{cases} 0 & \text{if } m \neq n > 0, \\ \frac{\pi^2}{m} & \text{if } m = n > 0, \\ -\frac{2\pi^2}{m^2} & \text{if } n = 0, m > 0, \\ \frac{2\pi^4}{3} & \text{if } n = m = 0. \end{cases} \quad (\text{A.9})$$

(The rest of the cases follow from the symmetry $n \leftrightarrow m$.) As a result we find

$$I_2^{(4-\varepsilon)} = \frac{\pi^2}{6} [c_0(\varepsilon)]^2 - 2c_0(\varepsilon) \sum_{n=1}^{\infty} \frac{c_n(\varepsilon)}{n^2} + \sum_{n=1}^{\infty} [c_n(\varepsilon)]^2. \quad (\text{A.10})$$

Notice that $c_0(\varepsilon) = O(\varepsilon)$ due to eq. (A.8). Therefore the first term in eq. (A.10) is of order $O(\varepsilon^2)$ and we will neglect it in what follows. One might similarly conclude that the second term is of order $O(\varepsilon)$, but this would be incorrect. This is because $c_0(\varepsilon) = O(\varepsilon)$ is multiplied by a sum which is logarithmically divergent for $\varepsilon = 0$, as it can be noticed using $c_n(0)/n^2 = -\pi/n$.

The sum therefore results in a $1/\varepsilon$ pole in dimensional regularization, which compensates the simple zero of $c_0(\varepsilon)$ and leads to a finite result.

In conclusion, we need to evaluate the two infinite sums in eq. (A.10). This is easily achieved using the substitution [99]

$$c_n(\varepsilon) \rightarrow -\pi n^{1-\varepsilon}, \quad (\text{A.11})$$

which is exact up to $O(\varepsilon)$ corrections. One may further check from the asymptotic expansion of $c_n(\varepsilon)$ for $n \rightarrow \infty$ that the terms neglected in eq. (A.11) do not lead to logarithmically divergent sums in eq. (A.10), and therefore remain $O(\varepsilon)$ suppressed with respect to the leading order also after the summation. Using eq. (A.11) both infinite sums are convergent when ε is analytically continued to a sufficiently large value and can be evaluated using

$$\sum_{n=1}^{\infty} n^{\alpha} = \zeta(-\alpha). \quad (\text{A.12})$$

Expanding the final result in ε we finally arrive at eq. (2.22).

B Details of the semiclassical calculations in free theory

B.1 The $1/s$ corrections to the one-point function of ϕ_a^2 close to four dimensions

In this appendix we evaluate the correction in eq. (2.54) to the leading order result (2.47) for the one-point function $\langle \phi_a^2(\mathbf{x}, 0) \rangle$ in $d = 4 - \varepsilon$ with $\varepsilon \ll 1$. This amounts at evaluating the following integral in dimensional regularization:

$$\mathcal{I}_3 = \lim_{\eta \rightarrow 0^+} \int \frac{d\omega}{2\pi} G_{\chi}(\omega) \left[|h_{\mathbf{x}}(\omega)|^2 - e^{i\omega\eta} |h_{\mathbf{x}}(0)|^2 \right], \quad (\text{B.1})$$

where $G_{\chi}(\omega)$ is defined in eq. (2.52) and $h_{\mathbf{x}}(\omega)$ is in eq. (2.55).

It is convenient to further rewrite the integral as:

$$\mathcal{I}_3 = \lim_{\eta \rightarrow 0^+} \int_0^{\infty} \frac{d\omega}{2\pi} \left\{ [G_{\chi}(\omega) + G_{\chi}(-\omega)] |h_{\mathbf{x}}(\omega)|^2 - [G_{\chi}(\omega)e^{i\omega\eta} + G_{\chi}(-\omega)e^{-i\omega\eta}] |h_{\mathbf{x}}(0)|^2 \right\}. \quad (\text{B.2})$$

To evaluate the integral in eq. (B.1) we will expand the propagator as a series in α_0 and commute the sum with the integral. For this procedure to work, we must perform the expansion in both terms inside the first parenthesis of eq. (B.2). Indeed, only in this way do we obtain a series whose individual terms can be integrated without encountering an IR singularity. Using the identity

$$\begin{aligned} G_{\chi}(\omega)e^{i\omega\eta} + G_{\chi}(-\omega)e^{-i\omega\eta} = & -2 \frac{\sin(\eta\omega)}{\omega} \sum_{n=0}^{\infty} (-1)^n \alpha_0^{2n} \left(\frac{c^{(4-\varepsilon)}(\omega)}{\omega} \right)^{2n} \\ & + 2 \frac{\cos(\eta\omega)}{\omega} \sum_{n=0}^{\infty} (-1)^{n+1} \alpha_0^{2n+1} \left(\frac{c^{(4-\varepsilon)}(\omega)}{\omega} \right)^{2n+1}, \end{aligned} \quad (\text{B.3})$$

we recast the integral as:

$$\begin{aligned} \mathcal{I}_3 = \lim_{\eta \rightarrow 0^+} \int_0^\infty \frac{d\omega}{2\pi} \left\{ \left[|h_{\mathbf{x}}(\omega)|^2 - \cos(\eta\omega) |h_{\mathbf{x}}(0)|^2 \right] \frac{2}{\omega} \sum_{n=0}^\infty (-1)^{n+1} \alpha_0^{2n+1} \left(\frac{c^{(4-\varepsilon)}(\omega)}{\omega} \right)^{2n+1} \right. \\ \left. + 2 |h_{\mathbf{x}}(0)|^2 \frac{\sin(\eta\omega)}{\omega} \sum_{n=0}^\infty (-1)^n \alpha_0^{2n} \left(\frac{c^{(4-\varepsilon)}(\omega)}{\omega} \right)^{2n} \right\}. \end{aligned} \quad (\text{B.4})$$

One might naively conclude that the term proportional to $\sin(\eta\omega)$ in the second line can be set to zero, by commuting the limit with the integral. We shall momentarily see that this is not the case.

We can now commute the sum and the integral in eq. (B.4). Notice that $c^{(4-\varepsilon)}(\omega) = \omega^{1-\varepsilon} c^{(4-\varepsilon)}(1)$ from eq. (2.53). Therefore, we can evaluate the integrals in the first line in eq. (B.4) using the following identity in dimensional regularization:⁴⁶

$$\begin{aligned} \lim_{\eta \rightarrow 0^+} \int_0^\infty \frac{d\omega}{2\pi} \omega^{-(2n+1)\varepsilon-1} \left[|h_{\mathbf{x}}(\omega)|^2 - \cos(\eta\omega) |h_{\mathbf{x}}(0)|^2 \right] \\ = \frac{-\pi}{2(2n+1)\mathbf{x}^2} \left[\frac{1}{\varepsilon} + (2n+3) \log(2|\mathbf{x}|) + (2n+1)\gamma_E + O(\varepsilon) \right]. \end{aligned} \quad (\text{B.5})$$

The integrals in the second line are instead evaluated using:

$$\lim_{\eta \rightarrow 0^+} \int_0^\infty \frac{d\omega}{2\pi} \frac{\sin(\eta\omega)}{\omega^{1+2n\varepsilon}} = \begin{cases} \frac{1}{4} & \text{for } n = 0, \\ 0 & \text{for } n \geq 1. \end{cases} \quad (\text{B.6})$$

As anticipated, the limit and the integral do not commute for $n = 0$. Physically, this is because the propagator at $\alpha_0 = 0$ is discontinuous, $\langle \chi(\tau) \bar{\chi}(0) \rangle_{\alpha_0=0} = \frac{1}{2} \text{sgn}(\tau) + \text{const}$ (the constant term drops from all physical observables).

Performing the series over n we finally arrive at:

$$\mathcal{I}_3 = -\frac{1}{\varepsilon} \frac{2\pi \arctan(\pi\alpha_0)}{\mathbf{x}^2} - \frac{2\pi \arctan(\pi\alpha_0) \log(4\mathbf{x}^2)}{\mathbf{x}^2} - \frac{\pi^2 \alpha_0 [\log(4\mathbf{x}^2) + 2]}{(1 + \pi^2 \alpha_0^2) \mathbf{x}^2} + \frac{\pi^2}{2\mathbf{x}^2} + O(\varepsilon), \quad (\text{B.7})$$

where the last term in eq. (B.7) arises because of the point-splitting procedure from eq. (B.6). Restoring the prefactor in eq. (2.54), we arrive at the result (2.57).

⁴⁶Notice that the limit $\eta \rightarrow 0^+$ is taken within dimensional regularization, hence before the limit $\varepsilon \rightarrow 0$.

B.2 Calculation of the \tilde{f}_0 function

In this appendix, we provide some technical details associated with the calculation of the \tilde{f}_0 function (2.76) close to four and three dimensions. This follows from the one-loop fluctuation determinant around the saddle-point.

In terms of the fluctuations (2.44) the quadratic action (2.45) on the defect reads:

$$S^{(2)} \simeq \int d\phi \bar{\chi} \dot{\chi} - \frac{\tilde{\alpha}_0}{2R} \int d\phi \int d\phi' \frac{(\bar{\chi} \chi' + \bar{\chi}' \chi - \bar{\chi} \chi - \bar{\chi}' \chi')}{\left(4 \sin^2 \frac{\phi - \phi'}{2}\right)^{\frac{d-2}{2}}}, \quad (\text{B.8})$$

where we defined the dimensionless combination $\tilde{\alpha}_0 = \alpha_0 R^{4-d}$. It is useful to decompose the fields into Fourier modes on the circle

$$\chi(\phi) = \sum_n \frac{e^{-in\phi}}{\sqrt{2\pi}} \chi_n, \quad \bar{\chi}(\phi) = \sum_n \frac{e^{in\phi}}{\sqrt{2\pi}} \bar{\chi}_n. \quad (\text{B.9})$$

The action then reads:

$$S_{\text{eff}}^{(2)} = \sum_n \bar{\chi}_n \left[-in - \tilde{\alpha}_0 (c_n(\varepsilon) - e^{in\eta} c_0(\varepsilon)) \right] \chi_n, \quad (\text{B.10})$$

where $c_n(\varepsilon)$ is defined in eq. (A.8) and η is a positive infinitesimal parameter which follows from the point-splitting regularization in eq. (2.4). Notice the action (B.10) is independent of the zero modes, as expected since these are associated with the action of the symmetry group.

We now perform the Gaussian integration over the fields $\bar{\chi}_n$ and χ_n in eq. (B.10). Normalizing the result by the partition function g_0 of a decoupled defect, we find:

$$\begin{aligned} \tilde{f}_0(\gamma_0^2 s, R, d) &= - \lim_{\eta \rightarrow 0^+} \sum_{n \neq 0} \log \left[-in - \tilde{\alpha}_0 (c_n(\varepsilon) - e^{in\eta} c_0(\varepsilon)) \right] + \sum_{n \neq 0} \log(-in) \\ &= - \sum_{n=1}^{\infty} \log \left[1 + \tilde{\alpha}_0^2 \left(\frac{c_n(\varepsilon) - c_0(\varepsilon)}{n} \right)^2 \right] + \lim_{\eta \rightarrow 0^+} \sum_{n=1}^{\infty} \frac{2\tilde{\alpha}_0 c_0(\varepsilon) n \sin(n\eta)}{n^2 + \tilde{\alpha}_0^2 (c_n(\varepsilon) - c_0(\varepsilon))^2}, \end{aligned} \quad (\text{B.11})$$

where we already neglected terms that manifestly vanish in the limit $\eta \rightarrow 0$. The result (B.11) holds for any value of $d = 4 - \varepsilon$. Our task is thus to evaluate the sums in eq. (B.11) in dimensional regularization.

Let us first consider the limit $\varepsilon \rightarrow 0$. We start with the second term in the second line of eq. (B.11): it is a convergent sum times $c_0(\varepsilon) = O(\varepsilon)$, hence it vanishes in the $\varepsilon \rightarrow 0$ limit. One might naively conclude that $c_0(\varepsilon)$ may also be neglected also in the first term of eq. (B.11). However, similarly to the discussion in appendix A.2, this is not the case. Indeed it multiplies a $1/\varepsilon$ term arising from a logarithmically divergent sum. In light of this comment, we expand eq. (B.11) in $c_0(\varepsilon)$ and get

$$\tilde{f}_0(\gamma_0^2 s, R, 4) = - \lim_{\varepsilon \rightarrow 0} \sum_{n=1}^{\infty} \left\{ \log \left[1 + \tilde{\alpha}_0^2 \left(\frac{c_n(\varepsilon)}{n} \right)^2 \right] - c_0(\varepsilon) \frac{2c_n(\varepsilon) \tilde{\alpha}_0^2}{[c_n(\varepsilon)]^2 \tilde{\alpha}_0^2 + n^2} + O \left(\frac{(c_0(\varepsilon))^2}{n^2} \right) \right\}, \quad (\text{B.12})$$

where we retained the term linear in $c_0(\varepsilon)$, while all the higher order terms in $c_0(\varepsilon)$ are multiplied by sums which are finite in dimensional regularization and thus can be safely neglected in four dimensions. We finally evaluate the sums by expanding in α_0 and replacing (just as in (A.11))

$$c_n(\varepsilon) \rightarrow -\pi n^{1-\varepsilon}, \quad (\text{B.13})$$

which is exact up to $O(\varepsilon)$ terms. Performing the summation over n in dimensional regularization and then expanding for $\varepsilon \rightarrow 0$, we arrive at:

$$\begin{aligned} \tilde{f}_0(\gamma_0^2 S, R, 4) &= -\sum_{k=1}^{\infty} \frac{(-1)^k \pi^{2k} \alpha_0^{2k}}{2k} + \sum_{k=0}^{\infty} \frac{(-1)^k \pi^{2k+2} \alpha_0^{2k+2}}{2k+1} \\ &= \frac{1}{2} \log(1 + \pi^2 \alpha_0^2) + \pi \alpha_0 \arctan(\pi \alpha_0). \end{aligned} \quad (\text{B.14})$$

Let us now consider the case of $d < 4$. As for the correlation function $\langle \phi_a^2(\mathbf{x}, 0) \rangle$ in sec. 2.3.3, we focus on the IR limit $\tilde{\alpha}_0 \rightarrow \infty$. The second term in eq. (B.11) can be evaluated by expanding the summand in $\tilde{\alpha}_0$. Only the first term of the expansion contributes in the limit $\eta \rightarrow 0^+$ and thus we find

$$\lim_{\eta \rightarrow 0^+} \sum_{n=1}^{\infty} \frac{2\tilde{\alpha}_0 c_0(\varepsilon) n \sin(n\eta)}{n^2 + \tilde{\alpha}_0^2 (c_n(\varepsilon) - c_0(\varepsilon))^2} = 2\tilde{\alpha}_0 c_0(\varepsilon) \lim_{\eta \rightarrow 0^+} \sum_{n=1}^{\infty} \frac{\sin(n\eta)}{n} = \pi \tilde{\alpha}_0 I_1^{(d)}, \quad (\text{B.15})$$

where we used $c_0(\varepsilon) = I_1^{(d)}$ in the last line, where $I_1^{(d)}$ is given in eq. (2.21). Eq. (B.15) is the only contribution linear in $\tilde{\alpha}_0$ to $\log g$. Adding eq. (B.15) to the leading order result (2.72), one finds $\log g_\gamma/g_0 = \pi \alpha_0 (s+1) R^{4-d} I_1^{(d)}$ to linear order in $\alpha_0 R^{4-d}$, in agreement with the diagrammatic result (2.20).

We now turn to the evaluation of the first term in eq. (B.11). The sum converges for $d < 7/2$, and can be evaluated in dimensional regularization for general values of d . Each individual term in the sum scales as $\log(\tilde{\alpha}_0^2)$ and is therefore subleading with respect to eq. (B.15) in the IR. Large IR contributions can thus only arise from the large n tail of the sum. We therefore expand the argument of the summand using

$$c_n(\varepsilon) - c_0(\varepsilon) \stackrel{n \rightarrow \infty}{\simeq} \begin{cases} -\frac{\pi \sec(\frac{\pi d}{2})}{\Gamma(d-2)} n^{d-3} - c_0(\varepsilon) + O(n^{d-5}) & \text{for } d > 3, \\ -2(\log n + \gamma_E + \log 4) + O(n^{-2}) & \text{for } d = 3. \end{cases} \quad (\text{B.16})$$

We conclude that most relevant contribution of the sum arises from the region where $n^{4-d} \sim \tilde{\alpha}_0$ for $3 < d < 4$ and from the one in which $n \sim \tilde{\alpha}_0 \log \tilde{\alpha}_0$ for $d = 3$.

To obtain a honest asymptotic expansion of the result we should proceed as in appendix D of [91], separating the first sum in eq. (B.11) into two pieces with a cutoff $\Lambda = a\tilde{\alpha}_0^{\frac{1}{4-d}}$ with $a \ll 1$. The sum over *small* n 's must then be evaluated analytically by expanding the summand for large $\tilde{\alpha}_0$, while the sum of large n can be approximated to arbitrary precision

via the Euler-Maclaurin formula. In practice, if we are not interested in the $O(\tilde{\alpha}_0^0)$ terms (not counting logarithms) we can simply replace the sum with an integral:⁴⁷

$$-\sum_{n=1}^{\infty} \log \left[1 + \tilde{\alpha}_0^2 \left(\frac{c_n(\varepsilon) - c_0(\varepsilon)}{n} \right)^2 \right] = -\int_0^{\infty} dn \log \left[1 + \tilde{\alpha}_0^2 \left(\frac{c_n(\varepsilon) - c_0(\varepsilon)}{n} \right)^2 \right] + O(\tilde{\alpha}_0^0), \quad (\text{B.17})$$

where we can replace $c_n(\varepsilon) - c_0(\varepsilon)$ with the expansion (B.16). The evaluation of eq. (B.17) is conveniently performed separately for $d > 3$ and $d = 3$.

To compute the integral (B.17) in $d > 3$, we rescale $n \rightarrow \tilde{\alpha}_0^{\frac{1}{4-d}} n$ and expand the integrand for large $\tilde{\alpha}_0$. We obtain

$$-\int_0^{\infty} dn \log \left[1 + \tilde{\alpha}_0^2 \left(\frac{c_n(\varepsilon) - c_0(\varepsilon)}{n} \right)^2 \right] = -\pi \tilde{\alpha}_0^{\frac{1}{4-d}} \csc \left(\frac{\pi}{8-2d} \right) \left[\frac{\pi |\sec(\frac{d\pi}{2})|}{\Gamma(d-2)} \right]^{\frac{1}{4-d}} + \pi \tilde{\alpha}_0 \frac{2\pi\Gamma(3-d)}{(4-d)\Gamma(2-\frac{d}{2})^2} + O\left(\tilde{\alpha}_0^{1-\frac{d-3}{4-d}}\right). \quad (\text{B.18})$$

The first term on the right hand side of eq. (B.18) is proportional to $\tilde{\alpha}_0^{\frac{1}{4-d}} = R\alpha_0^{\frac{1}{4-d}}$. Thus this is a pure cosmological constant term and it can be renormalized away. The second term is the leading physical contribution and it is linear in $\tilde{\alpha}_0$ as the leading order (2.72). Adding eq. (B.18) to eq. (B.15) we obtain the result (2.83) in the main text.

In $d = 3$ the expansion is more subtle due to the logarithm in eq. (B.16). In this case it is convenient to rescale $n \rightarrow 2\tilde{\alpha}_0 \log \tilde{\alpha}_0 n$, so that the integral reads:

$$-2\tilde{\alpha}_0 \log \tilde{\alpha}_0 \int_0^{\infty} dn \log \left[1 + \frac{1}{n^2} \left(1 + \frac{\log(\log \tilde{\alpha}_0) + \log n + \gamma_E + \log 8}{\log \tilde{\alpha}_0} \right)^2 \right]. \quad (\text{B.19})$$

We may now expand the integrand for large $\log \tilde{\alpha}_0$ (notice $\log \tilde{\alpha}_0 \gg \log(\log \tilde{\alpha}_0)$ for $\tilde{\alpha}_0 \gg 1$) and evaluate the resulting integrals. We obtain:

$$-\int_0^{\infty} dn \log \left[1 + \tilde{\alpha}_0^2 \left(\frac{c_n(\varepsilon) - c_0(\varepsilon)}{n} \right)^2 \right] \stackrel{d=3}{=} -2\pi\tilde{\alpha}_0 \log \tilde{\alpha}_0 - 2\pi\tilde{\alpha}_0 [\log(\log \tilde{\alpha}_0) + \log 8 + \gamma_E] + O\left(\tilde{\alpha}_0 \frac{\log^2(\log \tilde{\alpha}_0)}{\log \tilde{\alpha}_0}\right). \quad (\text{B.20})$$

Adding eq. (B.20) with the limit $d \rightarrow 3$ of eq. (B.15) and neglecting the terms linear in $\tilde{\alpha}_0 = \alpha_0 R$, which represent a cosmological constant contribution, we obtain the result (2.85) in the main text. Notice that the term proportional to $\tilde{\alpha}_0 \log R$ cancels between eqs. (B.15) and (B.20).

⁴⁷More precisely, this is true because the resulting integral is convergent for $n \rightarrow 0$.

C Running from the classical profile for the defect coupling in the $O(3)$ model

In this appendix we obtain the four-dimensional beta function for the defect coupling γ in eq. (3.11) to leading order in the triple-scaling limit (3.12). As we explain below, remarkably, the beta function in this limit can be extracted from the solution of the classical saddle-point equations.

C.1 Beta function in the physical renormalization scheme

In this and the next section (and only in these two sections) it will prove useful to work in a *physical* regularization scheme, rather than within dimensional regularization. In particular, we will analyze the theory (3.11) directly in four spacetime dimensions with a cutoff scale M (whose precise definition will be given below). Thus, the couplings in the action (3.11) are to be interpreted directly as the physical couplings at the scale M .

The saddle-point equations demand $\bar{z}\frac{\sigma^a}{2}z = n^a$ with n^a a unit vector independent of the defect position, while varying (3.11) we get the bulk equation of motion:

$$-\partial^2\phi_a + \frac{1}{3!}\phi_a(\phi_b)^2 = -4\pi y \left(\bar{z}\frac{\sigma^a}{2}z \right) \delta^{d-1}(x_\perp). \quad (\text{C.1})$$

The source imposes the following boundary condition:

$$\phi_a \xrightarrow{r \rightarrow 0} -c_d \frac{y \left(\bar{z}\frac{\sigma^a}{2}z \right)}{r^{d-3}}, \quad (\text{C.2})$$

where r denotes the distance from the defect and $c_d = \Gamma((d-3)/2)/\pi^{(d-3)/2}$, which was chosen such that $c_4 = 1$. This implies that $\phi_a \propto \bar{z}\sigma^a z$. As in the free theory, there is really a family of saddle-points, related by the global action of the zero-mode in the path integral.

To leading order in the semiclassical limit (3.12) the saddle-point is given by the solution of the equation (C.1) in four spacetime dimensions. However, it turns out that in $d = 4$ the eq. (C.1) does not have a solution that is compatible with the boundary condition (C.2), since the cubic term unavoidably leads to logarithmic corrections to a power law profile, making the profile more singular than required at $r \rightarrow 0$. The resolution of this conundrum is to introduce a running coupling. This is how the beta function $\beta_0^{(4d)}(y)$ will emerge from classical physics.

Technically, the absence of solutions to the problem (C.1) in four dimensions is associated with the necessity of regularizing the source term on the right-hand side. In principle, this can be done by finding the solution in d spacetime dimensions. This would lead to a singular result in the limit $d \rightarrow 4$. By reabsorbing the singularities in the definition of the defect coupling as in eq. (2.58), we could then extract its beta function.⁴⁸ This strategy however suffers of some drawbacks. First, it requires finding an analytical solution to the nonlinear problem (C.1) for arbitrary values of d . Second, dimensional regularization hides the physical

⁴⁸Notice that in four dimensions and to leading order in the triple-scaling limit (3.12) we can neglect the beta function of the bulk coupling λ (3.4).

origin of the *classical* running. For these reasons, in the following we will introduce a more physically transparent approach, which allows studying the problem directly in four spacetime dimensions and that lends itself to a straightforward numerical implementation, bypassing the complication of finding an analytical solution to a nonlinear boundary value problem. Nonetheless, as a proof of concept, in app. C.3 we will show how to find the beta function from the equation (C.1) in dimensional regularization as a series expansion for small values of y .

To obtain a mathematically consistent formulation we require that the boundary conditions (C.2) are satisfied at a certain distance $r = M^{-1} > 0$ from the defect rather than for $r \rightarrow 0$:

$$\phi_a = -\frac{y \left(\bar{z} \frac{\sigma_a}{2} z \right)}{r} \Big|_{r=M^{-1}}. \quad (\text{C.3})$$

Physically, the length scale M^{-1} can be interpreted as the *thickness* of the line defect. The boundary condition (C.3) introduces a mass scale and thus breaks the scale invariance of the action (3.11); by requiring that observables be independent of the scale M we can thus obtain the beta function of the defect coupling.

To do so, let us define the function χ by

$$\phi_a \equiv -\frac{\left(\bar{z} \frac{\sigma_a}{2} z \right)}{r} \chi(\log(rM)), \quad (\text{C.4})$$

where henceforth we will use a new coordinate $u \equiv \log(rM)$. At $r = 1/M$ we have $u = 0$, and from comparing (C.2) and (C.4), we find that $\chi(0)$ has the interpretation of the running coupling y at the scale M .

$\chi(u)$ solves the translationally invariant equation:

$$0 = \chi''(u) - \chi'(u) - \frac{1}{6} \chi^3(u), \quad (\text{C.5})$$

where by $'$ we refer to derivatives with respect to u , such that $\chi'(u) \equiv \partial_u \chi(u)$. To solve this equation we need to choose boundary conditions. One is given by the interpretation of $\chi(u)$ as the running coupling; we also impose that $\chi(\infty) = 0$, which is consistent with the defect being infrared free in four dimensions. In summary, we have

$$\chi_y(0) = y, \quad \chi_y(\infty) = 0, \quad (\text{C.6})$$

where the subscript labels the boundary conditions.

Next, we use the fact that the modulus squared of the bulk scalar field coincides with the leading order value of the ϕ_a^2 one-point function and it is thus a measurable physical quantity given by

$$\frac{\phi_a^2}{\lambda} = \frac{\chi^2(u)}{\lambda r^2}, \quad (\text{C.7})$$

where we divided by λ to compensate for the field redefinition that we implemented in (3.11). Since $\chi_y(u)$ is proportional to a physical quantity, it satisfies the Callan-Symanzik equation:

$$\left[\frac{\partial}{\partial \log M} + \beta_y^{(4d)}(y) \frac{\partial}{\partial y} \right] \chi_y(\log(rM)) = 0. \quad (\text{C.8})$$

From eq. (C.8) we find the following result for the beta function of the coupling y :

$$\beta_y^{(4d)}(y) = -\frac{\chi'_y(u)}{\partial_y \chi_y(u)}. \quad (\text{C.9})$$

As promised, eq. (C.9) relates the beta function of the defect coupling with the classical solution to the saddle-point equations. Notice that eq. (C.9) does not depend on u , and we can exploit this u -independence to write a simpler formula. We use the translation invariance of (C.5) to write

$$\chi_y(u) = \chi_1(u + u_0(y)) \implies y = \chi_1(u_0(y)), \quad (\text{C.10})$$

which defines the function $u_0(y)$ as the inverse function of χ_1 , in terms of which

$$\begin{aligned} \beta_y^{(4d)}(y) &= -\frac{\chi'_y(u)}{\partial_y \chi_y(u)} \\ &= -\frac{\chi'_1(u + u_0(y))}{\partial_y \chi_1(u + u_0(y))} = -\frac{1}{u'_0(y)}, \end{aligned} \quad (\text{C.11})$$

or alternatively equal to $-\chi'_1(u_0(y))$. In practice, we can obtain $\beta_y(y)$ from the parametric plot $\{\chi_1(u_0), -\chi'_1(u_0)\}$, which is easy to make once we are in possession of $\chi_1(u)$; see fig. 12. This function does not have a nontrivial zero, it grows monotonically and diverges as $y \rightarrow \infty$.

Let us comment on one detail of the numerics. The way we set up the problem in eq. (C.11) is not ideal for numerics, since we have to shoot to find the ideal value of $\chi'_1(0)$ that gives a decaying function for $u \rightarrow \infty$. It is easier to choose a very small fixed initial value δ for $u = 0$, use the asymptotic solution (C.13) that we obtain below in the vicinity of $u = 0$, and numerically integrate forwards and backwards to obtain $\chi_\delta(u)$. (Or for $y < \delta$ simply use the perturbative beta function that can be read off from the asymptotic solution, see (C.19).) From the derivation of eq. (C.11) it should be clear that for any δ we have the formula

$$\beta_y^{(4d)}(y) = -\chi'_\delta(\chi_\delta^{-1}(y)). \quad (\text{C.12})$$

Then the parametric plot $\{\chi_\delta(u_0), -\chi'_\delta(u_0)\}$ will still give us the graph of $\beta_y(y)$, see fig. 12.

One may wonder if the salient features of the beta function can be understood analytically, without needing a numerical solution. Next, we show that this is indeed possible.

C.2 Analytic results on the semiclassical beta function

An elementary argument implies the absence of zero of the beta function. This is because such a zero would be unavoidably associated with a scale invariant solution to the equation (C.1) in four dimensions, which however does not exist for $\lambda \neq 0$ as we discussed at length. Technically this is reflected in the fact that the beta function (C.9) is proportional to $\chi'_y(u)$, while eq. (C.1) does not admit a constant nonzero solutions.

Notice that this observation alone does not rule out the possibility that the function $\beta_y^{(4d)}(y)$ tends to zero for $y \rightarrow \infty$, which would imply a strongly coupled fixed point for any

$\varepsilon > 0$. However, even this scenario is ruled out both by numerics and by the analytic argument presented below.

We continue with the analysis of $\chi(u)$ for large u . We are interested in a decaying positive solution to the equation of motion (C.5). Performing the asymptotic analysis with this input yields:

$$\chi(u) = \frac{\sqrt{3}}{\sqrt{u - u_*}} \left(1 + \frac{\log(u - u_*)}{u - u_*} + \dots \right), \quad (\text{C.13})$$

where u_* is a free parameter that can be used to match the solution at finite u .⁴⁹ Asymptotically, we have a positive, monotonically decreasing function.⁵⁰ Going towards smaller u , we wonder if the function can have a maximum. At this maximum at $u = u_m$, we would have $\chi''(u_m) < 0$, $\chi'(u_m) = 0$, $\chi(u_m) > 0$, which contradicts the equation of motion (C.5). We conclude that the function cannot have a maximum.

$\chi(u)$ thus continues to grow as we decrease u ; it can either asymptote to a constant at $u \rightarrow -\infty$ or diverge (either at a finite $u = u_s$ or $u \rightarrow -\infty$). A simple asymptotic analysis rules out the possibility of a finite limit as $u \rightarrow -\infty$. Inspired by Chap. 7 of the book [152], we make an attempt at understanding the large χ behavior of the equation of motion (C.5). We introduce the notation $p(\chi) \equiv \chi'(u)$ and rewrite eq. (C.5) as:

$$0 = p \frac{dp}{d\chi} - p - \frac{\chi^3}{6}. \quad (\text{C.14})$$

It is simple to guess that the large ϕ behavior of p is

$$p(\chi) = -\frac{\chi^2}{2\sqrt{3}} + \dots \quad (\text{C.15})$$

This result is rigorously established by Hardy's theorem, see Chap. 5 of [152]. We can then use the relation $p(\chi(u)) = d\chi/du$ to write

$$u(\chi) = u(\chi_0) + \int_{\chi_0}^{\chi} \frac{d\tilde{\chi}}{p(\tilde{\chi})} \quad (\text{C.16})$$

and using the asymptotics (C.15) derive that the position of the divergence of χ , u_s is finite:

$$u_s = u(\chi_0) + \int_{\chi_0}^{\infty} \frac{d\tilde{\chi}}{p(\tilde{\chi})} < \infty. \quad (\text{C.17})$$

For completeness, we have determined the near singularity behavior of $\chi(u)$:

$$\begin{aligned} \chi(u) = \frac{2\sqrt{3}}{u - u_s} & \left[1 + \frac{u - u_s}{6} - \frac{(u - u_s)^2}{36} + \frac{(u - u_s)^3}{54} \right. \\ & \left. + \left(\frac{2}{135} \log(u - u_s) + a \right) (u - u_s)^4 + \dots \right], \end{aligned} \quad (\text{C.18})$$

⁴⁹We could have further expanded (C.13) at large u , but that would have obscured the meaning of u_* .

⁵⁰This result is actually a theorem, see [152] Chap. 7.5 Theorem 4.

where the two undetermined parameters are u_s and a : these can be used to match to the solution of interest.

Thus we have established that $\chi_1(u)$ (or any $\chi_\delta(u)$) is a monotonically decreasing function on (u_s, ∞) and it goes from ∞ to 0. Then the function $u_0(y)$ defined in eq. (C.10) is a function on $(0, \infty)$ that interpolates monotonically between ∞ and u_s . In eq. (C.11) we derived that $\beta_y^{(4d)}(y) = -1/u'_0(y)$ and it follows that it is a function on $[0, \infty)$ monotonically increasing from 0 to ∞ .

The asymptotic formulas in eqs. (C.13) and (C.18) can be used to obtain the asymptotic behaviors of the beta function. We simply plug them in into eq. (C.12), and evaluate in the case of the large u asymptotics from eq. (C.13) for large u , and in the case for the near singularity behavior from eq. (C.18) small $(u - u_s)$ to obtain:

$$\beta_y^{(4d)}(y) = \begin{cases} \frac{y^3}{6} - \frac{y^5}{12} + \frac{y^7}{9} + \dots & y \ll 1, \\ \frac{y^2}{2\sqrt{3}} - \frac{y}{3} + \frac{2}{3\sqrt{3}} + \dots & y \gg 1. \end{cases} \quad (\text{C.19})$$

Note that in both cases the dependence on the shift of u , denoted by u_* and u_s , is guaranteed to drop out, since the formula (C.12) works for any $\chi(u)$.⁵¹

Finally in fig. 13 we plot the numerical solution for $\chi_1(u)$ together with the asymptotics from eqs. (C.13) and (C.18).⁵² Recall that we used this numerical solution to obtain the beta function in fig. 12.

Finally, we also present a series solution (in the amplitude y) of the equation of motion (C.5). The linearized equation has an exponentially blowing up solution $\chi \sim e^u$. We tune its amplitude to zero to satisfy the boundary condition (C.6), and get the small y solution

$$\chi_y(u) = y - \frac{u}{6} y^3 + \frac{u(u+2)}{24} y^5 - \frac{u(5u^2 + 24u + 48)}{432} y^7 + O(y^9), \quad (\text{C.20})$$

which if plugged into eq. (C.9) reproduces the beta function we got in eq. (C.19):

$$\beta_y^{(4d)}(y) = \frac{y^3}{6} - \frac{y^5}{12} + \frac{y^7}{9} + O(y^9). \quad (\text{C.21})$$

This had to be the case, as the series solution can be matched to the asymptotic solution from eq. (C.13).⁵³ To compare (C.21) with the diagrammatic result $\beta_0^{(4d)} = \frac{1}{3}y^2 + \dots$, remember that $\gamma^2 \beta_0^{(4d)}$ described the flow of γ^2 , which can then be translated to the flow of y since we are strictly in four dimensions and the flow of λ can be ignored.

⁵¹On the other hand, the constant a from (C.18) shows up in the large y expansion of the beta function at $\mathcal{O}(1/y^2)$. Its value can only be determined numerically. (At the same order we also have a $\log(y)$ correction to the power series in $1/y$.)

⁵²We obtained this function by shifting $\chi_\delta(u)$ appropriately in u , as discussed around eq. (C.10).

⁵³To match the two expressions, we have to set

$$u_* = -\frac{3}{y^2} \left(1 + \frac{y^2}{2} \log\left(\frac{3}{y^2}\right) + \dots \right). \quad (\text{C.22})$$

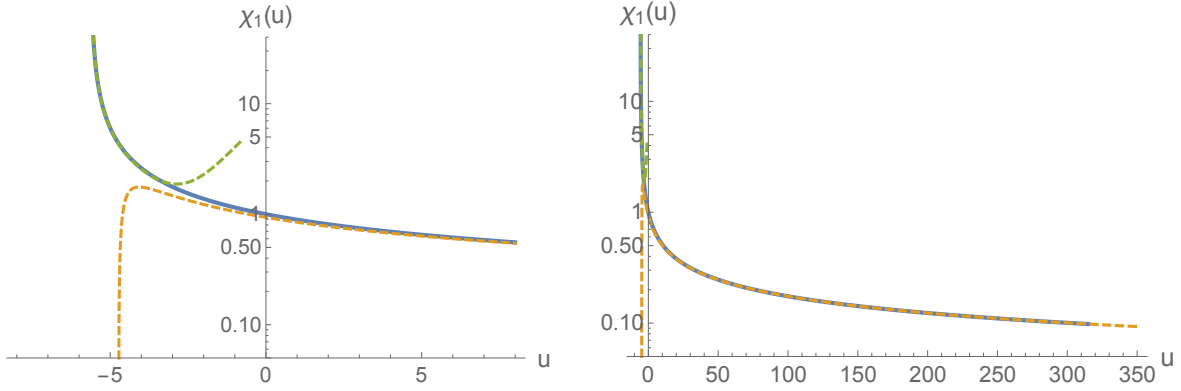


Figure 13: Plot of $\chi_1(u)$ together with its asymptotic behaviors. On the left we are showing a zoomed in version of the plot on the right. The solid line is the numerical solution for $\chi_1(u)$ and the green and orange dashed lines are the near singularity and large u asymptotics respectively. Note that except for a small window of u these asymptotics describe the full curve very accurately. The fitted values of the matching parameters for the asymptotics are $u_* = -5.2$ (from eq. (C.13)) and $u_s = -5.63$ (from eq. (C.18); also note we did not obtain a reliable value for a).

C.3 Beta function in the interacting $O(3)$ model in dimensional regularization

The dimensional regularization method we present here will follow the conventional machinery. However, it hides the physical meaning of the running coupling as a saddle-point field profile, which was abundantly clear in the previous computation presented in apps. C.1 and C.2.

Our starting point is to solve eq. (C.1) in fractional dimension with the boundary condition (C.2). The equation is not scale invariant for $d < 4$, therefore we were not able to find an exact solution. Nonetheless one can find a solution perturbatively in the bare double scaling parameter y_0 :

$$\begin{aligned} \phi_a(r) &= -c_d \frac{y_0 \left(\bar{z} \frac{\sigma^a}{2} z \right)}{r^{d-3}} \left[1 + a_1 U^2 + a_2 U^4 + \dots \right], \\ U &\equiv y_0 r^{4-d}, \end{aligned} \quad (\text{C.23})$$

where we have determined the first 20 a_i coefficients, e.g.

$$a_1 = \frac{c_d^2}{12(d-4)(3d-11)}, \quad a_2 = \frac{c_d^4}{96(d-4)^2(3d-11)(5d-19)}. \quad (\text{C.24})$$

We notice the pattern that as $d \rightarrow 4$ these coefficients blow up as $a_k \sim 1/\varepsilon^k$. As a result, we have that

$$a_k U^{2k} \sim \left[y_0^2 \left(\frac{1}{\varepsilon} + \log r + O(\varepsilon) \right) \right]^k. \quad (\text{C.25})$$

We renormalize these divergences by requiring that ϕ_a^2/λ_0 , which is a physical expectation value, is finite. The only way to consistently do so is to shift the coupling γ_0 . We do so in the following way:

$$\gamma_0^2 = \frac{M^\varepsilon}{c_{4-\varepsilon}^2} \left[\gamma_{\text{DR}}^2 + \frac{\delta\gamma^2(y_{\text{DR}})}{\varepsilon} + \frac{\delta_2\gamma^2(y_{\text{DR}})}{\varepsilon^2} + \dots \right], \quad (\text{C.26})$$

which is equivalent to

$$y_0 = \frac{M^\varepsilon}{c_{4-\varepsilon}} \left[y_{\text{DR}} + \frac{\delta y(y_{\text{DR}})}{\varepsilon} + \frac{\delta_2 y(y_{\text{DR}})}{\varepsilon^2} + \dots \right], \quad (\text{C.27})$$

where the DR subscript stands for dimensional regularization, and we conventionally divided by the factor $c_{4-\varepsilon}^2 = 1 + O(\varepsilon)$ for convenience; therefore the physical coupling defined by eqs. (C.26), (C.27) does not coincide with the one in the usual minimal subtraction scheme. To the order we are working we can neglect the running of the coupling λ , the counterterms for γ_{DR} and y_{DR} are identical and they are functions of the renormalized triple-scaled coupling y_{DR} .

The beta functions of the defect coupling is conveniently written in terms of y and is obtained from

$$\beta_{y_{\text{DR}}} = -\varepsilon y_{\text{DR}} + \beta_{y_{\text{DR}}}^{(4d)}, \quad \beta_{y_{\text{DR}}}^{(4d)} = y_{\text{DR}} \frac{d\delta y(y_{\text{DR}})}{dy_{\text{DR}}} - \delta y(y_{\text{DR}}). \quad (\text{C.28})$$

Our result reads:

$$\begin{aligned} \beta_{y_{\text{DR}}}^{(4d)} = & \frac{y_{\text{DR}}^3}{6} - \frac{y_{\text{DR}}^5}{12} + \frac{11y_{\text{DR}}^7}{144} - \frac{59y_{\text{DR}}^9}{648} + \frac{2609y_{\text{DR}}^{11}}{20736} - \frac{14869y_{\text{DR}}^{13}}{77760} + \frac{2318219y_{\text{DR}}^{15}}{7464960} \\ & - \frac{1729831y_{\text{DR}}^{17}}{3265920} + \frac{14116674883y_{\text{DR}}^{19}}{15049359360} - \frac{241476805y_{\text{DR}}^{21}}{141087744} + O(y_{\text{DR}}^{23}), \end{aligned} \quad (\text{C.29})$$

where we reported several orders to illustrate the simplicity of the procedure compared to standard loop calculations. The first two terms of eq. (C.29) agree with the result for $\beta_y^{(4d)}$ given in eq. (C.19), which was obtained in a different renormalization scheme as discussed in app. C.1. Indeed, to the order we are working y is the only running coupling in four dimensions, and it is a well known fact that for such a setup the first two coefficients of the beta function are scheme-independent [89]. This does not apply to the higher order terms, and indeed eq. (C.29) differs from the eq. (C.19) in the $O(y_{\text{DR}}^7)$ term (and beyond). As a consistency check, in the following we independently determine the translation between y and y_{DR} and show that the beta functions computed from the classical profile and from minimal subtraction match precisely once this is taken into account.

The renormalization procedure described above leads to the following bulk scalar profile in 4 dimensions:

$$\frac{\phi_a}{\sqrt{\lambda}} = -\frac{(\bar{z}\frac{\sigma_a}{2}z)}{\sqrt{\lambda}r} y_{\text{DR}} \left[1 - \frac{2u+3}{12} y_{\text{DR}}^2 + \frac{4u^2+20u+31}{96} y_{\text{DR}}^4 + \dots \right]. \quad (\text{C.30})$$

where to simplify formulas we use the coordinate $u = \log(rM)$. Recalling the definition $\chi(u=0) = y$ in the scheme used in app. C.1, we get the relation:

$$y = y_{\text{DR}} \left[1 - \frac{1}{4} y_{\text{DR}}^2 + \frac{31}{96} y_{\text{DR}}^4 + \dots \right]. \quad (\text{C.31})$$

Inverting this relation, it is simple to verify that the beta functions from eqs. (C.19) and (C.29) match on the nose.

References

- [1] S. Sachdev, C. Buragohain and M. Vojta, *Quantum impurity in a nearly critical two-dimensional antiferromagnet*, *Science* **286** (1999) 2479 [[cond-mat/0004156](#)].
- [2] M. Vojta, C. Buragohain and S. Sachdev, *Quantum impurity dynamics in two-dimensional antiferromagnets and superconductors*, *Physical Review B* **61** (2000) 15152 [[cond-mat/9912020](#)].
- [3] K. G. Wilson, *Confinement of Quarks*, *Phys. Rev. D* **10** (1974) 2445.
- [4] G. 't Hooft, *On the Phase Transition Towards Permanent Quark Confinement*, *Nucl. Phys. B* **138** (1978) 1.
- [5] I. Affleck, *Conformal field theory approach to the Kondo effect*, *Acta Phys. Polon. B* **26** (1995) 1869 [[cond-mat/9512099](#)].
- [6] I. Affleck and A. W. W. Ludwig, *Universal noninteger 'ground state degeneracy' in critical quantum systems*, *Phys. Rev. Lett.* **67** (1991) 161.
- [7] D. Friedan and A. Konechny, *On the boundary entropy of one-dimensional quantum systems at low temperature*, *Phys. Rev. Lett.* **93** (2004) 030402 [[hep-th/0312197](#)].
- [8] H. Casini, I. Salazar Landea and G. Torroba, *The g-theorem and quantum information theory*, *JHEP* **10** (2016) 140 [[1607.00390](#)].
- [9] G. Cuomo, Z. Komargodski and A. Raviv-Moshe, *Renormalization Group Flows on Line Defects*, *Phys. Rev. Lett.* **128** (2022) 021603 [[2108.01117](#)].
- [10] N. Andrei et al., *Boundary and Defect CFT: Open Problems and Applications*, *J. Phys. A* **53** (2020) 453002 [[1810.05697](#)].
- [11] N. B. Agmon and Y. Wang, *Classifying Superconformal Defects in Diverse Dimensions Part I: Superconformal Lines*, [2009.06650](#).
- [12] S. Penati, *Superconformal Line Defects in 3D*, *Universe* **7** (2021) 348 [[2108.06483](#)].
- [13] N. Lashkari, A. Dymarsky and H. Liu, *Eigenstate Thermalization Hypothesis in Conformal Field Theory*, *J. Stat. Mech.* **1803** (2018) 033101 [[1610.00302](#)].
- [14] A. Belin and J. de Boer, *Random statistics of OPE coefficients and Euclidean wormholes*, *Class. Quant. Grav.* **38** (2021) 164001 [[2006.05499](#)].
- [15] L. V. Delacretaz, *Heavy Operators and Hydrodynamic Tails*, *SciPost Phys.* **9** (2020) 034 [[2006.01139](#)].
- [16] L. F. Alday and J. M. Maldacena, *Comments on operators with large spin*, *JHEP* **11** (2007) 019 [[0708.0672](#)].

- [17] Z. Komargodski and A. Zhiboedov, *Convexity and Liberation at Large Spin*, *JHEP* **11** (2013) 140 [[1212.4103](#)].
- [18] A. L. Fitzpatrick, J. Kaplan, D. Poland and D. Simmons-Duffin, *The Analytic Bootstrap and AdS Superhorizon Locality*, *JHEP* **12** (2013) 004 [[1212.3616](#)].
- [19] S. Hellerman, D. Orlando, S. Reffert and M. Watanabe, *On the CFT Operator Spectrum at Large Global Charge*, *JHEP* **12** (2015) 071 [[1505.01537](#)].
- [20] A. Monin, D. Pirtskhalava, R. Rattazzi and F. K. Seibold, *Semiclassics, Goldstone Bosons and CFT data*, *JHEP* **06** (2017) 011 [[1611.02912](#)].
- [21] S. Hellerman, S. Maeda and M. Watanabe, *Operator Dimensions from Moduli*, *JHEP* **10** (2017) 089 [[1706.05743](#)].
- [22] F. Parisen Toldin, F. F. Assaad and S. Wessel, *Critical behavior in the presence of an order-parameter pinning field*, *Phys. Rev. B* **95** (2017) 014401 [[1607.04270](#)].
- [23] G. Cuomo, Z. Komargodski and M. Mezei, *Localized magnetic field in the $O(N)$ model*, [2112.10634](#).
- [24] A. Pelissetto and E. Vicari, *Critical phenomena and renormalization group theory*, *Phys. Rept.* **368** (2002) 549 [[cond-mat/0012164](#)].
- [25] D. Poland, S. Rychkov and A. Vichi, *The Conformal Bootstrap: Theory, Numerical Techniques, and Applications*, *Rev. Mod. Phys.* **91** (2019) 015002 [[1805.04405](#)].
- [26] J. Henriksson, *The critical $O(N)$ CFT: Methods and conformal data*, [2201.09520](#).
- [27] A. M. Sengupta, *Spin in a fluctuating field: The bose(+fermi) kondo models*, *Phys. Rev. B* **61** (2000) 4041 [[cond-mat/9707316](#)].
- [28] S. Sachdev, *Static hole in a critical antiferromagnet: Field theoretic renormalization group*, *Physica C* **357** (2001) 78 [[cond-mat/0011233](#)].
- [29] S. Sachdev and M. Vojta, *Quantum impurity in an antiferromagnet: Nonlinear sigma model theory*, *Phys. Rev. B* **68** (2003) 064419 [[cond-mat/0303001](#)].
- [30] K. H. Höglund, A. W. Sandvik and S. Sachdev, *Impurity induced spin texture in quantum critical 2d antiferromagnets*, *Phys. Rev. Lett.* **98** (2007) 087203 [[cond-mat/0611418](#)].
- [31] K. H. Höglund and A. W. Sandvik, *Anomalous curie response of impurities in quantum-critical spin-1/2 heisenberg antiferromagnets*, *Phys. Rev. Lett.* **99** (2007) 027205 [[cond-mat/0701472](#)].
- [32] S. Liu, H. Shapourian, A. Vishwanath and M. A. Metlitski, *Magnetic impurities at quantum critical points: Large- N expansion and connections to symmetry-protected topological states*, *Phys. Rev. B* **104** (2021) 104201 [[2104.15026](#)].
- [33] S. Florens, L. Fritz and M. Vojta, *Kondo effect in bosonic spin liquids*, *Phys. Rev. Lett.* **96** (2006) 036601 [[cond-mat/0507188](#)].
- [34] A. Kolezhuk, S. Sachdev, R. R. Biswas and P. Chen, *Theory of quantum impurities in spin liquids*, *Phys. Rev. B* **74** (2006) 165114 [[cond-mat/0606385](#)].
- [35] S. Florens, L. Fritz and M. Vojta, *Boundary quantum criticality in models of magnetic impurities coupled to bosonic baths*, *Phys. Rev. B* **75** (2007) 224420 [[cond-mat/0703609](#)].

- [36] R. R. Biswas, S. Sachdev and D. T. Son, *Coulomb impurity in graphene*, *Phys. Rev. B* **76** (2007) 205122 [[0706.3907](#)].
- [37] M. A. Metlitski and S. Sachdev, *Valence bond solid order near impurities in two-dimensional quantum antiferromagnets*, *Phys. Rev. B* **77** (2008) 054411 [[0710.0626](#)].
- [38] F. F. Assaad and I. F. Herbut, *Pinning the order: the nature of quantum criticality in the Hubbard model on honeycomb lattice*, *Phys. Rev. X* **3** (2013) 031010 [[1304.6340](#)].
- [39] A. Allais, *Magnetic defect line in a critical Ising bath*, [1412.3449](#).
- [40] A. Allais and S. Sachdev, *Spectral function of a localized fermion coupled to the Wilson-Fisher conformal field theory*, *Phys. Rev. B* **90** (2014) 035131 [[1406.3022](#)].
- [41] M. Billó, M. Caselle, D. Gaiotto, F. Gliozzi, M. Meineri and R. Pellegrini, *Line defects in the 3d Ising model*, *JHEP* **07** (2013) 055 [[1304.4110](#)].
- [42] D. Gaiotto, D. Mazac and M. F. Paulos, *Bootstrapping the 3d Ising twist defect*, *JHEP* **03** (2014) 100 [[1310.5078](#)].
- [43] A. Söderberg, *Anomalous Dimensions in the WF $O(N)$ Model with a Monodromy Line Defect*, *JHEP* **03** (2018) 058 [[1706.02414](#)].
- [44] L. Bianchi, A. Chalabi, V. Procházka, B. Robinson and J. Sisti, *Monodromy defects in free field theories*, *JHEP* **08** (2021) 013 [[2104.01220](#)].
- [45] S. Giombi, E. Helfenberger, Z. Ji and H. Khanchandani, *Monodromy Defects from Hyperbolic Space*, [2102.11815](#).
- [46] A. Tsvelick and P. Wiegmann, *Exact solution of the multichannel kondo problem, scaling, and integrability*, *Journal of Statistical Physics* **38** (1985) 125.
- [47] V. J. Emery and S. Kivelson, *Mapping of the two-channel kondo problem to a resonant-level model*, *Phys. Rev. B* **46** (1992) 10812.
- [48] O. Parcollet, A. Georges, G. Kotliar and A. Sengupta, *Overscreened multichannel $SU(n)$ kondo model: Large- n solution and conformal field theory*, *Phys. Rev. B* **58** (1998) 3794 [[cond-mat/9711192](#)].
- [49] M. Moshe and J. Zinn-Justin, *Quantum field theory in the large N limit: A Review*, *Phys. Rept.* **385** (2003) 69 [[hep-th/0306133](#)].
- [50] V. A. Miransky, *Dynamics of Spontaneous Chiral Symmetry Breaking and Continuum Limit in Quantum Electrodynamics*, *Nuovo Cim. A* **90** (1985) 149.
- [51] D. B. Kaplan, J.-W. Lee, D. T. Son and M. A. Stephanov, *Conformality Lost*, *Phys. Rev. D* **80** (2009) 125005 [[0905.4752](#)].
- [52] V. Gorbenko, S. Rychkov and B. Zan, *Walking, Weak first-order transitions, and Complex CFTs*, *JHEP* **10** (2018) 108 [[1807.11512](#)].
- [53] E. Lauria, P. Liendo, B. C. Van Rees and X. Zhao, *Line and surface defects for the free scalar field*, *JHEP* **01** (2021) 060 [[2005.02413](#)].
- [54] T. Nishioka and Y. Sato, *Free energy and defect C -theorem in free scalar theory*, *JHEP* **05** (2021) 074 [[2101.02399](#)].

- [55] D. Friedan, A. Konechny and C. Schmidt-Colinet, *Lower bound on the entropy of boundaries and junctions in 1+1d quantum critical systems*, *Phys. Rev. Lett.* **109** (2012) 140401 [[1206.5395](#)].
- [56] S. Collier, D. Mazac and Y. Wang, *Bootstrapping Boundaries and Branes*, [2112.00750](#).
- [57] P. Argyres, M. Lotito, Y. Lü and M. Martone, *Geometric constraints on the space of $\mathcal{N} = 2$ SCFTs. Part I: physical constraints on relevant deformations*, *JHEP* **02** (2018) 001 [[1505.04814](#)].
- [58] P. C. Argyres, M. Lotito, Y. Lü and M. Martone, *Geometric constraints on the space of $\mathcal{N} = 2$ SCFTs. Part II: construction of special Kähler geometries and RG flows*, *JHEP* **02** (2018) 002 [[1601.00011](#)].
- [59] P. Argyres, M. Lotito, Y. Lü and M. Martone, *Geometric constraints on the space of $\mathcal{N} = 2$ SCFTs. Part III: enhanced Coulomb branches and central charges*, *JHEP* **02** (2018) 003 [[1609.04404](#)].
- [60] P. C. Argyres, M. Lotito, Y. Lü and M. Martone, *Expanding the landscape of $\mathcal{N} = 2$ rank 1 SCFTs*, *JHEP* **05** (2016) 088 [[1602.02764](#)].
- [61] J. M. Maldacena, *Wilson loops in large N field theories*, *Phys. Rev. Lett.* **80** (1998) 4859 [[hep-th/9803002](#)].
- [62] S.-J. Rey and J.-T. Yee, *Macroscopic strings as heavy quarks in large N gauge theory and anti-de Sitter supergravity*, *Eur. Phys. J. C* **22** (2001) 379 [[hep-th/9803001](#)].
- [63] J. K. Erickson, G. W. Semenoff and K. Zarembo, *Wilson loops in $N=4$ supersymmetric Yang-Mills theory*, *Nucl. Phys. B* **582** (2000) 155 [[hep-th/0003055](#)].
- [64] N. Drukker and D. J. Gross, *An Exact prediction of $N=4$ SUSYM theory for string theory*, *J. Math. Phys.* **42** (2001) 2896 [[hep-th/0010274](#)].
- [65] K. Zarembo, *Supersymmetric Wilson loops*, *Nucl. Phys. B* **643** (2002) 157 [[hep-th/0205160](#)].
- [66] J. Gomis and F. Passerini, *Holographic Wilson Loops*, *JHEP* **08** (2006) 074 [[hep-th/0604007](#)].
- [67] V. Pestun, *Localization of gauge theory on a four-sphere and supersymmetric Wilson loops*, *Commun. Math. Phys.* **313** (2012) 71 [[0712.2824](#)].
- [68] D. Gaiotto, G. W. Moore and A. Neitzke, *Framed BPS States*, *Adv. Theor. Math. Phys.* **17** (2013) 241 [[1006.0146](#)].
- [69] D. Correa, J. Henn, J. Maldacena and A. Sever, *An exact formula for the radiation of a moving quark in $N=4$ super Yang Mills*, *JHEP* **06** (2012) 048 [[1202.4455](#)].
- [70] C. Córdova and A. Neitzke, *Line Defects, Tropicalization, and Multi-Centered Quiver Quantum Mechanics*, *JHEP* **09** (2014) 099 [[1308.6829](#)].
- [71] A. Lewkowycz and J. Maldacena, *Exact results for the entanglement entropy and the energy radiated by a quark*, *JHEP* **05** (2014) 025 [[1312.5682](#)].
- [72] F. Fucito, J. F. Morales and R. Poghossian, *Wilson loops and chiral correlators on squashed spheres*, *JHEP* **11** (2015) 064 [[1507.05426](#)].
- [73] B. Fiol, E. Gerchkovitz and Z. Komargodski, *Exact Bremsstrahlung Function in $N = 2$ Superconformal Field Theories*, *Phys. Rev. Lett.* **116** 081601 [[1510.01332](#)].

- [74] C. Cordova, D. Gaiotto and S.-H. Shao, *Infrared Computations of Defect Schur Indices*, *JHEP* **11** (2016) 106 [[1606.08429](#)].
- [75] L. Bianchi, M. Lemos and M. Meineri, *Line Defects and Radiation in $\mathcal{N} = 2$ Conformal Theories*, *Phys. Rev. Lett.* **121** (2018) 141601 [[1805.04111](#)].
- [76] L. Bianchi, M. Billò, F. Galvagno and A. Lerda, *Emitted Radiation and Geometry*, *JHEP* **01** (2020) 075 [[1910.06332](#)].
- [77] F. Galvagno, *Emitted radiation in superconformal field theories*, *Eur. Phys. J. Plus* **137** (2022) 143 [[2112.03841](#)].
- [78] K. Hosomichi, *$\mathcal{N} = 2$ SUSY gauge theories on S^4* , *J. Phys. A* **50** (2017) 443010 [[1608.02962](#)].
- [79] M. Beccaria, S. Giombi and A. A. Tseytlin, *Wilson loop in general representation and RG flow in 1d defect QFT, to appear*.
- [80] S. Sachdev, *Quantum Phase Transitions*. Cambridge University Press, 2 ed., 2011, [10.1017/CBO9780511973765](#).
- [81] E. H. Lieb, *The classical limit of quantum spin systems*, *Communications in Mathematical Physics* **31** (1973) 327.
- [82] E. Rabinovici, A. Schwimmer and S. Yankielowicz, *Quantization in the Presence of Wess-Zumino Terms*, *Nucl. Phys. B* **248** (1984) 523.
- [83] M. P. Clark, *A Semi-classical analysis of the Wilson Loop in a 2+1 Dimensional Yang-Mills theory with a monopole gas*, Ph.D. thesis, University of British Columbia, 1997. <http://dx.doi.org/10.14288/1.0085080>.
- [84] T. T. Wu and C. N. Yang, *Dirac monopole without strings: Monopole harmonics*, *Nuclear Physics B* **107** (1976) 365.
- [85] G. V. Dunne, R. Jackiw and C. A. Trugenberger, *Topological (Chern-Simons) Quantum Mechanics*, *Phys. Rev. D* **41** (1990) 661.
- [86] K. Hasebe, *Hopf Maps, Lowest Landau Level, and Fuzzy Spheres*, *SIGMA* **6** (2010) 071 [[1009.1192](#)].
- [87] J. Negele and H. Orland, *Quantum Many-particle Systems*. CRC Press, 2018.
- [88] S. R. Coleman and B. R. Hill, *No More Corrections to the Topological Mass Term in QED in Three-Dimensions*, *Phys. Lett. B* **159** (1985) 184.
- [89] S. Weinberg, *The quantum theory of fields. Vol. 2: Modern applications*. Cambridge University Press, 8, 2013.
- [90] A. J. Bray and M. A. Moore, *Critical behaviour of semi-infinite systems*, *Journal of Physics A: Mathematical and General* **10** (1977) 1927.
- [91] G. Cuomo, M. Mezei and A. Raviv-Moshe, *Boundary conformal field theory at large charge*, *JHEP* **10** (2021) 143 [[2108.06579](#)].
- [92] J. Padayasi, A. Krishnan, M. A. Metlitski, I. A. Gruzberg and M. Meineri, *The extraordinary boundary transition in the 3d $O(N)$ model via conformal bootstrap*, [2111.03071](#).
- [93] C. P. Herzog and K.-W. Huang, *Boundary Conformal Field Theory and a Boundary Central Charge*, *JHEP* **10** (2017) 189 [[1707.06224](#)].

- [94] G. Badel, G. Cuomo, A. Monin and R. Rattazzi, *The Epsilon Expansion Meets Semiclassics*, [*JHEP* **11** \(2019\) 110](#) [[1909.01269](#)].
- [95] V. A. Rubakov, *Nonperturbative aspects of multiparticle production*, in *2nd Rencontres du Vietnam: Consisting of 2 parallel conferences: Astrophysics Meeting: From the Sun and Beyond / Particle Physics Meeting: Physics at the Frontiers of the Standard Model*, 10, 1995, [hep-ph/9511236](#).
- [96] D. T. Son, *Semiclassical approach for multiparticle production in scalar theories*, [*Nucl. Phys. B* **477** \(1996\) 378](#) [[hep-ph/9505338](#)].
- [97] D. H. Correa and F. I. Schaposnik Massolo, *Ladder exponentiation for generic large symmetric representation Wilson loops*, [*JHEP* **11** \(2015\) 060](#) [[1510.02345](#)].
- [98] D. H. Correa, F. I. Schaposnik Massolo and D. Trancanelli, *Cusped Wilson lines in symmetric representations*, [*JHEP* **08** \(2015\) 091](#) [[1506.01680](#)].
- [99] M. Beccaria, S. Giombi and A. Tseytlin, *Non-supersymmetric Wilson loop in $\mathcal{N} = 4$ SYM and defect 1d CFT*, [*JHEP* **03** \(2018\) 131](#) [[1712.06874](#)].
- [100] N. Kobayashi, T. Nishioka, Y. Sato and K. Watanabe, *Towards a C-theorem in defect CFT*, [*JHEP* **01** \(2019\) 039](#) [[1810.06995](#)].
- [101] L. Alvarez-Gaume, D. Orlando and S. Reffert, *Large charge at large N*, [*JHEP* **12** \(2019\) 142](#) [[1909.02571](#)].
- [102] G. Badel, G. Cuomo, A. Monin and R. Rattazzi, *Feynman diagrams and the large charge expansion in $3 - \varepsilon$ dimensions*, [*Phys. Lett. B* **802** \(2020\) 135202](#) [[1911.08505](#)].
- [103] O. Antipin, J. Bersini, F. Sannino, Z.-W. Wang and C. Zhang, *Charging the $O(N)$ model*, [*Phys. Rev. D* **102** \(2020\) 045011](#) [[2003.13121](#)].
- [104] I. Jack and D. R. T. Jones, *Anomalous dimensions at large charge in $d=4$ $O(N)$ theory*, [*Phys. Rev. D* **103** \(2021\) 085013](#) [[2101.09820](#)].
- [105] J. Gomis, P.-S. Hsin, Z. Komargodski, A. Schwimmer, N. Seiberg and S. Theisen, *Anomalies, Conformal Manifolds, and Spheres*, [*JHEP* **03** \(2016\) 022](#) [[1509.08511](#)].
- [106] A. Schwimmer and S. Theisen, *Moduli Anomalies and Local Terms in the Operator Product Expansion*, [*JHEP* **07** \(2018\) 110](#) [[1805.04202](#)].
- [107] A. Schwimmer and S. Theisen, *Osborn Equation and Irrelevant Operators*, [*J. Stat. Mech.* **1908** \(2019\) 084011](#) [[1902.04473](#)].
- [108] H. Kleinert and V. Schulte-Frohlinde, *Critical properties of ϕ^4 -theories*. 2001.
- [109] M. A. Metlitski, *Boundary criticality of the $O(N)$ model in $d = 3$ critically revisited*, [2009.05119](#).
- [110] C. P. Herzog and A. Shrestha, *Two point functions in defect CFTs*, [*JHEP* **04** \(2021\) 226](#) [[2010.04995](#)].
- [111] M. Billò, V. Gonçalves, E. Lauria and M. Meineri, *Defects in conformal field theory*, [*JHEP* **04** \(2016\) 091](#) [[1601.02883](#)].
- [112] T. DeGrand, *Lattice tests of beyond Standard Model dynamics*, [*Rev. Mod. Phys.* **88** \(2016\) 015001](#) [[1510.05018](#)].

- [113] A. Kapustin, *Wilson-'t Hooft operators in four-dimensional gauge theories and S-duality*, *Phys. Rev. D* **74** (2006) 025005 [[hep-th/0501015](#)].
- [114] D. Jafferis, B. Mukhametzhanov and A. Zhiboedov, *Conformal Bootstrap At Large Charge*, *JHEP* **05** (2018) 043 [[1710.11161](#)].
- [115] Z. Komargodski, M. Mezei, S. Pal and A. Raviv-Moshe, *Spontaneously broken boosts in CFTs*, *JHEP* **09** (2021) 064 [[2102.12583](#)].
- [116] G. Cuomo, A. de la Fuente, A. Monin, D. Pirtskhalava and R. Rattazzi, *Rotating superfluids and spinning charged operators in conformal field theory*, *Phys. Rev. D* **97** (2018) 045012 [[1711.02108](#)].
- [117] A. De La Fuente, *The large charge expansion at large N* , *JHEP* **08** (2018) 041 [[1805.00501](#)].
- [118] G. Murthy and S. Sachdev, *Action of Hedgehog Instantons in the Disordered Phase of the $(2+1)$ -dimensional CP^{N-1} Model*, *Nucl. Phys. B* **344** (1990) 557.
- [119] E. Dyer, M. Mezei and S. S. Pufu, *Monopole Taxonomy in Three-Dimensional Conformal Field Theories*, [1309.1160](#).
- [120] E. Dyer, M. Mezei, S. S. Pufu and S. Sachdev, *Scaling dimensions of monopole operators in the CP^{N_b-1} theory in $2 + 1$ dimensions*, *JHEP* **06** (2015) 037 [[1504.00368](#)].
- [121] S. M. Chester, M. Mezei, S. S. Pufu and I. Yaakov, *Monopole operators from the $4 - \epsilon$ expansion*, *JHEP* **12** (2016) 015 [[1511.07108](#)].
- [122] S. Giombi, S. Komatsu and B. Offertaler, *Large Charges on the Wilson Loop in $\mathcal{N} = 4$ SYM: Matrix Model and Classical String*, [2110.13126](#).
- [123] J. S. Schwinger, *On gauge invariance and vacuum polarization*, *Phys. Rev.* **82** (1951) 664.
- [124] G. W. Semenoff and K. Zarembo, *Holographic Schwinger Effect*, *Phys. Rev. Lett.* **107** (2011) 171601 [[1109.2920](#)].
- [125] S. Bolognesi, F. Kiefer and E. Rabinovici, *Comments on Critical Electric and Magnetic Fields from Holography*, *JHEP* **01** (2013) 174 [[1210.4170](#)].
- [126] J. Polchinski and J. Sully, *Wilson Loop Renormalization Group Flows*, *JHEP* **10** (2011) 059 [[1104.5077](#)].
- [127] M. Beccaria and A. A. Tseytlin, *On non-supersymmetric generalizations of the Wilson-Maldacena loops in $N = 4$ SYM*, *Nucl. Phys. B* **934** (2018) 466 [[1804.02179](#)].
- [128] M. Beccaria, S. Giombi and A. A. Tseytlin, *Higher order RG flow on the Wilson line in $\mathcal{N} = 4$ SYM*, *JHEP* **01** (2022) 056 [[2110.04212](#)].
- [129] P. C. Argyres, A. M. Awad, G. A. Braun and F. P. Esposito, *Higher derivative terms in $N=2$ supersymmetric effective actions*, *JHEP* **07** (2003) 060 [[hep-th/0306118](#)].
- [130] A. Schwimmer and S. Theisen, *Spontaneous Breaking of Conformal Invariance and Trace Anomaly Matching*, *Nucl. Phys. B* **847** (2011) 590 [[1011.0696](#)].
- [131] Z. Komargodski and A. Schwimmer, *On Renormalization Group Flows in Four Dimensions*, *JHEP* **12** (2011) 099 [[1107.3987](#)].
- [132] B. de Wit, M. T. Grisaru and M. Rocek, *Nonholomorphic corrections to the one loop $N=2$ superYang-Mills action*, *Phys. Lett. B* **374** (1996) 297 [[hep-th/9601115](#)].

- [133] M. Henningson, *Extended superspace, higher derivatives and $SL(2, \mathbb{Z})$ duality*, *Nucl. Phys. B* **458** (1996) 445 [[hep-th/9507135](#)].
- [134] M. Dine and N. Seiberg, *Comments on higher derivative operators in some SUSY field theories*, *Phys. Lett. B* **409** (1997) 239 [[hep-th/9705057](#)].
- [135] S. Hellerman and S. Maeda, *On the Large R -charge Expansion in $\mathcal{N} = 2$ Superconformal Field Theories*, *JHEP* **12** (2017) 135 [[1710.07336](#)].
- [136] S. Giombi and I. R. Klebanov, *Interpolating between a and F* , *JHEP* **03** (2015) 117 [[1409.1937](#)].
- [137] K. Papadodimas, *Topological Anti-Topological Fusion in Four-Dimensional Superconformal Field Theories*, *JHEP* **08** (2010) 118 [[0910.4963](#)].
- [138] S. Hellerman, S. Maeda, D. Orlando, S. Reffert and M. Watanabe, *Universal correlation functions in rank 1 SCFTs*, *JHEP* **12** (2019) 047 [[1804.01535](#)].
- [139] V. Pestun et al., *Localization techniques in quantum field theories*, *J. Phys. A* **50** (2017) 440301 [[1608.02952](#)].
- [140] G. W. Moore, N. Nekrasov and S. Shatashvili, *Integrating over Higgs branches*, *Commun. Math. Phys.* **209** (2000) 97 [[hep-th/9712241](#)].
- [141] N. A. Nekrasov, *Seiberg-Witten prepotential from instanton counting*, *Adv. Theor. Math. Phys.* **7** (2003) 831 [[hep-th/0206161](#)].
- [142] N. Nekrasov and A. Okounkov, *Seiberg-Witten theory and random partitions*, *Prog. Math.* **244** (2006) 525 [[hep-th/0306238](#)].
- [143] A. Grassi, Z. Komargodski and L. Tizzano, *Extremal correlators and random matrix theory*, *JHEP* **04** (2021) 214 [[1908.10306](#)].
- [144] S. Hellerman, *On the exponentially small corrections to $\mathcal{N} = 2$ superconformal correlators at large R -charge*, [2103.09312](#).
- [145] S. Hellerman and D. Orlando, *Large R -charge EFT correlators in $N=2$ SQCD*, [2103.05642](#).
- [146] A. Klemm, M. Marino and S. Theisen, *Gravitational corrections in supersymmetric gauge theory and matrix models*, *JHEP* **03** (2003) 051 [[hep-th/0211216](#)].
- [147] S. Hellerman, S. Maeda, D. Orlando, S. Reffert and M. Watanabe, *S -duality and correlation functions at large R -charge*, *JHEP* **04** (2021) 287 [[2005.03021](#)].
- [148] M. Beccaria, *On the large R -charge $\mathcal{N} = 2$ chiral correlators and the Toda equation*, *JHEP* **02** (2019) 009 [[1809.06280](#)].
- [149] M. Beccaria, F. Galvagno and A. Hasan, *$\mathcal{N} = 2$ conformal gauge theories at large R -charge: the $SU(N)$ case*, *JHEP* **03** (2020) 160 [[2001.06645](#)].
- [150] E. D'Hoker, J. Estes and M. Gutperle, *Gravity duals of half-BPS Wilson loops*, *JHEP* **06** (2007) 063 [[0705.1004](#)].
- [151] J. Gomis, S. Matsuura, T. Okuda and D. Trancanelli, *Wilson loop correlators at strong coupling: From matrices to bubbling geometries*, *JHEP* **08** (2008) 068 [[0807.3330](#)].
- [152] R. Bellman, *Stability Theory of Differential Equations*, Dover Books on Mathematics. Dover Publications, 2013.